united nations
educational, scientific
and cultural
organization

international atomic
energy agency

the
abdus salam
international centre for theoretical physics

School on "Exploring the Atmosphere by Remote Sensing Techniques"
18 October - 5 November 1999

1151-22

"Improvements of DOAS"

K. Pfeilsticker
University of Heidelberg
Germany

Please note: These are preliminary notes intended for internal distribution only.

strada costiera 11 - 34014 trieste italy

Improvements of DOAS

Differential Optical Absorption Spectroscopy

Dr. Klaus Pfeilsticker
University of Heidelberg
Germany

also with

NOAA
Aeronomy Lab
Boulder, CO
USA

Structure of the presentation

1.) **Introduction**
What is DOAS about ?
- **principles**
- **list of atmospheric absorbers**
- **absorbers versus wavelength**

2.) **Typical questions related to instrumental outline**
- **What is the proper spectral resolution ?**
- **What is the best spectral range ?**
- **What is the best light detector (S/N) ?**

3.) **Some instrumental characteristics**
- **Spectrometers (gratings, FT-IR) (dispersion, light throughput, stray light, etc.)**
- **Detectors (diode array, CCD, slit disks with PMT's) (spectral sensitivity, noise, etc.**
- **Lights sources (lamps, diodes, laser, Sun, Moon, Stars)**

4.) **Problems**
- **Imaging (constant T, P's) illumination dependence and causes, sampling rate FWHM/pixel, etc. therapies**
- **detector noise, linearity**
- **spectrometer stray light**

5.) **Improvements**
- **non-linear spectral fitting**

- MCT - (Multi Channel Technique)
- Mode mixing
- etc.
-

6.) Applications
- zenith, off axis skylight
- direct Sun, Moon, Stars
- long path absorption
- photon path length
- satellite (GOME)

7.) Summary

8.) Literature

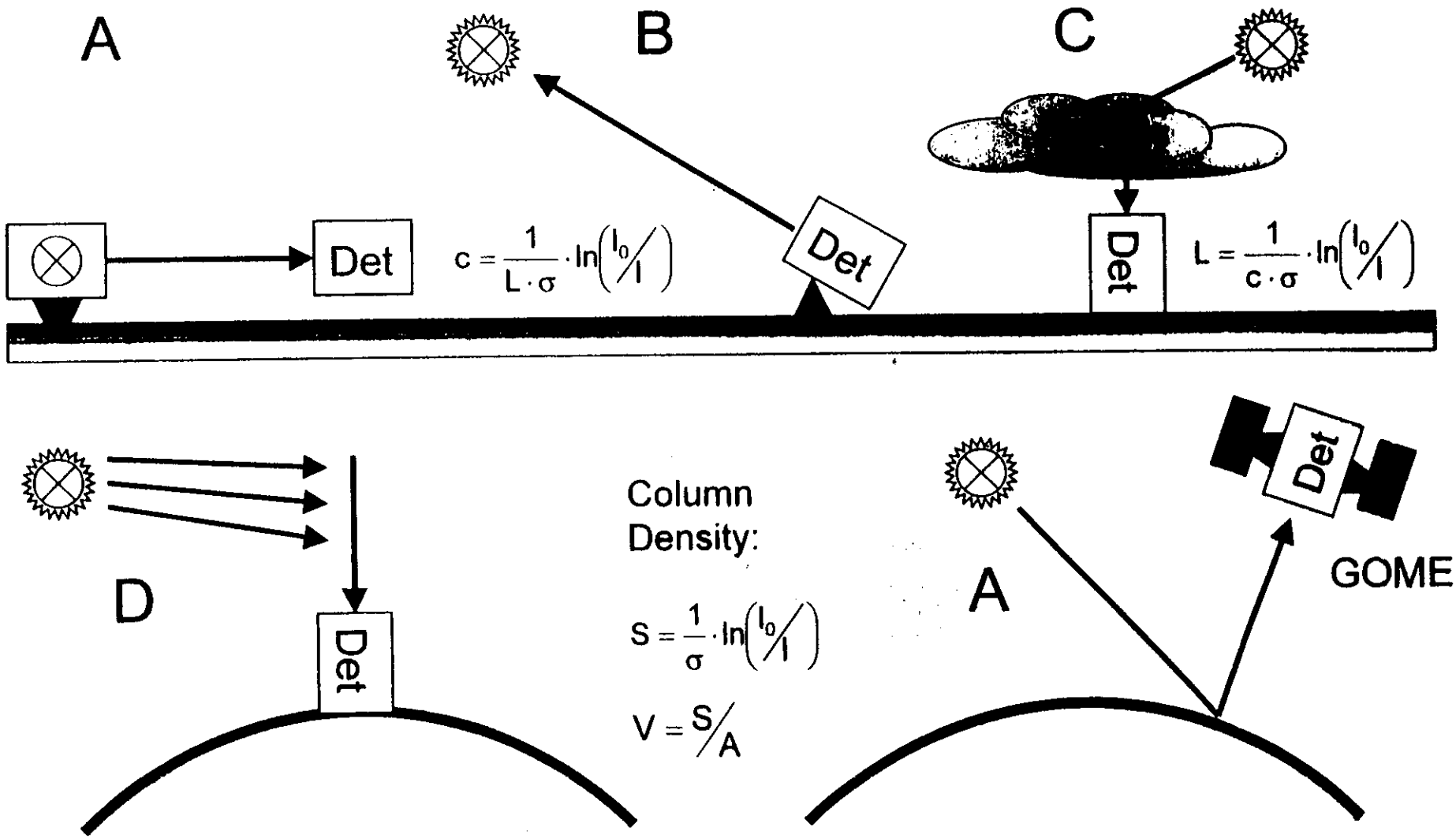
A
B
C
Det
Det
Det
$c = \frac{1}{L \cdot \sigma} \cdot \ln\left(I_0/I\right)$
$L = \frac{1}{c \cdot \sigma} \cdot \ln\left(I_0/I\right)$
D
Det
Column Density:
$S = \frac{1}{\sigma} \cdot \ln\left(I_0/I\right)$
$V = S/A$
A
Det
GOME

The DOAS Principle

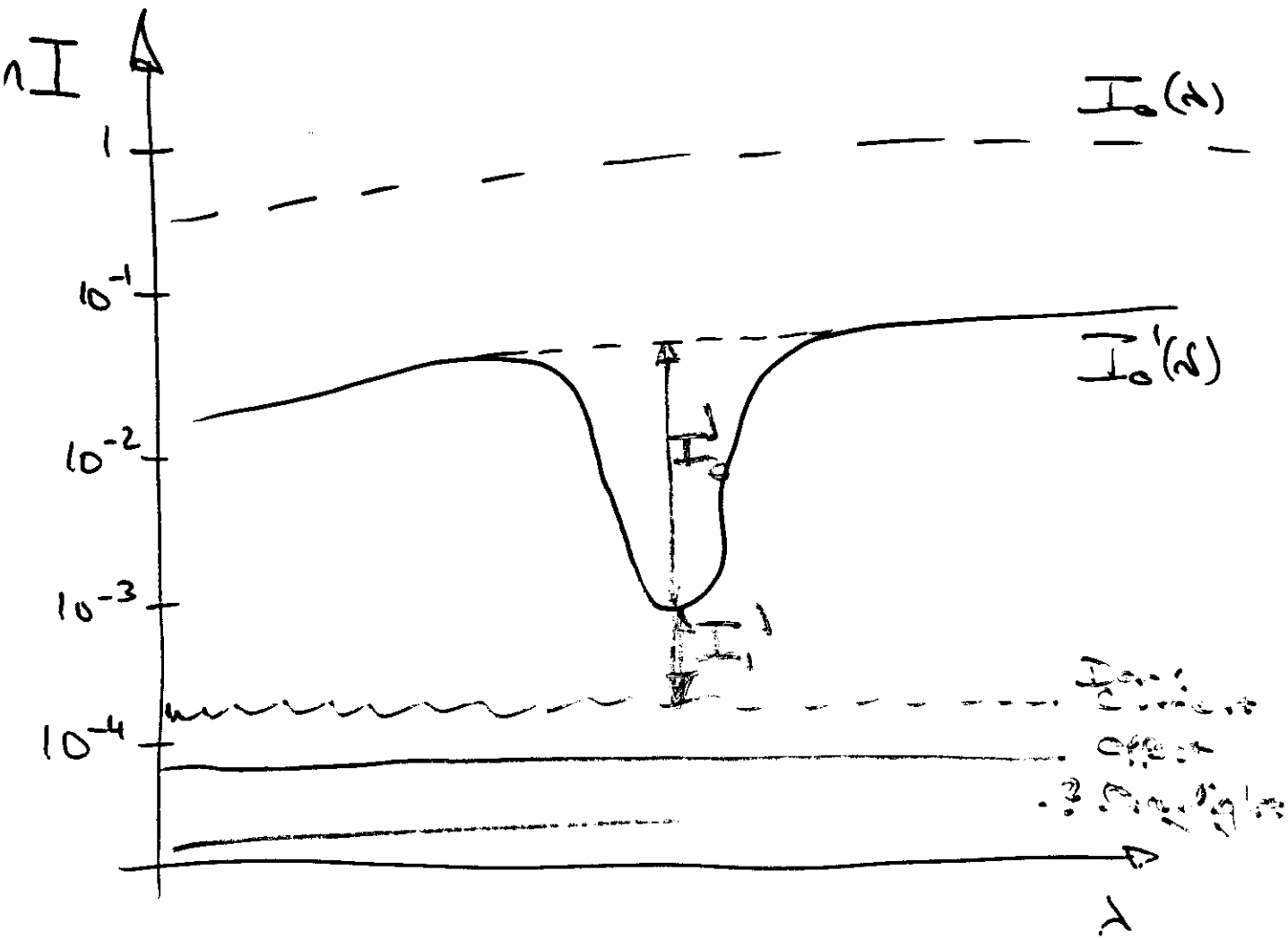

Lambert Beer's Law

$$I(\lambda) = I_0(\lambda) \exp(-\sigma(\lambda) \cdot n \cdot \ell)$$

$\sigma(\lambda)$: cross section

n : gas density (absorber)

ℓ : path length

$$I'_0(\lambda) = P(\lambda) \cdot I_0(\lambda)$$

$P(\lambda)$: broad band Extinction

$a\lambda^{-4}$ Rayleigh Scattering

$b\lambda^{-1}$ Mie Scattering

$c\lambda^{-k}$ broad band absorption

$$\sigma(\lambda) = \sigma'(\lambda) + \varepsilon(\lambda)$$

small — broad

Band Absorption

$$I'(\lambda) = \underbrace{I_0(\lambda) \cdot (a\lambda^{-4} + b\lambda^{-1} + \dots) \exp(-\varepsilon(\lambda) \cdot n \cdot \ell)}_{\text{broad band}} \cdot \underbrace{\exp(-\sigma'(\lambda) \cdot n \cdot \ell)}_{\text{small band}}$$

$$I'_1(\lambda) = I'_0(\lambda) \exp(-\sigma'(\lambda) \cdot n \cdot \ell)$$

Differential Optical Density:

$$D' = -\ln \frac{I'_1(\lambda)}{I'_0(\lambda)} = \sigma'(\lambda) \cdot \vec{n} \cdot \vec{\ell}$$

Errors in measured D's

Let δ be an unknown contribution to the measured I_0' and I_1' i.e. due to

(1) Noise in the dark current
(2) Electronic offset
(3) stray light
(4) etc.

$$D' = -\ln \frac{I_1'(d) + \delta}{I_0(d) + \delta}$$

$$\Delta D = \left(\frac{I_1'}{I_1' + \delta} - \frac{I_0'}{I_0' + \delta} \right) \cdot \delta$$

Error ΔD:

Problem: blackbars may overlap and cover range of $D = \underbrace{1 \ldots 10^{-4}}_{\text{dynamic range}}$

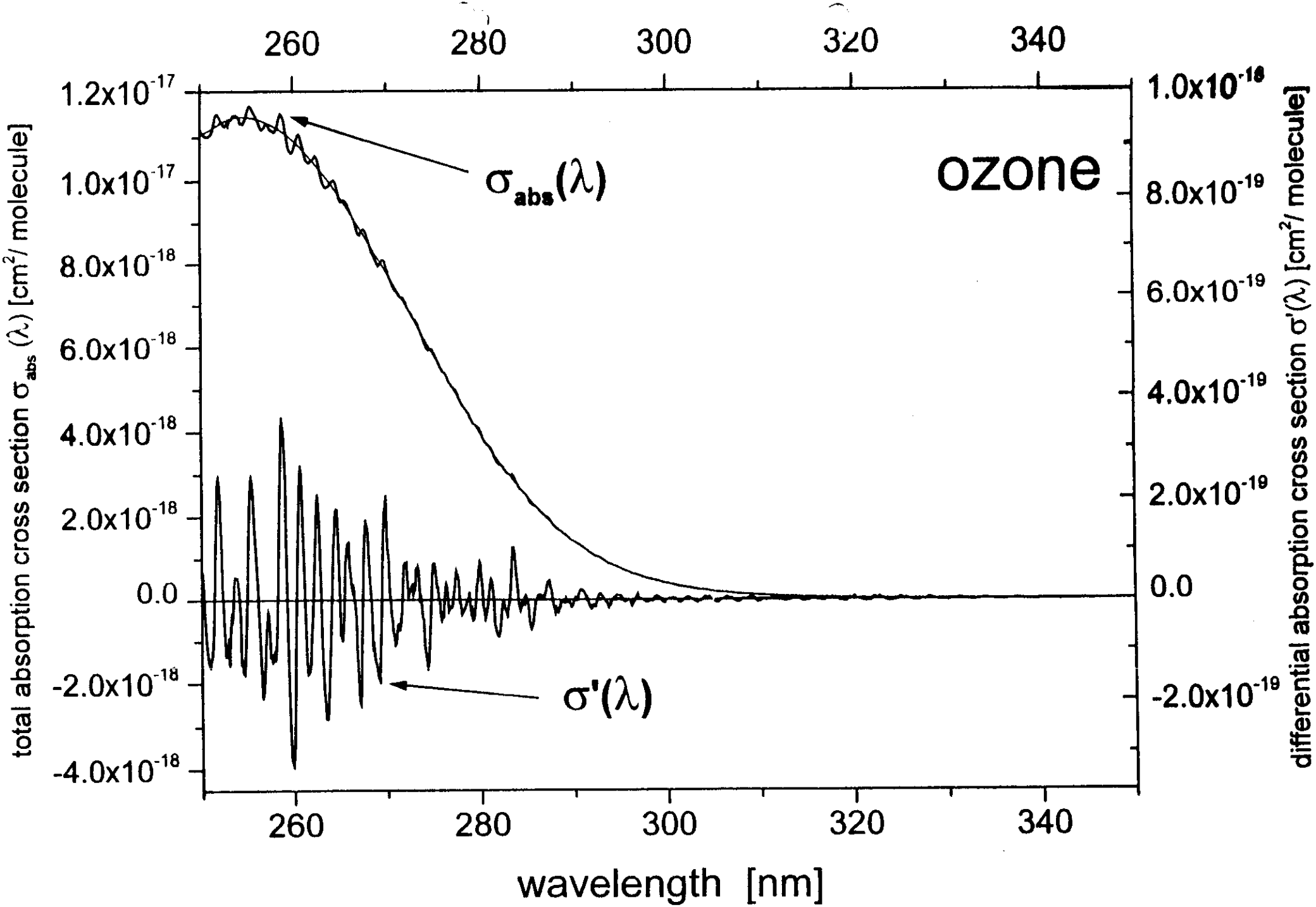
ozone
$\sigma_{abs}(\lambda)$
$\sigma'(\lambda)$
wavelength [nm]
total absorption cross section $\sigma_{abs}(\lambda)$ [cm^2/ molecule]
differential absorption cross section $\sigma'(\lambda)$ [cm^2/ molecule]
260
280
300
320
340
1.2x10^{-17}
1.0x10^{-17}
8.0x10^{-18}
6.0x10^{-18}
4.0x10^{-18}
2.0x10^{-18}
0.0
-2.0x10^{-18}
-4.0x10^{-18}
1.0x10^{-18}
8.0x10^{-19}
6.0x10^{-19}
4.0x10^{-19}
2.0x10^{-19}
0.0
-2.0x10^{-19}

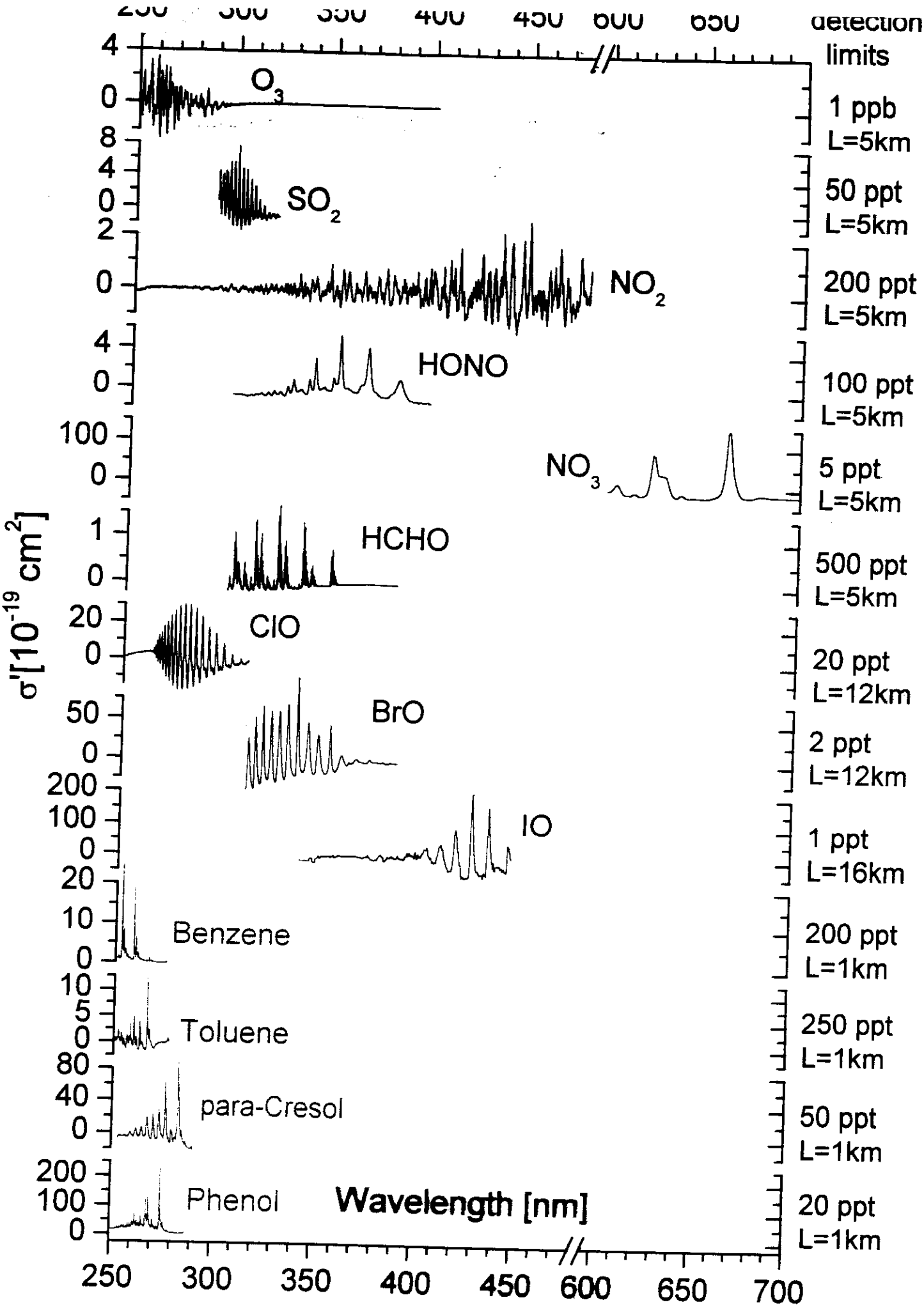
detection limits
O3
1 ppb L=5km
SO2
50 ppt L=5km
NO2
200 ppt L=5km
HONO
100 ppt L=5km
NO3
5 ppt L=5km
HCHO
500 ppt L=5km
ClO
20 ppt L=12km
BrO
2 ppt L=12km
IO
1 ppt L=16km
Benzene
200 ppt L=1km
Toluene
250 ppt L=1km
para-Cresol
50 ppt L=1km
Phenol
20 ppt L=1km
σ'[10-19 cm2]
Wavelength [nm]
250 300 350 400 450 600 650 700

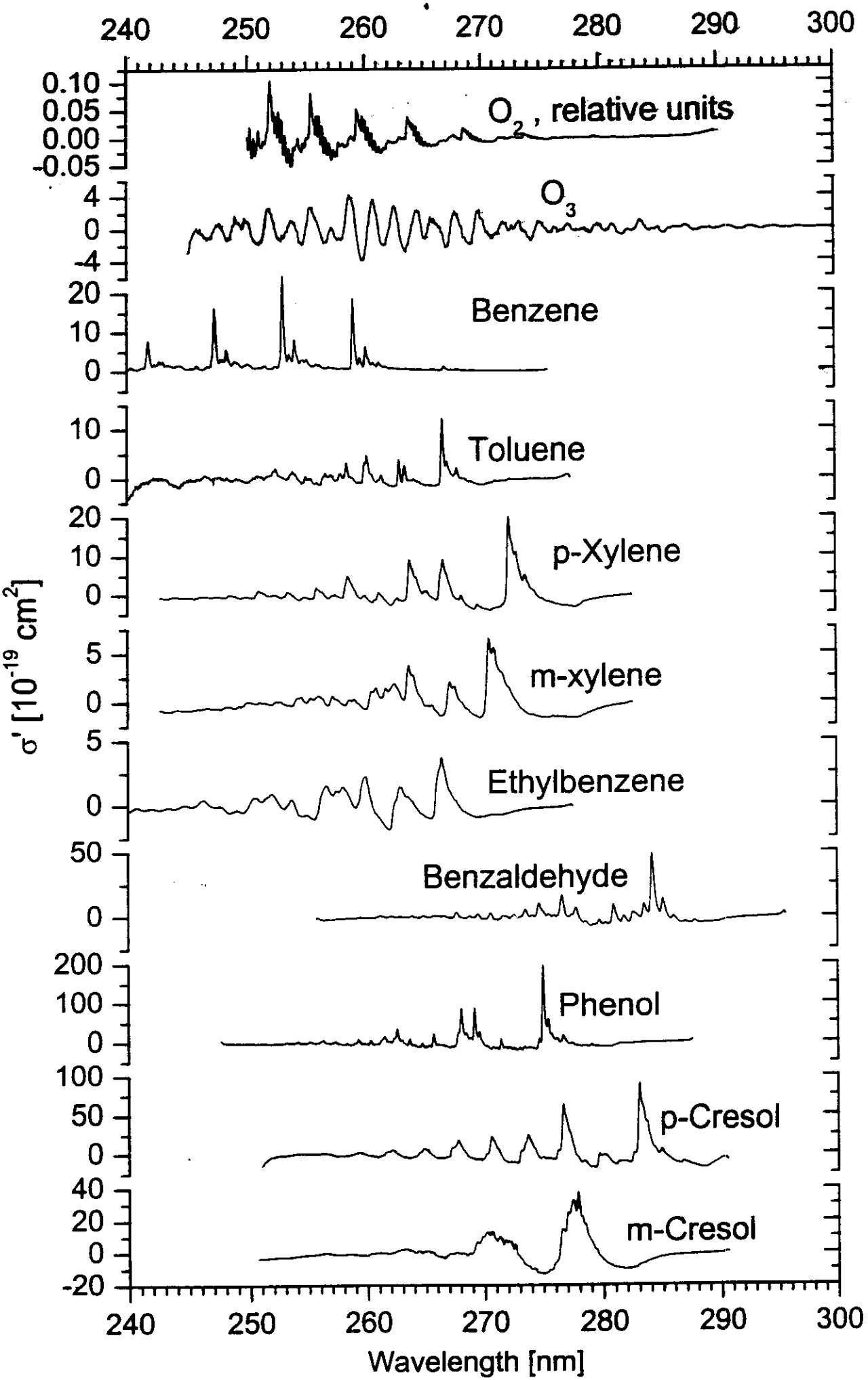
240
250
260
270
280
290
300
0.10
0.05
0.00
-0.05
O_2, relative units
4
0
-4
O_3
20
10
0
Benzene
10
0
Toluene
20
10
0
p-Xylene
5
0
m-xylene
5
0
Ethylbenzene
50
0
Benzaldehyde
200
100
0
Phenol
100
50
0
p-Cresol
40
20
0
-20
m-Cresol
σ' [10^{-19} cm^2]
Wavelength [nm]

Species measurable by UV/vis DOAS

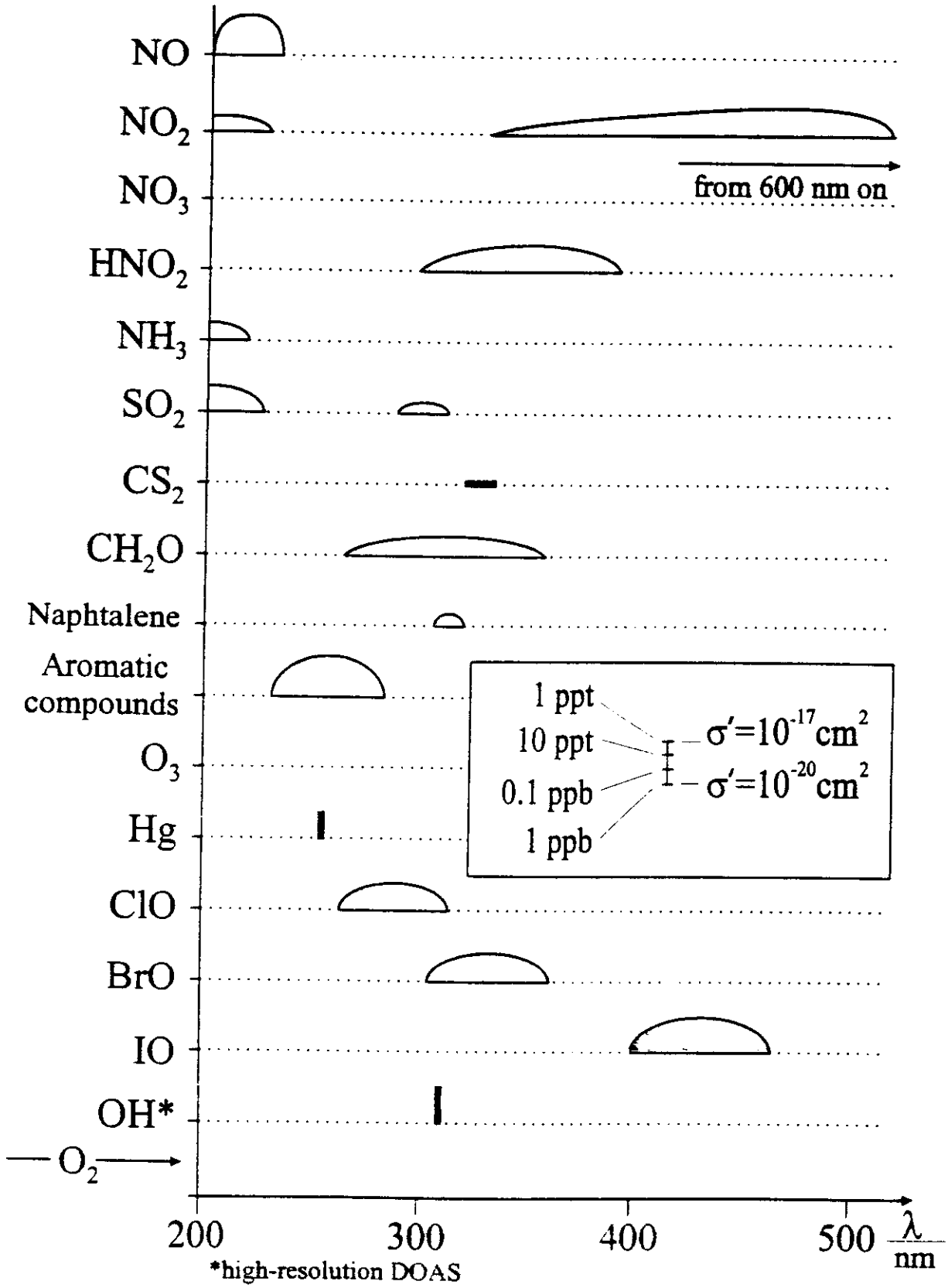

Table 1: Substances detectable by UV/visible absorption spectroscopy
Detection limits in ppt (1 ppt = 1 part in 10^{12})

Species	Wavelength interval nm	Differential Absorption Cross section 10^{-19} cm^2/Molec.	Detection Limit (5km Lightpath) ppt
SO_2	200-230	65	100[a]
	290-310	5.7	35
CS_2	320-340	0.4	500
NO	200-230	24	350[a]
NO_2	330-500	2.5	80
NO_3	600-670	200	1
NH_3	200-230	180	40[a]
HNO_2	330-380	5.1	40
O_3	300-330	0.045	4000
CH_2O	300-360	0.48	400
ClO	260-300	35	6
BrO	300-360	104	2
IO	400-470	170	1
Benzene	240-270?	21.9	400[a]
Toluene	250-280?	12.8	660[a]
Xylene (o/m/p)[b]	250-280?	2.1/6.6/20.3	4000/1300/420[a]
Phenol	260-290?	198	40[a]
Cresol (o/m/p)		20.1/31.8/87.2	420/270/100[a]
Benzaldehyde	280-290?	44	200[a]

a 500m Light path, 0.001 minimum detectable optical density

Principle steps in DOAS Spectrometry

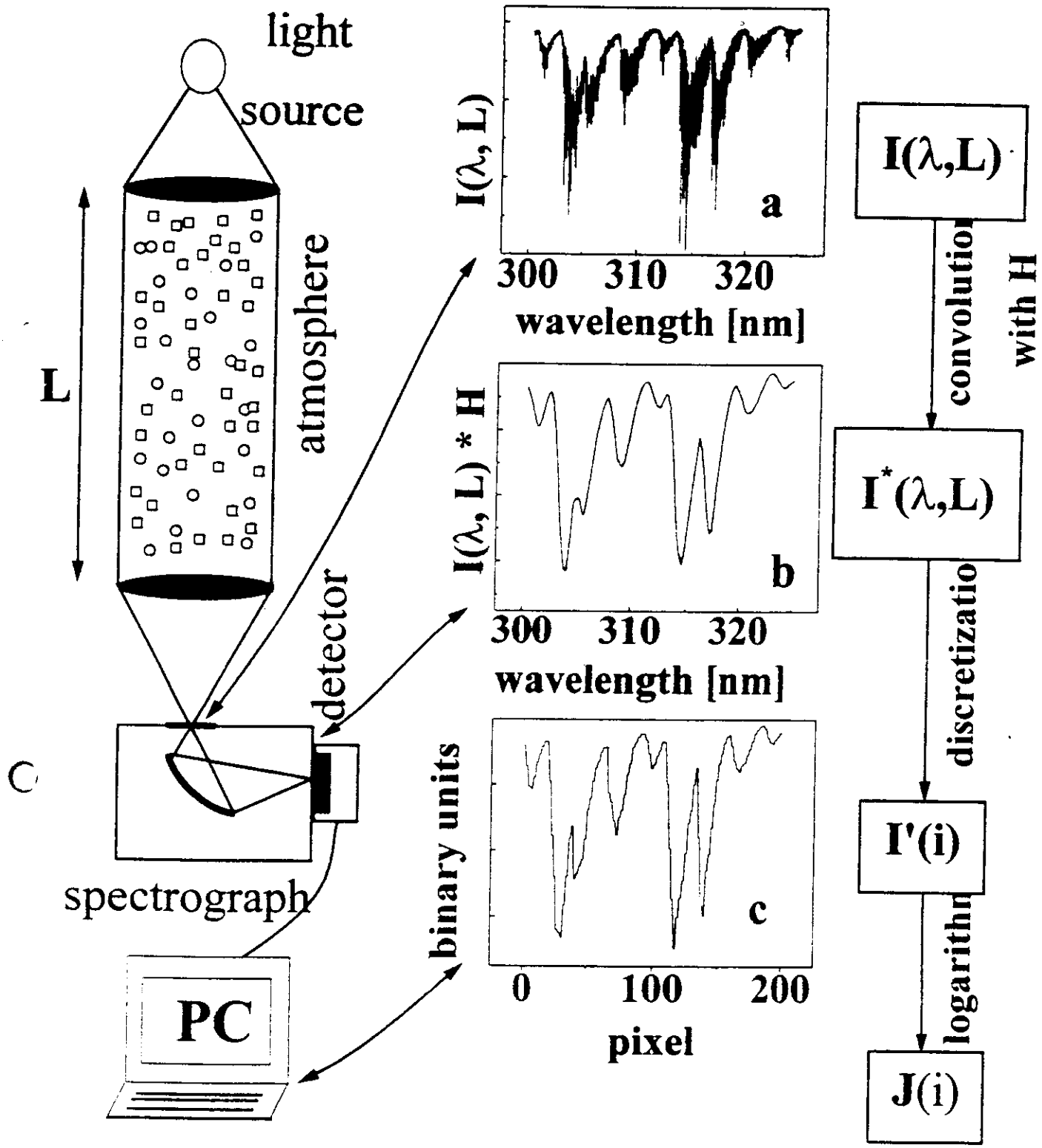

Principle steps in DOAS Spectrometry

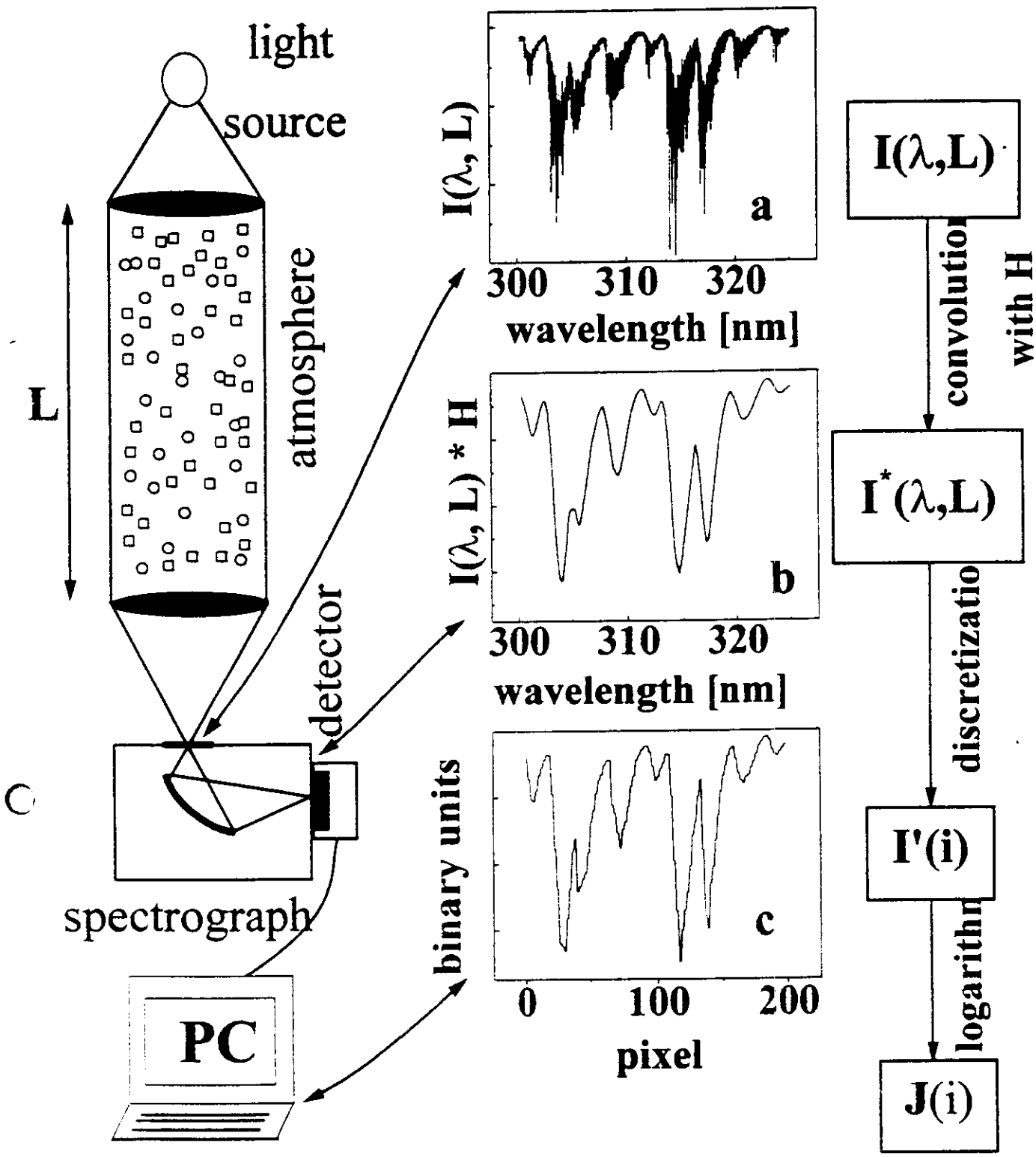

How to choose the best spectrometer for the desired application ?

Some Criteria:

1.) **What is the typical line width of the absorbers under consideration and what is the required spectral resolution ?**
- **vibrational lines (0.1 nm to several nm)**
- **rotational line (several 10^{-3} nm)**

Answer: A good choice allows for a sampling of at least 6 data points per full width at half maximum (FWHM) !

2.) **What is the light throughput ($TP = A/f^2$) of the required spectrometer ?**

(A pupil area and f the spectrometer's f-number)

Answer: The f-number usually increases with decreasing FWHM, hence the TP decreases. Increasing A , i.e. the area of the slit, causes a increases the FWHM. Hence a cost effective compromise allows for sufficient large A's and small f numbers !

3.) **How is the stability of the spectrometer with respect to changing ambient conditions (changes in T, and P) (is that important at all) ?**

(an issue addressed in detailed later !)

4.) **How large is the spectrometer stray light ?**

(an issue addressed in detailed later !)

Possible solutions:

- FT spectrometer allow for a very high resolution, are very stable respect to the wavelength registration, but tend to use only a small fraction of the light (only the interfering photons) and are not very stable when not operated at constant T and P.

- Grating spectrometers are easy to be operated at constant T and P.

- Both spectrometers do have problems with stray light but FT-spectrometers usually do not process strayed photons.

- FT spectrometer's are much more expensive than grating spectrometer's.

Answer: By far, most DOAS measurements are performed with grating spectrometers !

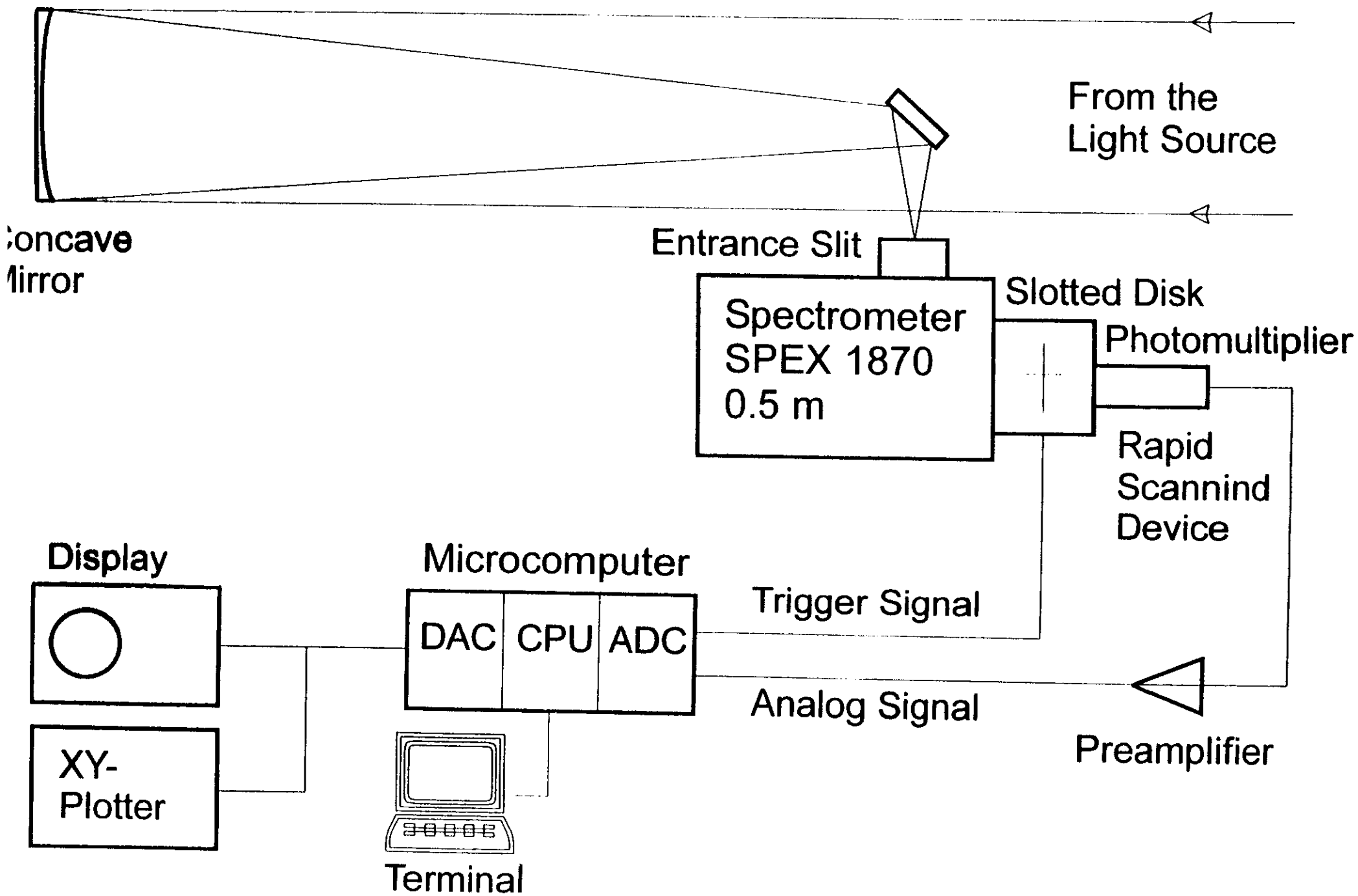
From the
Light Source
Concave
Mirror
Entrance Slit
Spectrometer
SPEX 1870
0.5 m
Slotted Disk
Photomultiplier
Rapid
Scannind
Device
Display
Microcomputer
DAC
CPU
ADC
Trigger Signal
Analog Signal
Preamplifier
XY-
Plotter
Terminal

I. INTRODUCTION

The Digikrom 240 is a classical *Czerny-Turner* monochromator in its optical configuration, with a 240mm focal length.

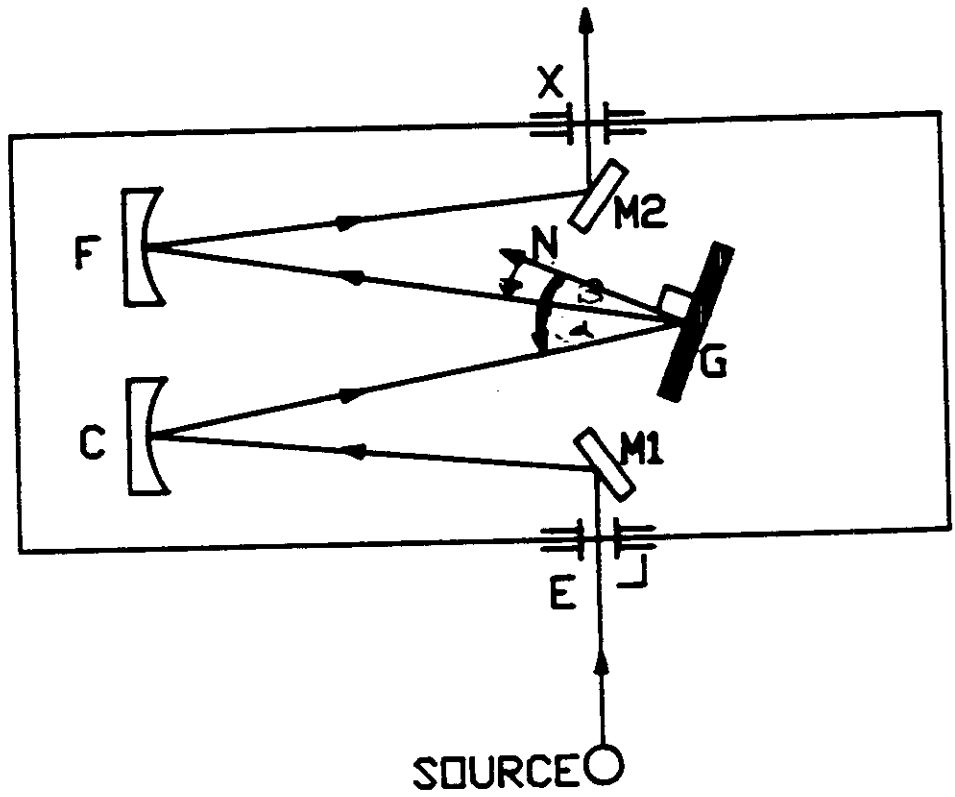

Figure 1. Optical Diagram of Digikrom 240

As indicated in Fig. 1, light from a source is focused on the entrance slit, E, and directed by the turning mirror, M1, to the collimating mirror, C. The focused beam is collimated and directed to the grating, G, which diffracts and reflects the radiation. A particular wavelength of the light, determined by rotation of the grating, is directed to the focusing mirror, F, which focuses it onto the exit slit, X, via the second turning mirror, M2.

Optical baffles are utilized to minimize stray light due to scattering from slit edges and dust or imperfections in the optical elements.

Gratings

- Positive interferences:

$$\sin\alpha + \sin\beta = \frac{k \cdot \lambda}{a} = k \cdot n \cdot \lambda$$

λ: wavelength

k: order $0 \pm 1 \pm 2 \ldots$

n: number of grooves per unit length

- Resolution:

$$\frac{\lambda}{d\lambda} = k \cdot N$$

- Dispersion:

$$\frac{dB}{d\lambda} = \frac{1}{\lambda} \cdot \frac{\sin\alpha + \sin\beta}{\cos\beta}$$

or

$$\frac{d\lambda}{dx} = \frac{\cos\beta}{k \cdot n \cdot F}$$

F: Focal length

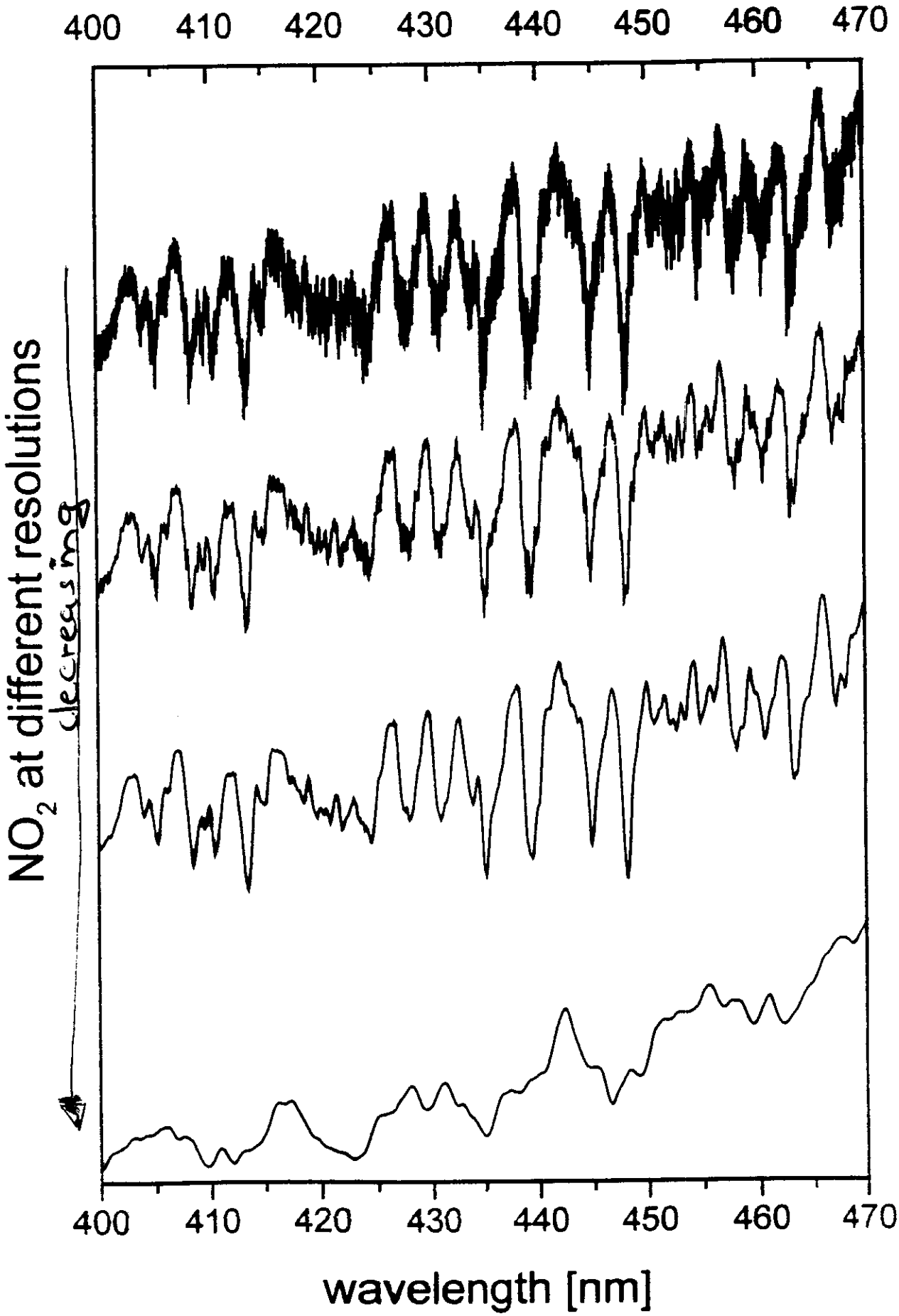
400
410
420
430
440
450
460
470
NO_2 at different resolutions
decreasing
wavelength [nm]

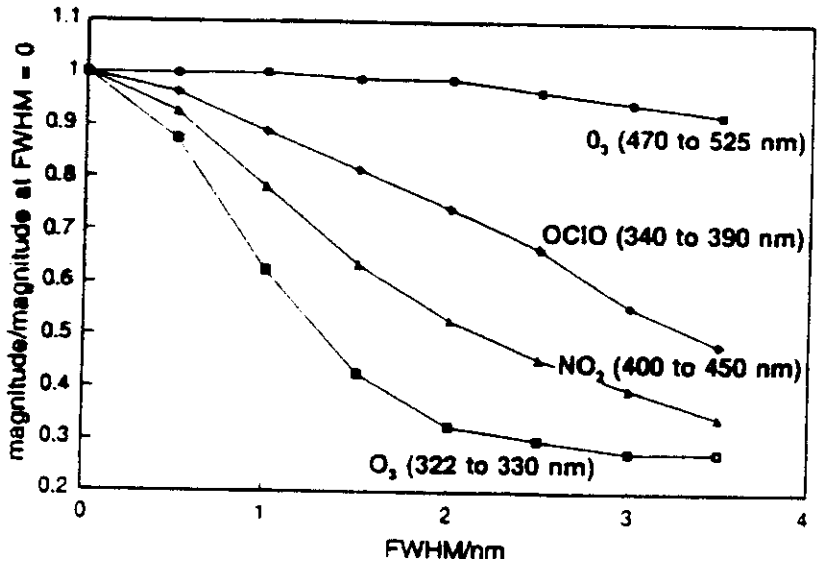

Fig. 10. Ratio of the average magnitude of differential cross sections of O_3, NO_2, and OClO, after smoothing with Gaussian functions, to those at high resolution. This magnitude is proportional to the amount of signal available for spectral analysis. Except for UV measurements of O_3, smoothing must reach 1 nm FWHM before the magnitude is reduced by 1/4.

Roscoe et al (1996)
Appl. Optics 35, 427

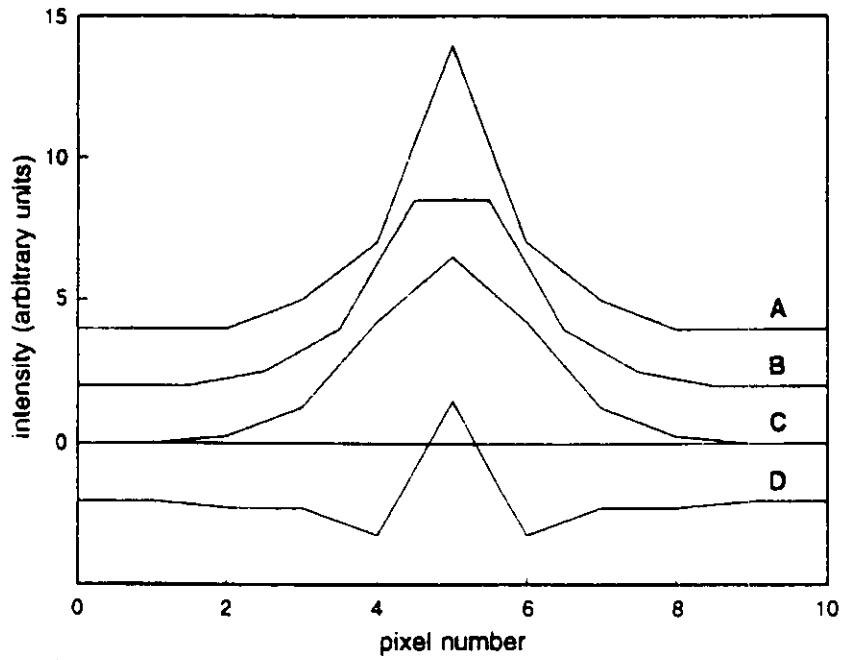

Fig. 1. Illustration of how the initial spectrum of a single Gaussian line (curve A) is degraded through two successive linear interpolations (curves B and C) to a much broader spectrum. The difference between curves A and C (i.e., the residual after interpolation) is plotted as curve D. In each case, the values at each pixel are joined by straight lines to illustrate linear interpolation. The curves are vertically displaced by 2 units for clarity.

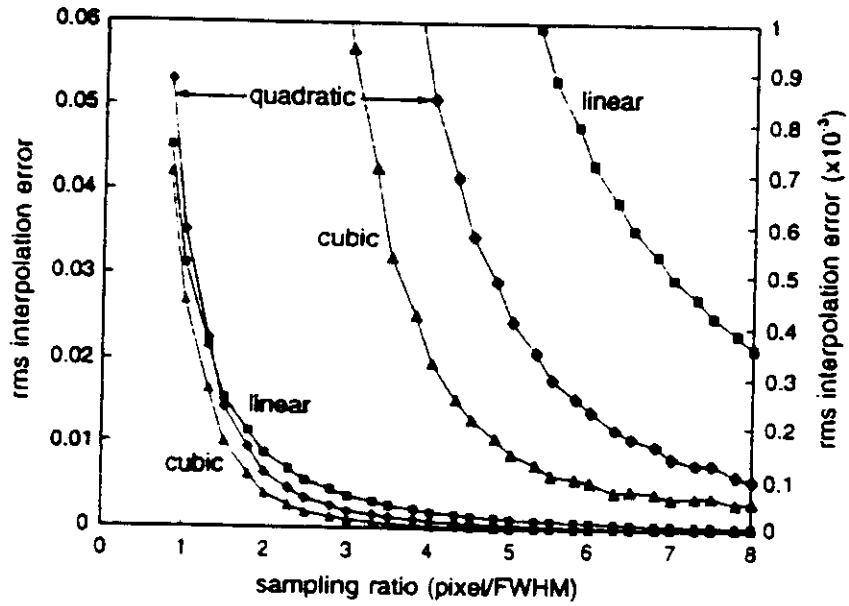

Fig. 3. Root-mean-square interpolation error for linear, quadratic, and cubic interpolation schemes as the number of pixels in each FWHM, commonly called the sampling ratio, increases. The errors shown are for a shift of 0.5 pixels, hence they are the maximum errors. A Gaussian slit function was used. The curves are expanded on the right-hand y axis. Note that the scale for errors is arbitrary relative to those of a real spectrum.

Ruscoe et al (1996)
App. Optics 35; 427

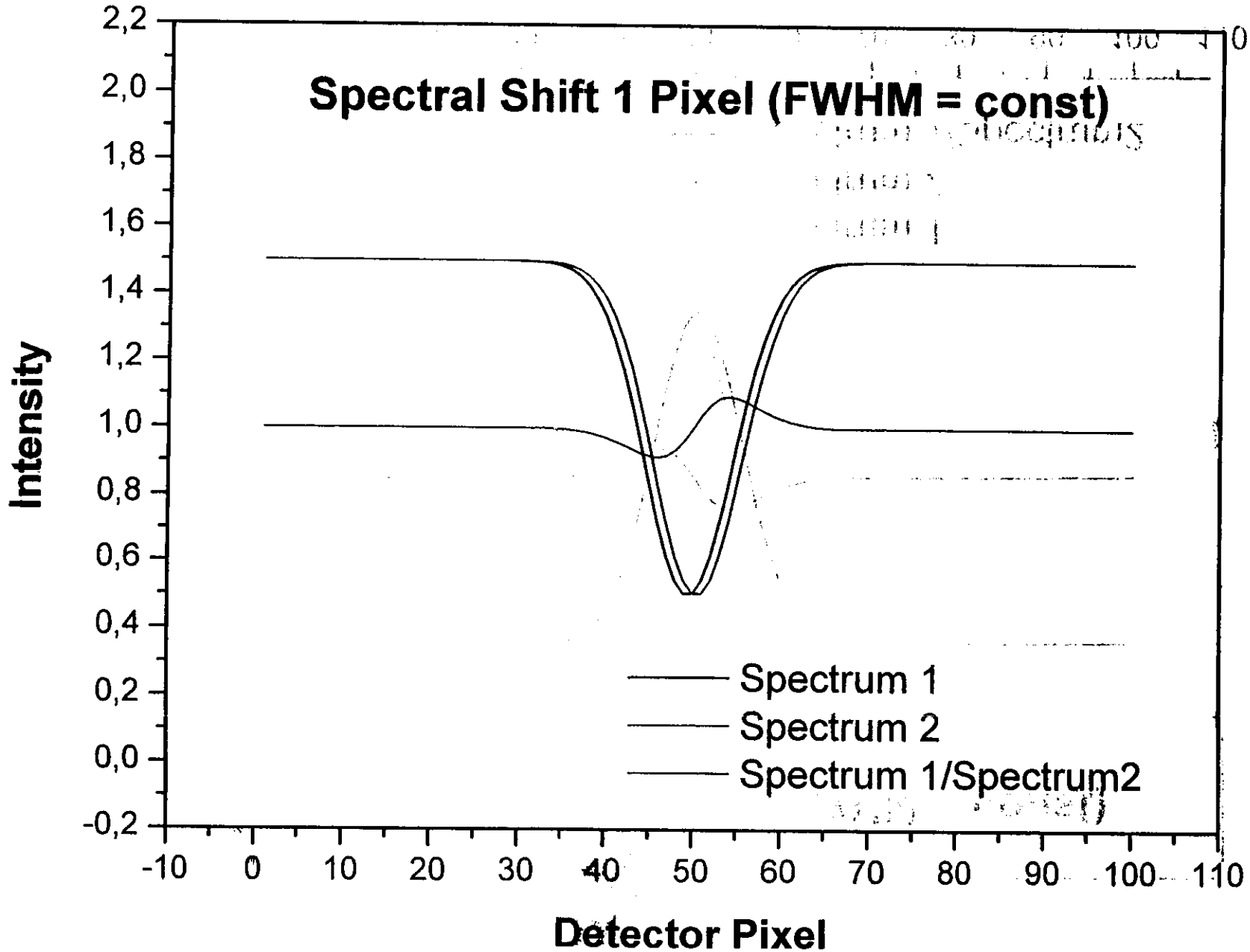
Spectral Shift 1 Pixel (FWHM = const)
Intensity
Detector Pixel
2,2
2,0
1,8
1,6
1,4
1,2
1,0
0,8
0,6
0,4
0,2
0,0
-0,2
-10
0
10
20
30
40
50
60
70
80
90
100
110
Spectrum 1
Spectrum 2
Spectrum 1/Spectrum2

Imaging

The spectrometer imaging may change with changing atmospheric/lab pressure (P) and (T). This is because $\Delta n/n = 2.7*10^{-4}$ (n refraction index) for a $\Delta p = 1$ atm, and likewise ΔT's cause thermal expansions of the optical setup.
Changing T's and P' causes imaging two effects:

(a) **Resolution (FWHM) changes due to a change (ΔL) in the focal length:**

$(n - 1)*L = \Delta L$, i.e., for $L = 30$ cm and $\Delta p = 1$ atm

$$\Delta L = 80\ \mu m$$

$\Delta FWHM = \Delta L$/f-number, i.e., by assuming f/3

$$\Delta FWHM = 24.2\ \mu m$$

(b) **Spectral Shift:**

$\Delta\lambda/\lambda = \Delta n/n = 2.7*10^{-4}$ or $\Delta x = 0.16$ nm at $\lambda = 430$ nm.

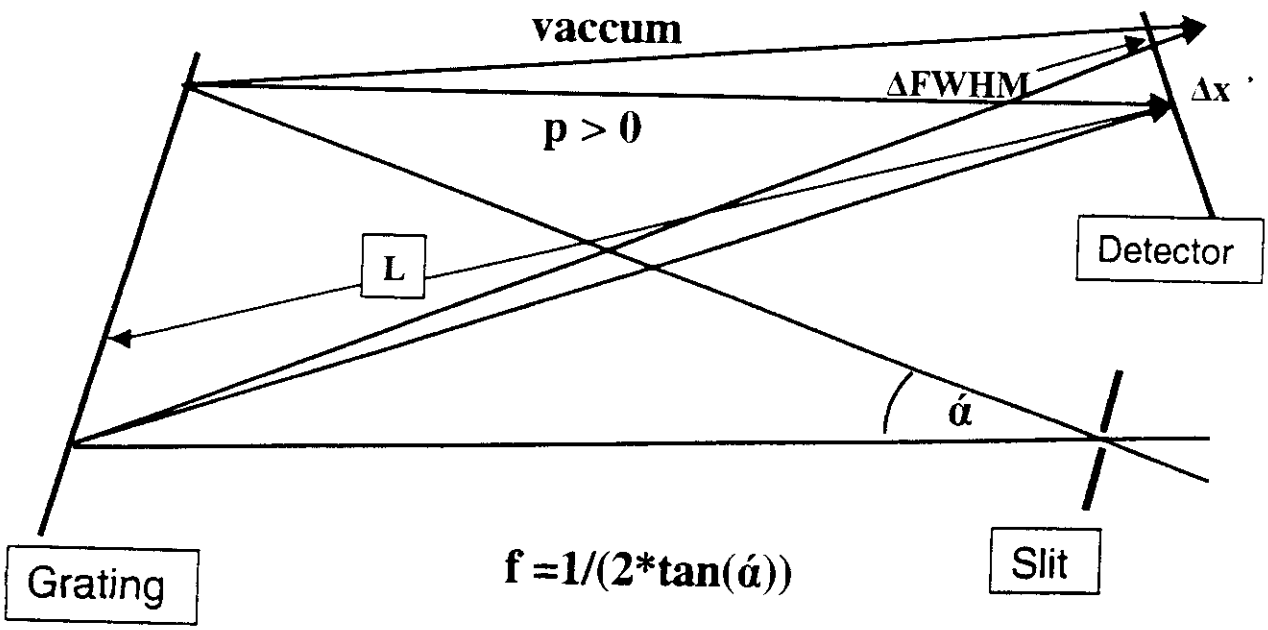

$$f = 1/(2*\tan(\alpha))$$

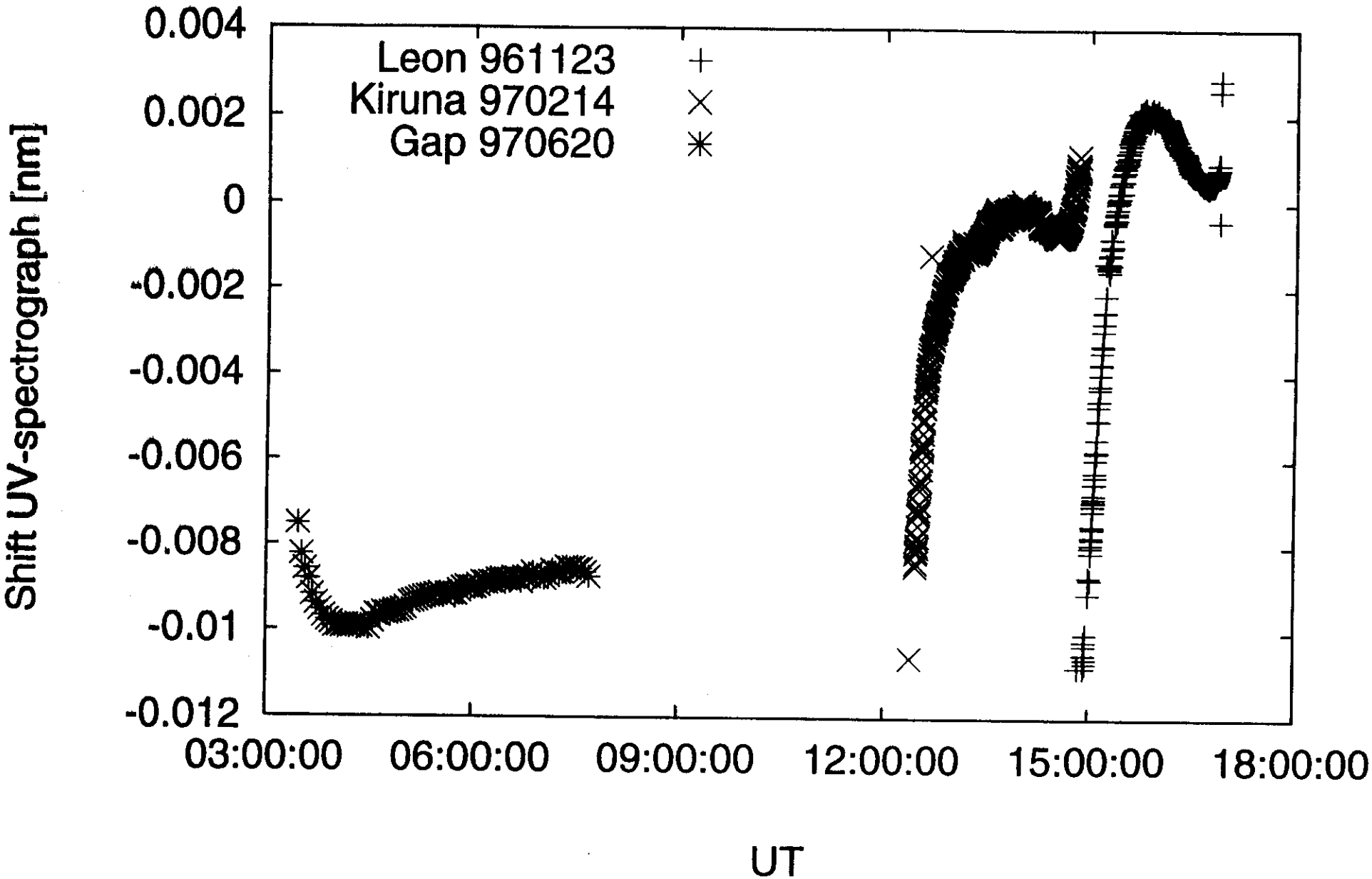
Leon 961123
Kiruna 970214
Gap 970620
Shift UV-spectrograph [nm]
0.004
0.002
0
-0.002
-0.004
-0.006
-0.008
-0.01
-0.012
03:00:00
06:00:00
09:00:00
12:00:00
15:00:00
18:00:00
UT

Fig. 3a

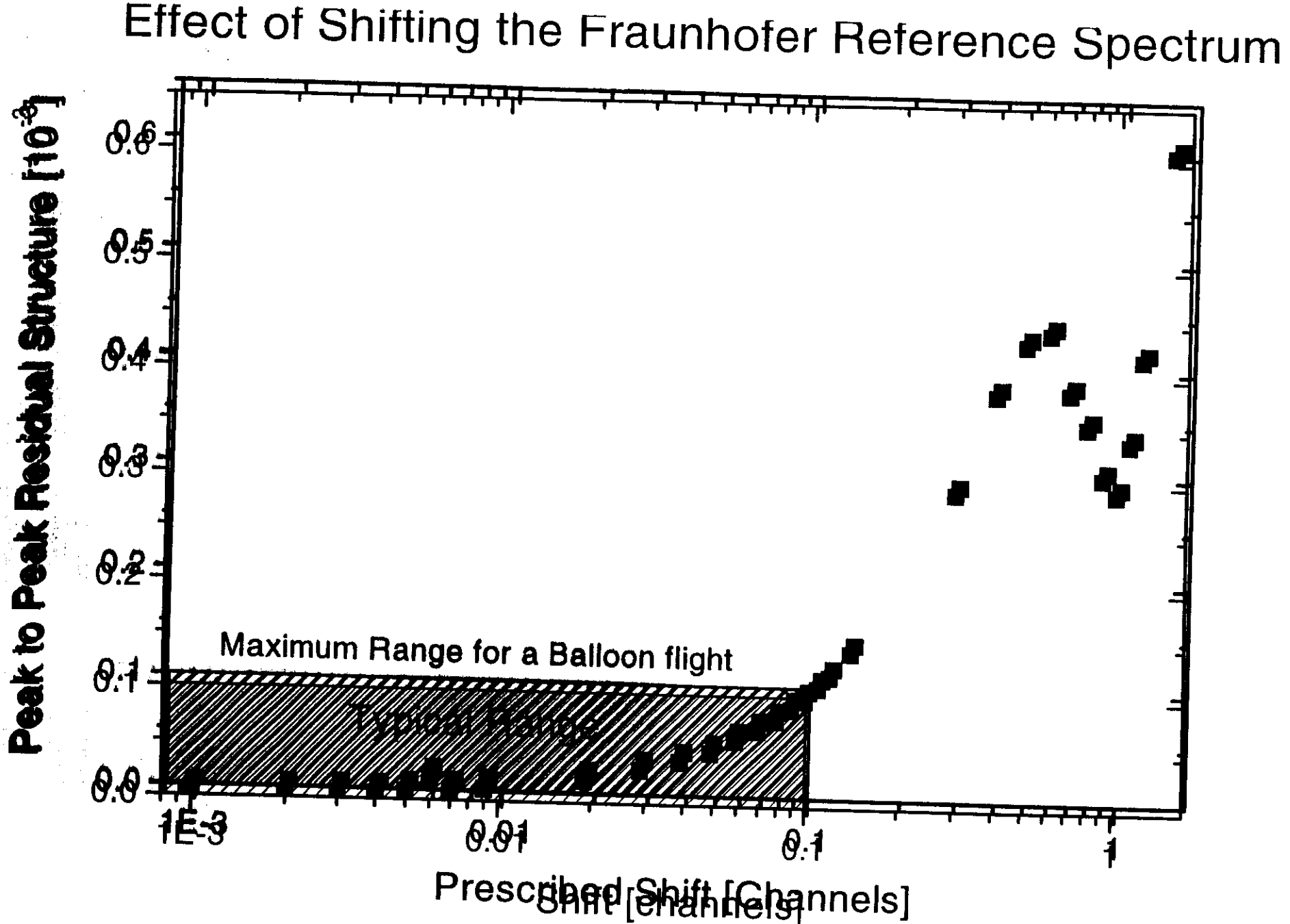
Effect of Shifting the Fraunhofer Reference Spectrum
Peak to Peak Residual Structure [10^-3]
0.6
0.5
0.4
0.3
0.2
0.1
0.0
Maximum Range for a Balloon flight
Typical Range
1E-3
0.01
0.1
1
Prescribed Shift [Channels]
Shift [channels]

Fig. 3d

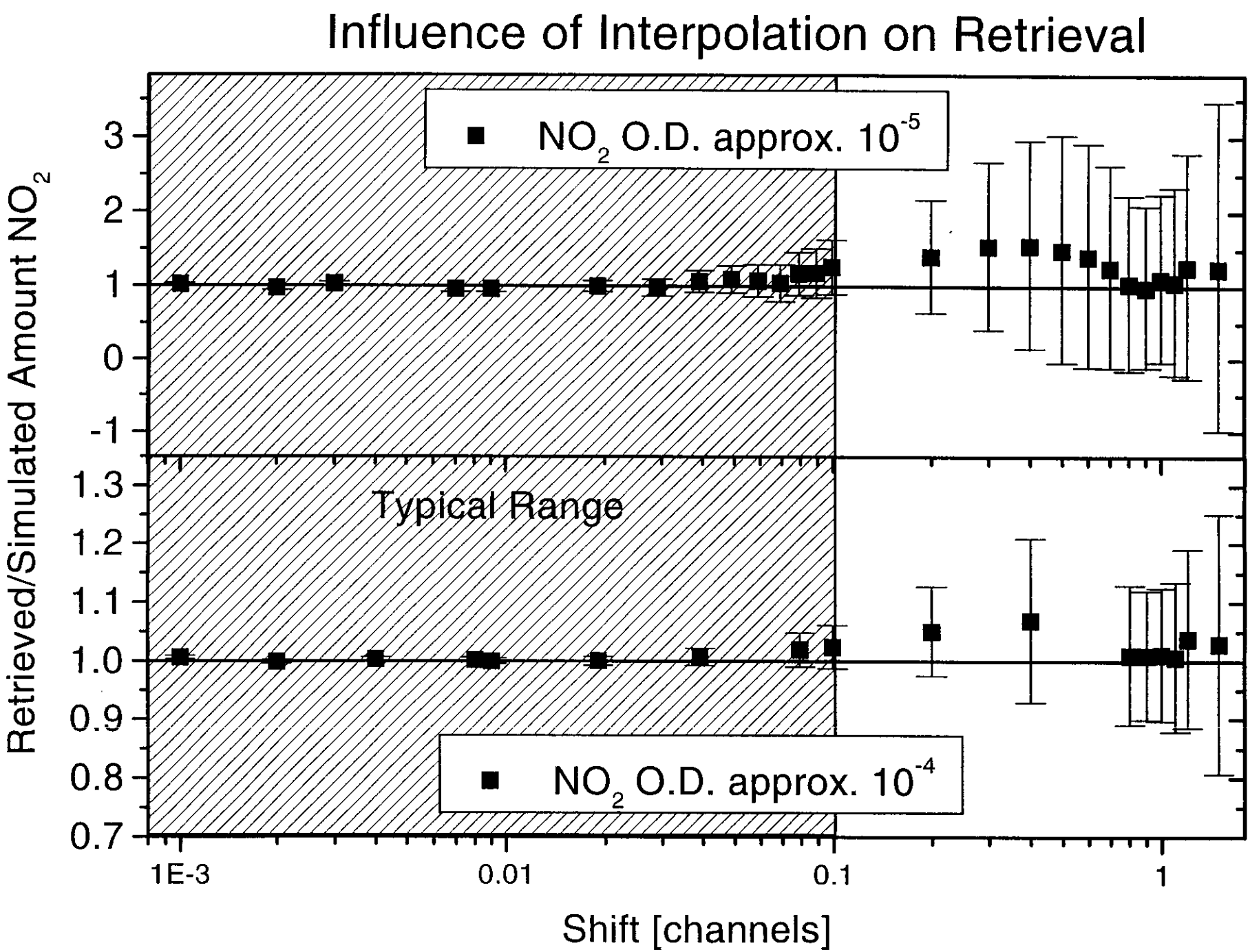
Influence of Interpolation on Retrieval
NO2 O.D. approx. 10-5
Typical Range
NO2 O.D. approx. 10-4
Retrieved/Simulated Amount NO2
Shift [channels]
3
2
1
0
-1
1.3
1.2
1.1
1.0
0.9
0.8
0.7
1E-3
0.01
0.1
1

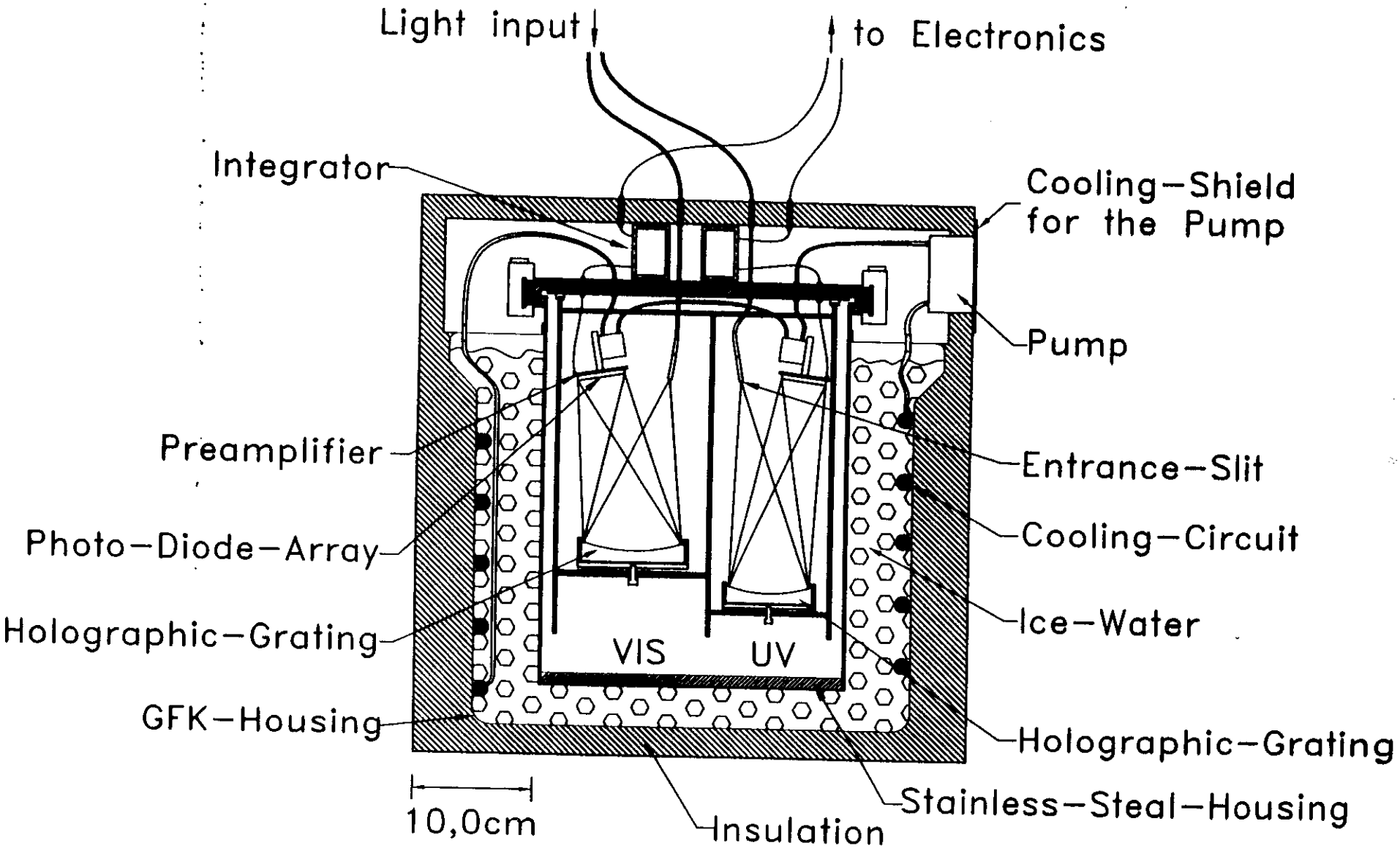

Fellemann et al,
Appl Optics (in press)

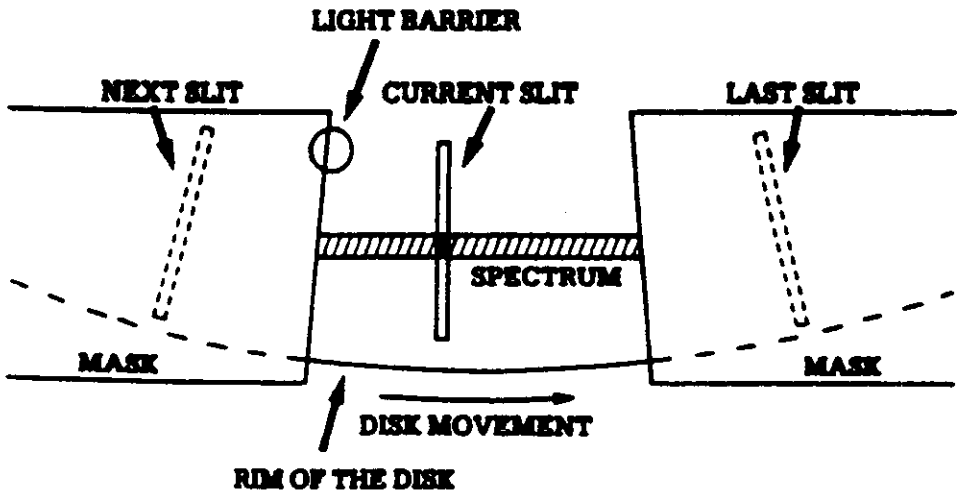

Figure 2.11. Optomechanical rapid scanning device. At any given moment one of the radial slits etched into a thin metal disk ("slotted disk") rotating in the focal plane of the spectrometer acts as an exit slit sweeping over the spectrum. A photomultiplier receives the portion of the spectrum falling through that slit.

ANDOR TECHNOLOGY

Specifications

Front Ill. / Back Ill. Evacuated CCD (EEV 42-10)

Pixels	2048 x 512, 13.5 μm²
	Typical
Pixel Well depth	150,000 e⁻
Readout Register Well Depth	600,000 e⁻
Node Well Depth (Low Noise) #1	300,000 e⁻
Node Well Depth (High Signal) #1	900,000 e⁻

CCD Readout Noise #2	2 electrons @ 20 kHz	6 electrons @ 1MHz

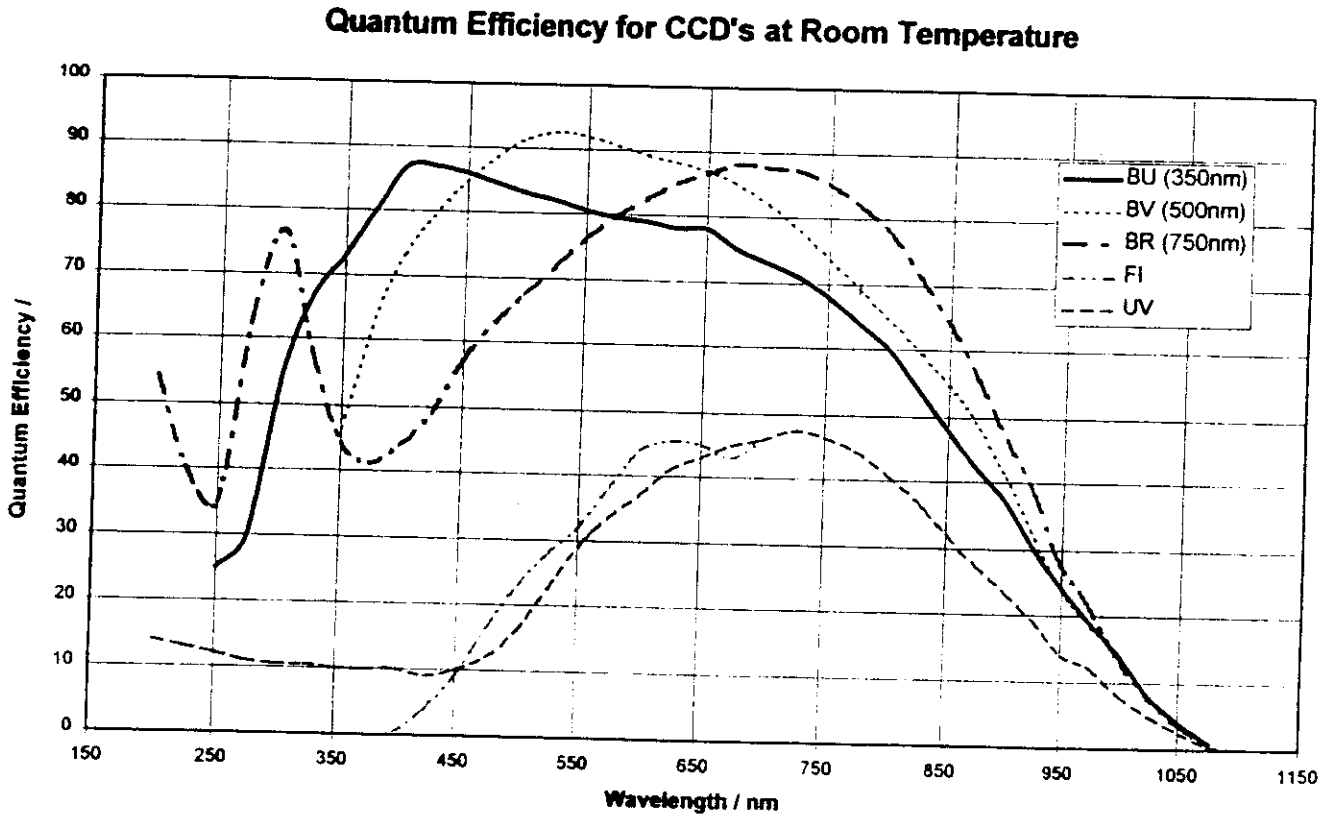

	Minimum	***Typical***	***Maximum***
Peak Quantum Efficiency #3 FI [BI]	40% [78%]	47% [85%]	
Linearity #4			1%

Dark Current Specification

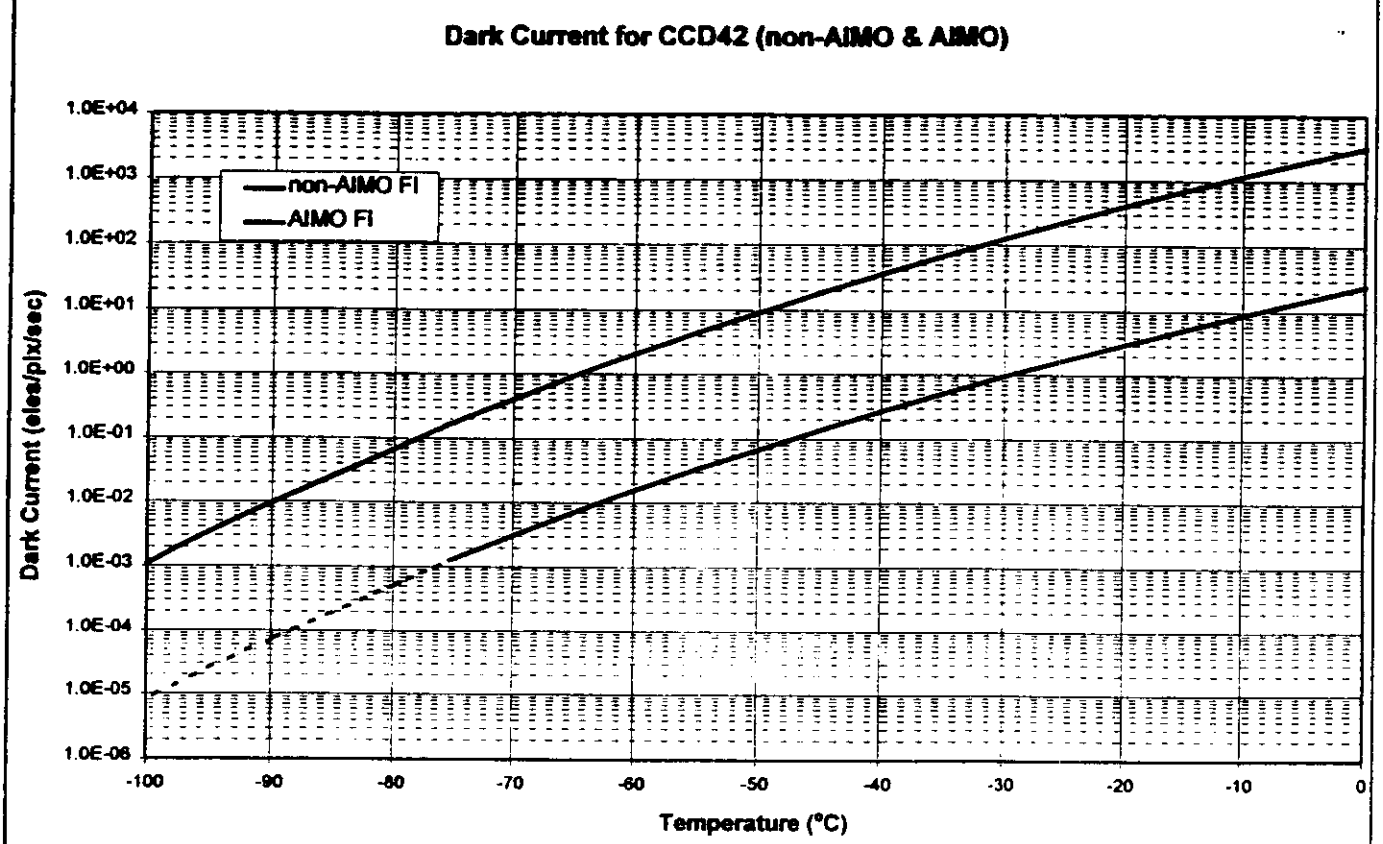

[Back Illuminated CCDs have dark currents approximately 4 times the level of Front Illuminated CCDs]

Blemish Specification #6	Spectroscopic Mode #7		Image Mode #8	
	Front Illuminated	*Back Illuminated*	*Front Illuminated*	*Back Illuminated*
Dark Current	0 columns	1 columns #9	30 spots #10	30 spots
Response	2 columns over 10 % contrast	2 columns #11 over 10 % contrast	80 spots #12 >25% contrast	80 spots >25% contrast
	2 traps over 200 electrons	2 traps #13 over 200 electrons		
	Minimum separation between column defects is 50 pixels			

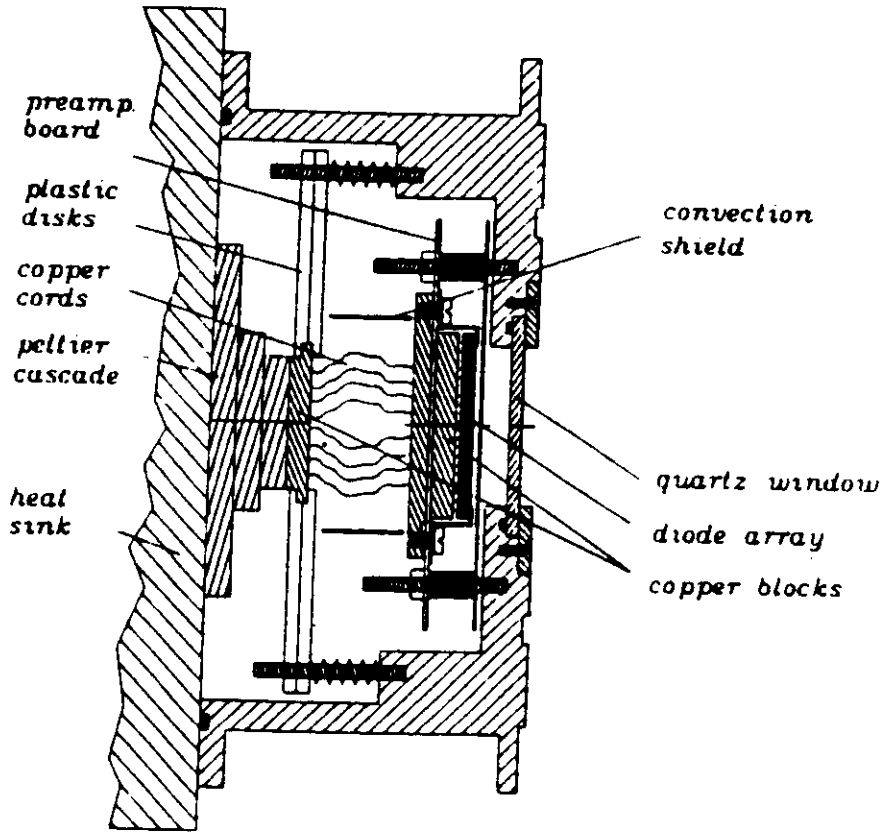

Figure 2.12. Cross section of a solid state photodetector (photodiode array). An air-cooled three-state Peltier device allows cooling to about -40 °C. Adapted from Stutz and Platt (1992).

Detector Noise:

a.) Photon Shot Noise N_{ph} (Poisson statistics)

$$N_{ph} = \sqrt{S} = \sqrt{C_{diode} * U * \acute{\alpha} / e^-} = 10^4\ e^-$$

With signal ($S * \acute{\alpha} = 10^8$ photons), diode or full well capacity ($C_{diode} = 10$ pF), voltage (U = 2.06 V), e^- electron charge, saturation ($\acute{\alpha} = 0.8$)

b.) Dark Current Noise N_{dark} (manufacturing dependent, for Hamamatsu S5931)

$$N_{dark} = \sqrt{S_{dark}} = 8296\ e^-/sec$$

c.) Preamplier Noise (N_{pre})

$$N_{pre} = 1/e^- \sqrt{(i_n * t_n)^2 + (u_n * C_t)^2} = 249\ e^-$$

For current and voltage noises ($i_n = 3.5 * 10^{-13}$ A - for OPA 627 - and $u_n = 1 * 10^{-6}$ V and for a read out time (t_n) (or bandwidth) of 20 µsec

d.) Read-out Noise (N_{read})

$$N_{read} = 1/e^- \sqrt{k * T * (2 * C_{diode} + C_{vc})} = 4124\ e^-$$

with cross talk capacity (C_{ve} = 20 pF), k Boltzmann Constant and T temperature

e.) ADC Noise (N_{ADC})

$$N_{ADC} = 2694\ e^-$$

Total Noise (N_{read})

$$\underline{N_{total} = 10983\ e^-\ \text{or}\ 5.3\ \text{binary Units}}$$

(for a 16 bit AD converter with the given numbers above)

Questions:

(1) What is the determining noise contribution.
(2) How can you measure it ?
(3) How can you reduce ?

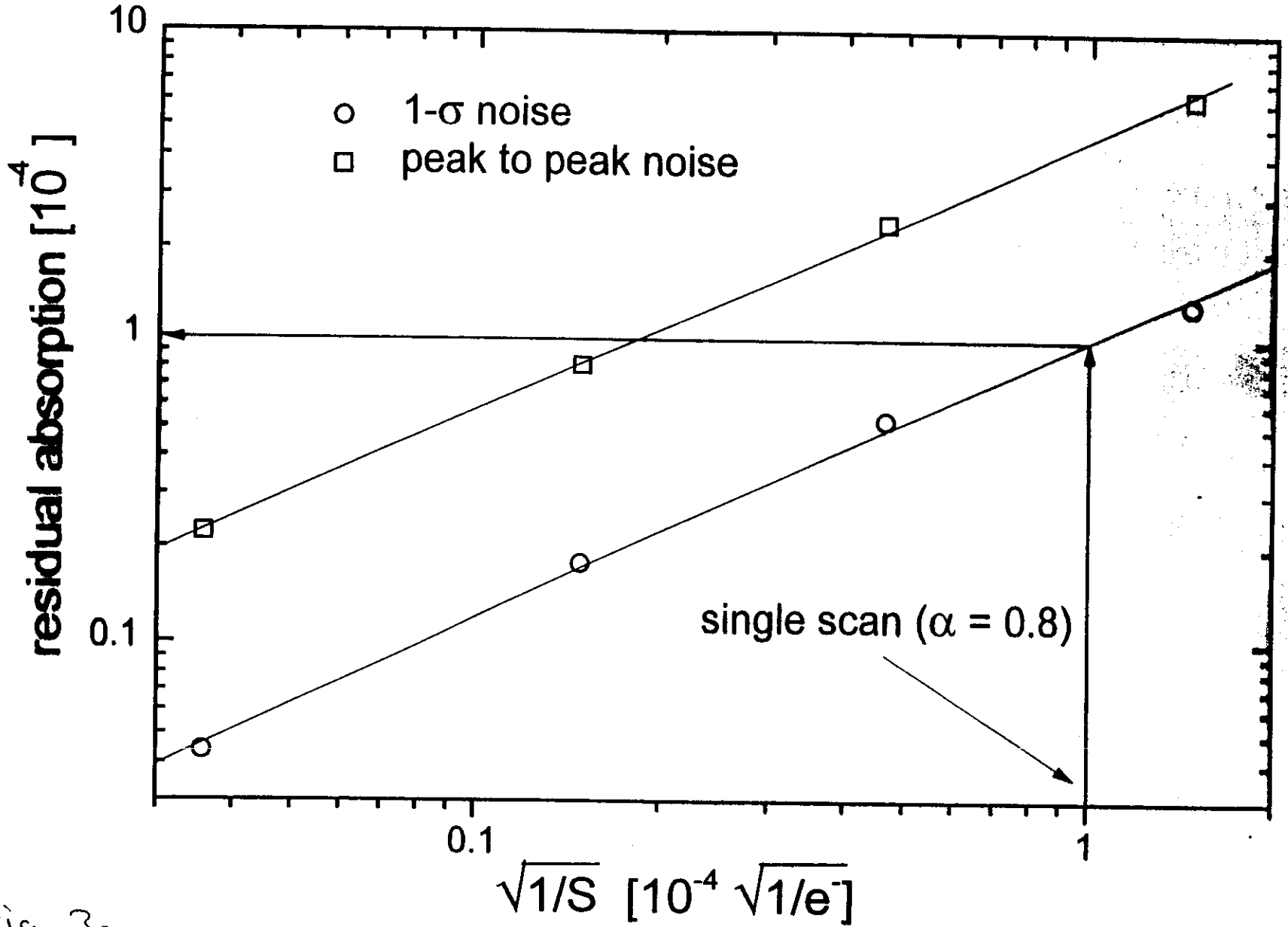
10
1
0.1
residual absorption [10^{-4}]
1-σ noise
peak to peak noise
single scan (α = 0.8)
0.1
1
$\sqrt{1/S}$ [10^{-4} $\sqrt{1/e^-}$]

Fig. 3a

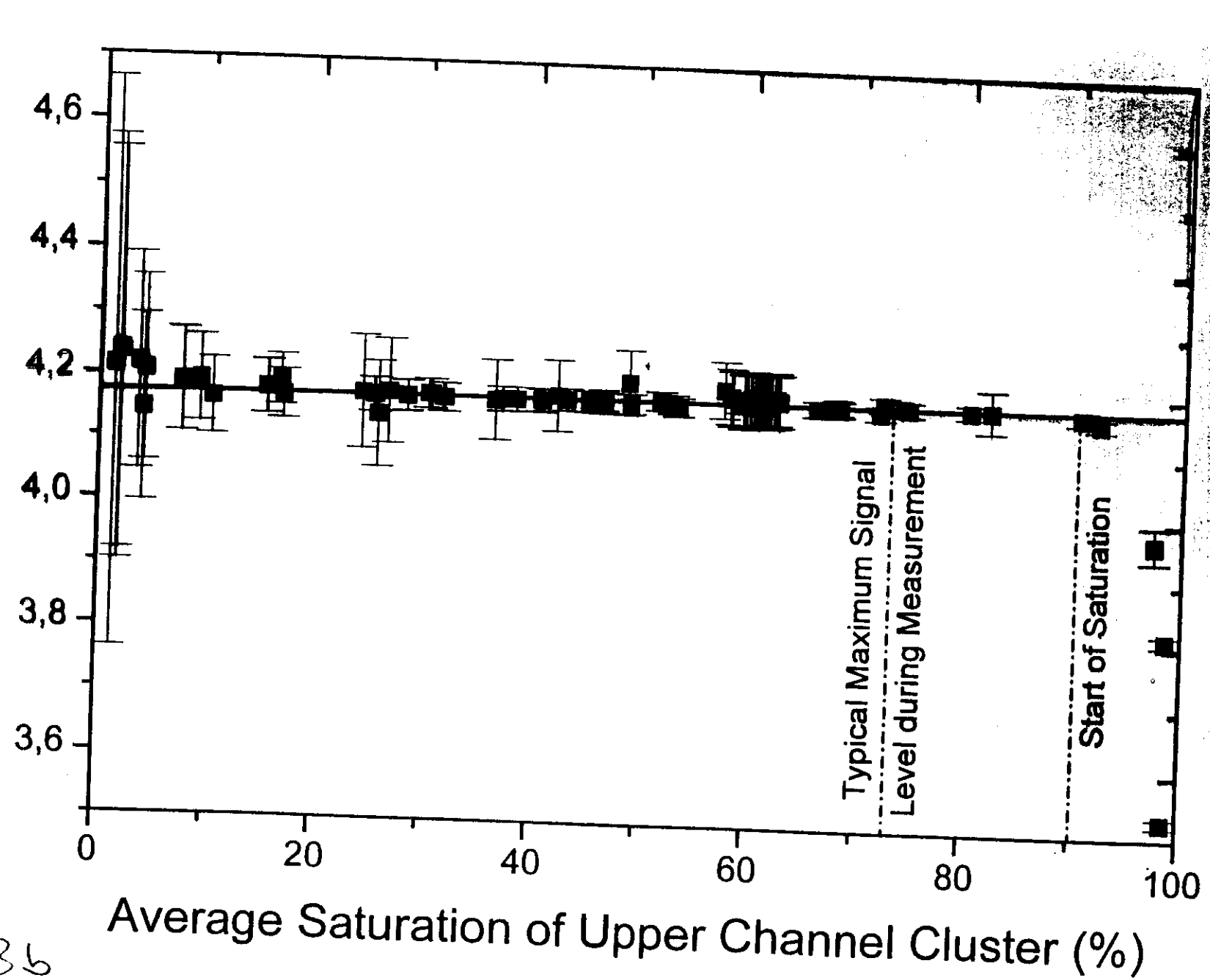
Count Ratio Upper/Lower Channel Clusters
4,6
4,4
4,2
4,0
3,8
3,6
0
20
40
60
80
100
Average Saturation of Upper Channel Cluster (%)
Typical Maximum Signal Level during Measurement
Start of Saturation

Fig. 3b

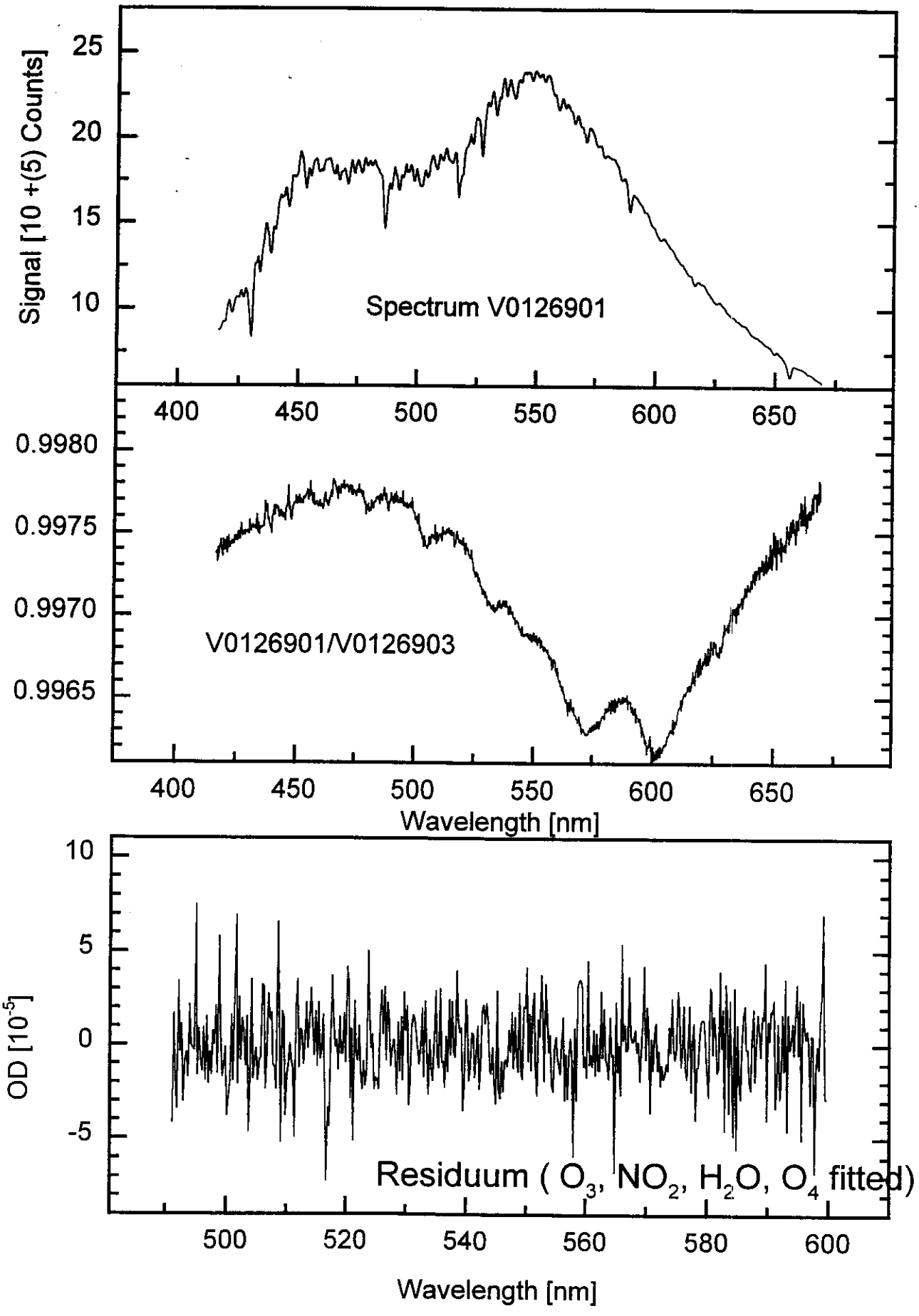
Signal [10 +(5) Counts]
25
20
15
10
Spectrum V0126901
400
450
500
550
600
650
0.9980
0.9975
0.9970
0.9965
V0126901/V0126903
400
450
500
550
600
650
Wavelength [nm]
OD [10-5]
10
5
0
-5
Residuum (O3, NO2, H2O, O4 fitted)
500
520
540
560
580
600
Wavelength [nm]

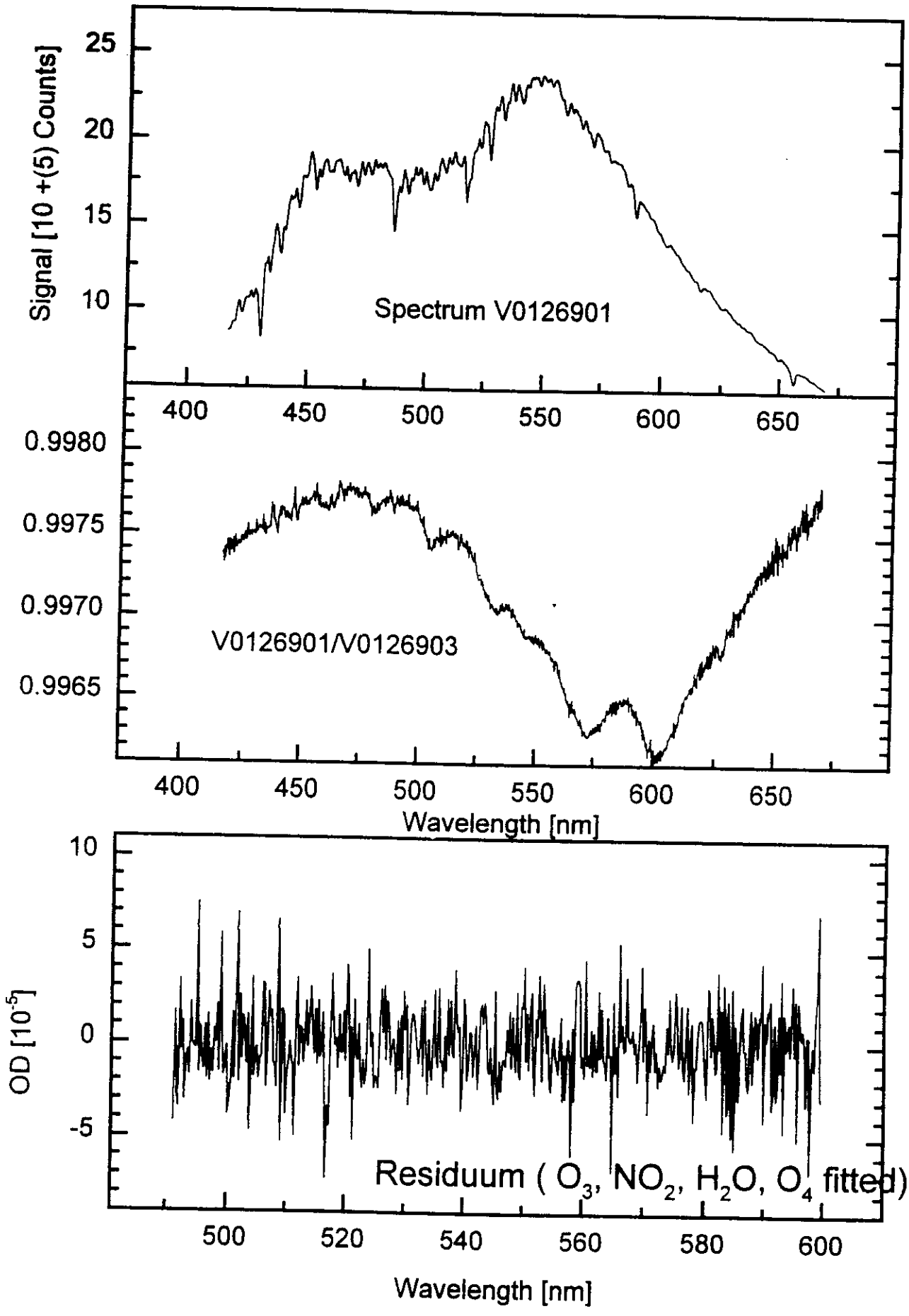
Signal [10 +(5) Counts]
25
20
15
10
Spectrum V0126901
400
450
500
550
600
650
0.9980
0.9975
0.9970
0.9965
V0126901/V0126903
400
450
500
550
600
650
Wavelength [nm]
OD [10-5]
10
5
0
-5
Residuum (O3, NO2, H2O, O4 fitted)
500
520
540
560
580
600
Wavelength [nm]

Principle of MCT technique

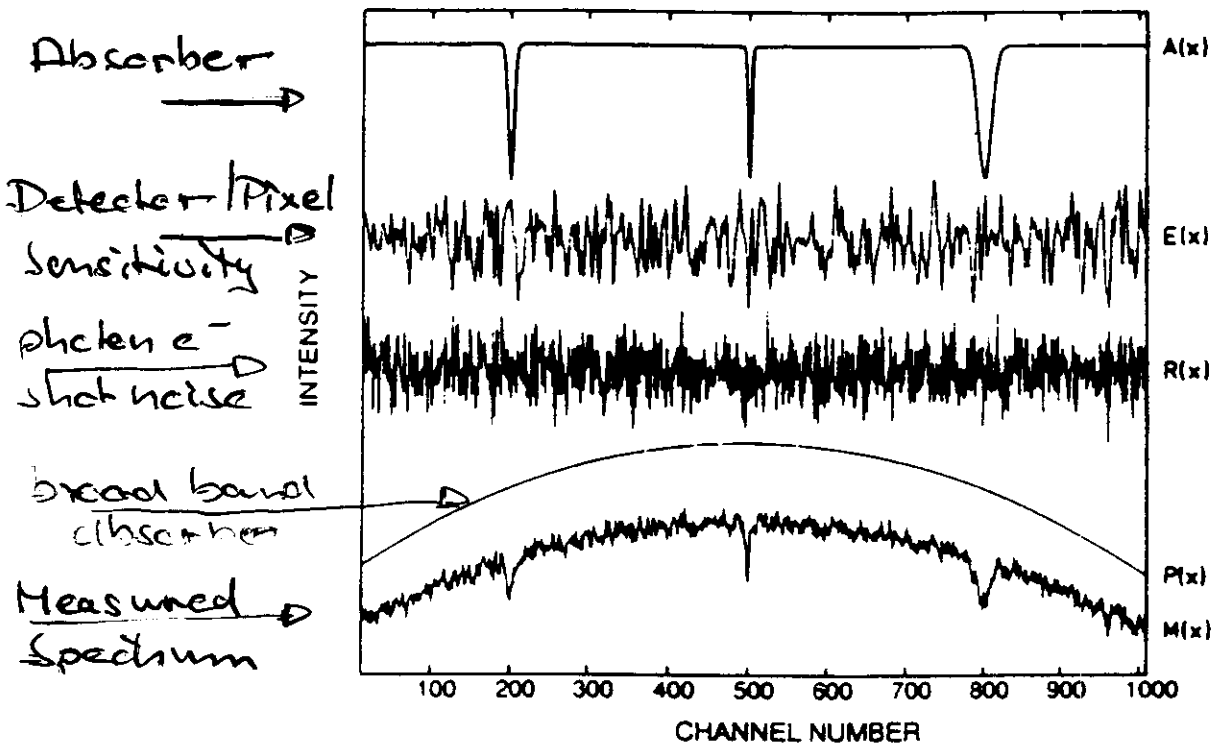

Fig. 2. Breakdown of the individual contributions to an example DOAS spectrum of atmospheric trace species as it is recorded with an OMA as a spectral detector (from top to bottom): Simulated differential absorption spectrum $A(x)$, where the differential optical density of all bands is 1×10^{-3}; pixel sensitivity pattern $E(x)$ of a photodiode array having 1024 pixels (peak-to-peak variation $p/p = 1\%$); photoelectron shot noise $R(x)$ ($p/p = 6.5 \times 10^{-4}$); broad-band term $P(x)$ ($p/p = 26\%$) containing the wavelength dependence of the light source, unstructured absorptions, and scattering; product $M(x)$ of all contributions, which is the observed spectrum.

Bauers et al. (1995)
Appl Optics, 34, 4472

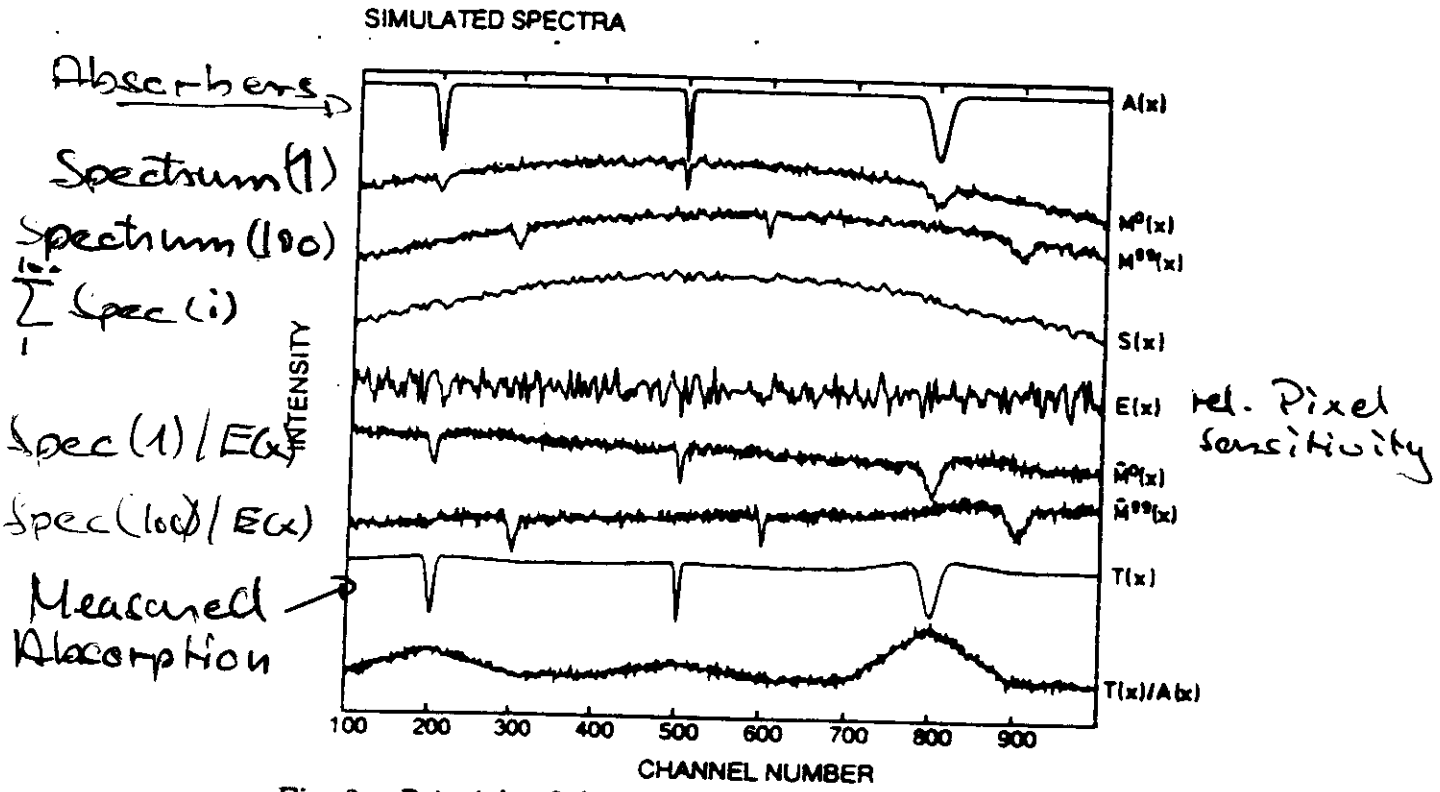

Fig. 3. Principle of the MCST with $N = 100$ simulated readouts containing three absorption lines ($D' = 0.001$) of different half-widths (10, 5, or 20 pixels). The lines are centered at pixels 200, 500, 800 at the first readout ($j = 0$) and at pixels 299, 599, 899 for the last readout ($j = 99$). A fixed pattern structure $E(x)$ (p/p = 0.001) and random noise $R^k(x)$ (p/p = 6×10^{-4}) were also applied. Top to bottom, sample absorption $A(x)$ (from Fig. 2); $M^0(x)$ and $M^{99}(x)$, first and last readouts of the set, where the spectral shift between two consecutive readouts was 1 pixel channel ($\alpha = 1$); sum $S(x)$ of all readouts of the set according to Eq. (10); relative pixel sensitivity $E(x)$ for comparison (different scaling); new readouts $\tilde{M}^0(x)$ and $\tilde{M}^{99}(x)$, where any contribution of $E(x)$ was removed according to Eq. (11); final spectrum $T(x)$ after the spectra $\tilde{M}^k(x)$ were reshifted and added at the spectral position of the first spectrum. The optical densities in this spectrum D' (at $x = 200$, 500, and 800) are reduced by 1.3%, 0.7%, and 6%, respectively, compared with the original values, depending on the half-width of the original line (see Table 1 for details). From the residual (magnified 10 times) it becomes obvious that the MCST generates no spurious narrow-band modulations. Compared with the random noise added to each spectrum at the beginning of the procedure, the final noise level is reduced by a factor of $\sqrt{N} = 10$.

Ruerend, (1995)
Appl. Optics, 34, 4472

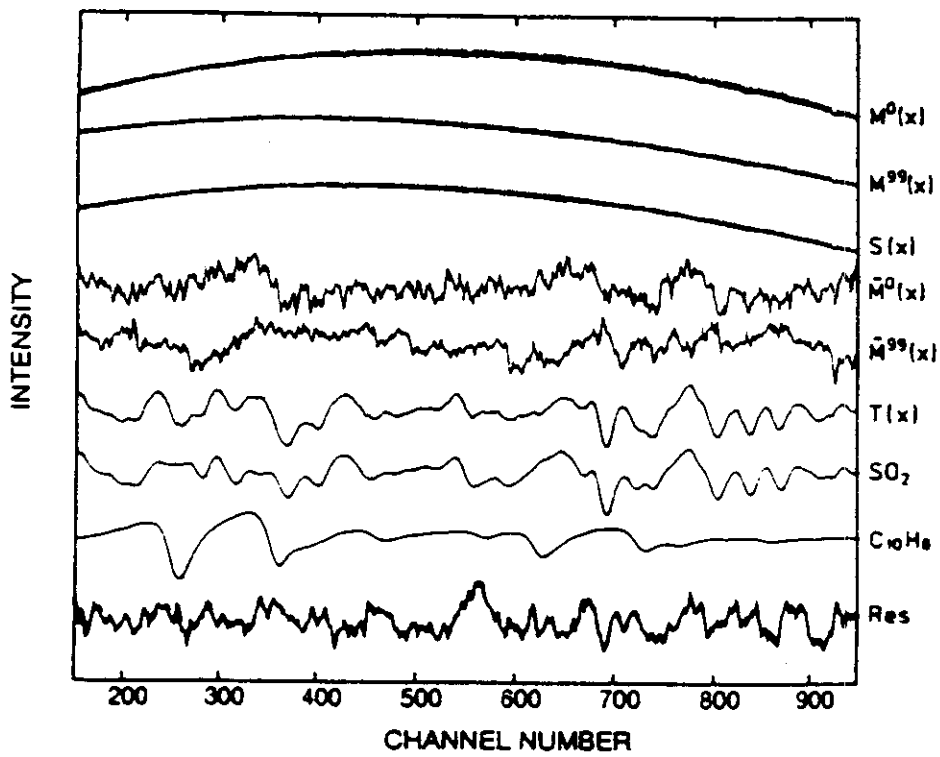

Fig. 5. Example of an air spectrum recorded with our OH-DOAS instrument by the use of the MCST. Top to bottom, the first $M^0(x)$ and the last readout $M^{99}(x)$, which were shifted by 0.94 channels after each readout; the sum $S(x)$ of the 100 readouts according to Eq. (10); $\tilde{M}^0(x)$ and $\tilde{M}^{99}(x)$ with $E(x)$ removed according to Eq. (11); the final spectrum $T(x)$ after the individual quotient spectra $\tilde{M}^k(x)$ are shifted back to the spectral position of the first spectrum and added up; SO_2 reference spectrum recorded with the same procedure of MCST; naphthalene reference spectrum; residual spectrum after removal of the atmospheric SO_2 and naphthalene absorptions, where the peak-to-peak value is 7×10^{-5}.

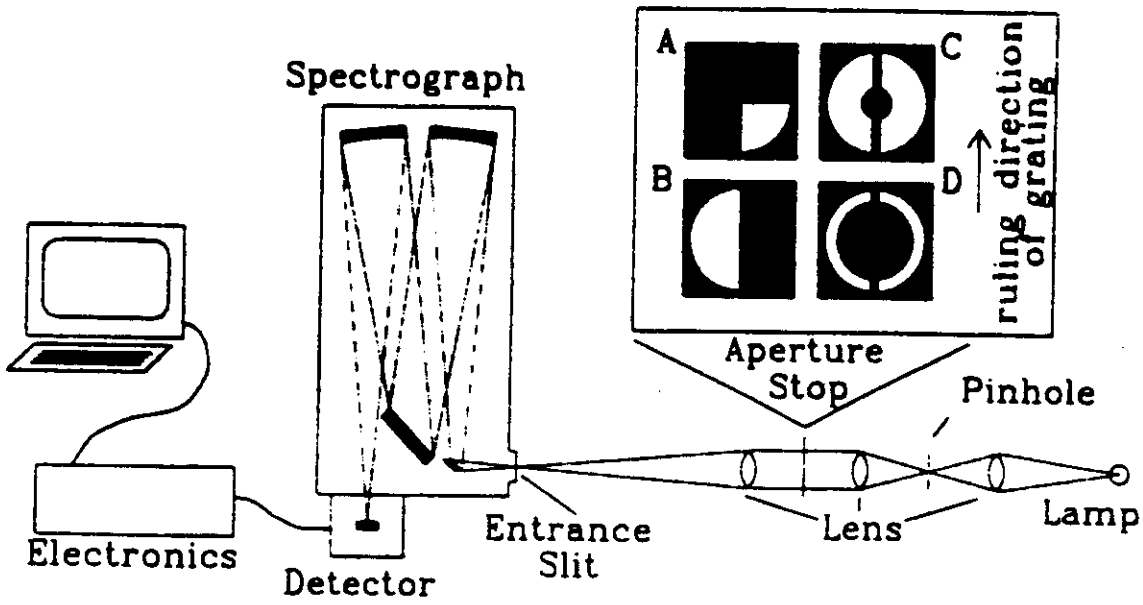

Fig. 1. Experimental setup to investigate the dependence of the spectrograph–detector system on the illumination. The aperture stops *A*, *B*, *C*, and *D* are inserted into the collimated light beam, which is produced by two lenses and a 200-μm pinhole. The light is focused on the entrance slit of the spectrograph by another lens.

Stutz and Plett (1997)
App Opt. 36, 1105

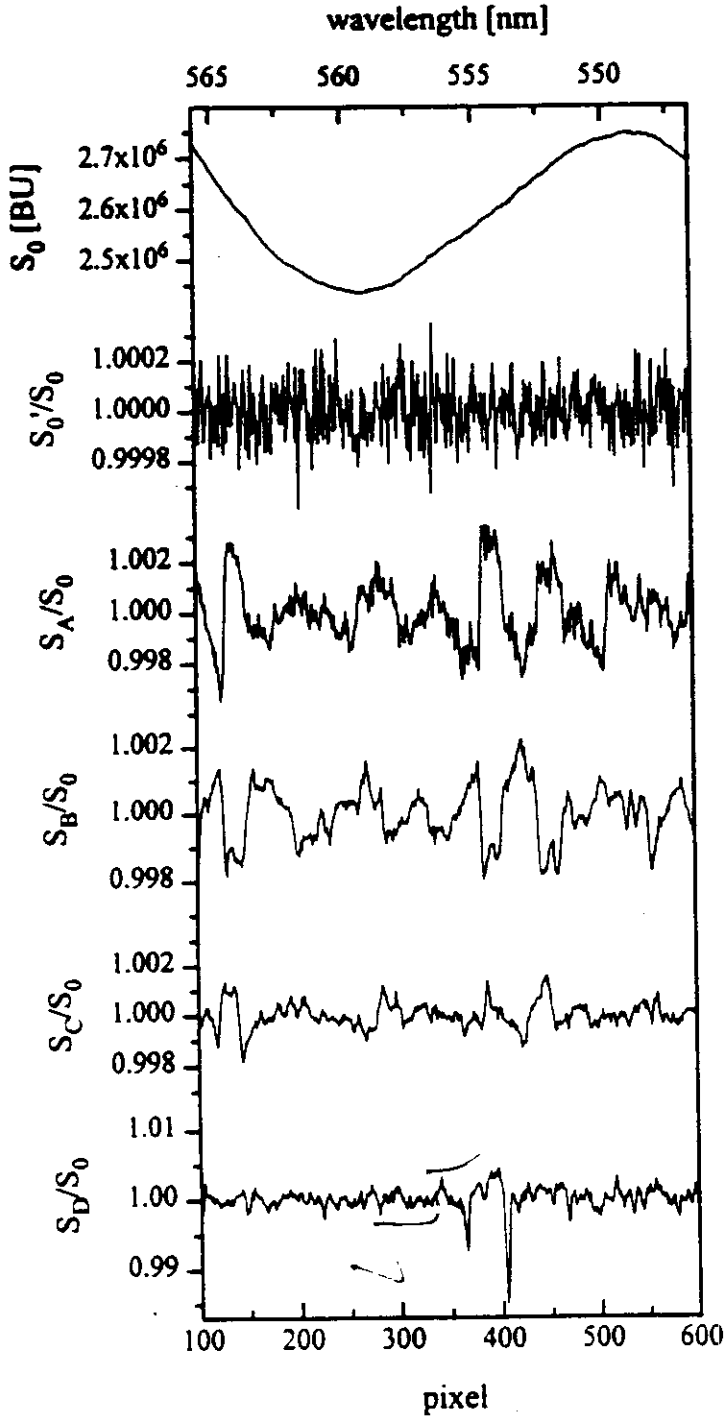

Fig. 2. Structures produced by changes in illumination of the spectrograph–detector system. The top spectrum shows a typical lamp spectrum with its sinusoidal étalon structure. The noise level in the ratio of two spectra taken under identical conditions without aperture stop S_0'/S_0 is lower than the spectral structures found in the ratios of spectra taken with different illuminations (i.e., aperture stops *A–D* inserted), S_A/S_0, S_B/S_0, S_C/S_0, and S_D/S_0. The *y* scale of S_D/S_0 was changed to show the complete spectrum. The aperture stops used to change the illuminations are shown in Fig. 1.

Stutz and Platt (199

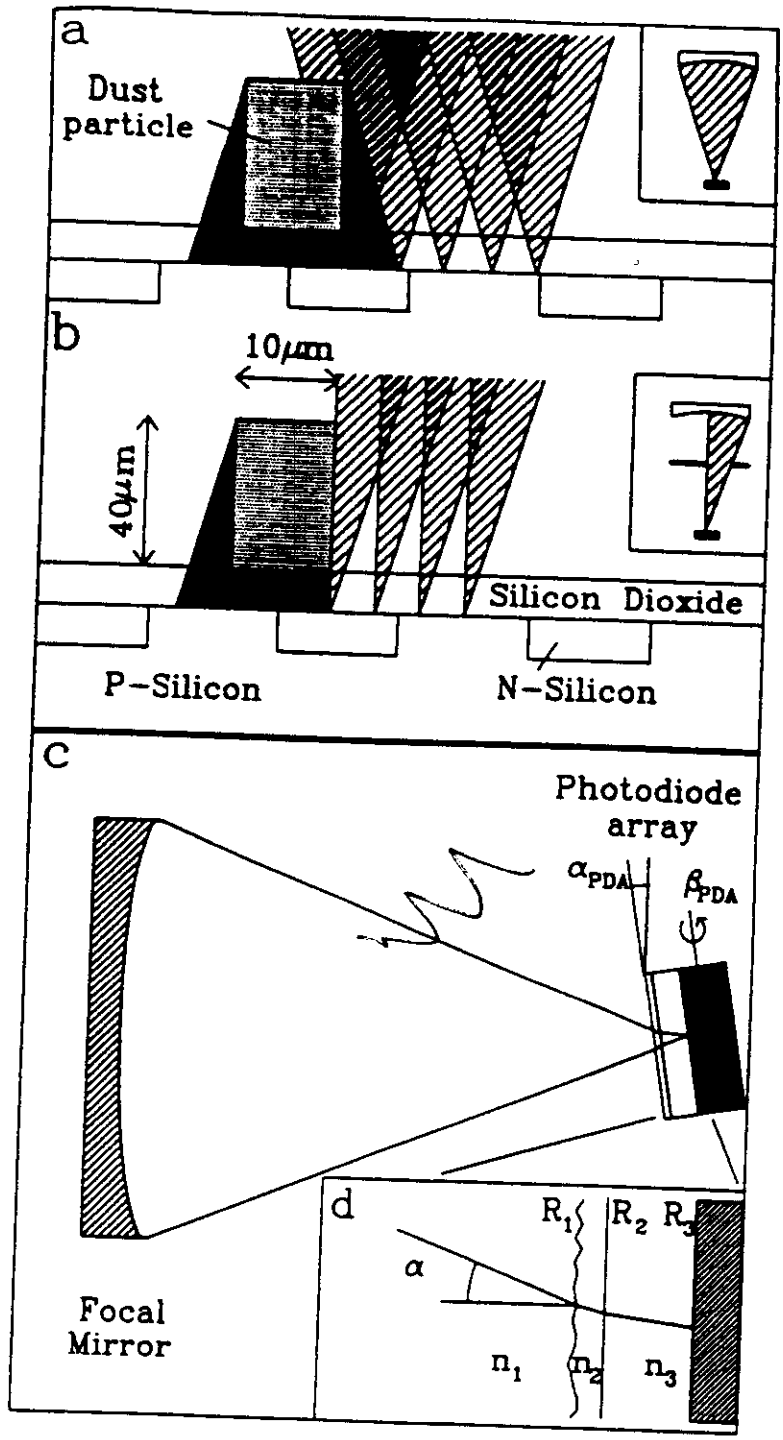

Fig. 3. Effects that give rise to illumination-sensitive response of the diode of a PDA: a, a dust particle illustrated with a rectangular cross section throws a shadow on the diode on the right of the particle. The diode is illuminated by a full cone of light (i.e., no aperture stop present); b, if only the right half of the cone is illuminated (e.g., owing to the presence of aperture stop *A* or *B*) the shadow is not present; c, d, an irregular surface changes the interferences in the protective layer of the PDA. The figure explains the model calculations performed to investigate this effect in two dimensions: A ray enters the layers on the PDA with angles α; the light path in the layer is therefore longer compared with a vertical ray; as a cone of light is thrown from the focusing mirror of the spectrograph on the PDA, the intensity must be integrated over all angles to derive the total intensity I_{tot}.

Stutz and Platt (1997)
App. Opt. 36. 1105

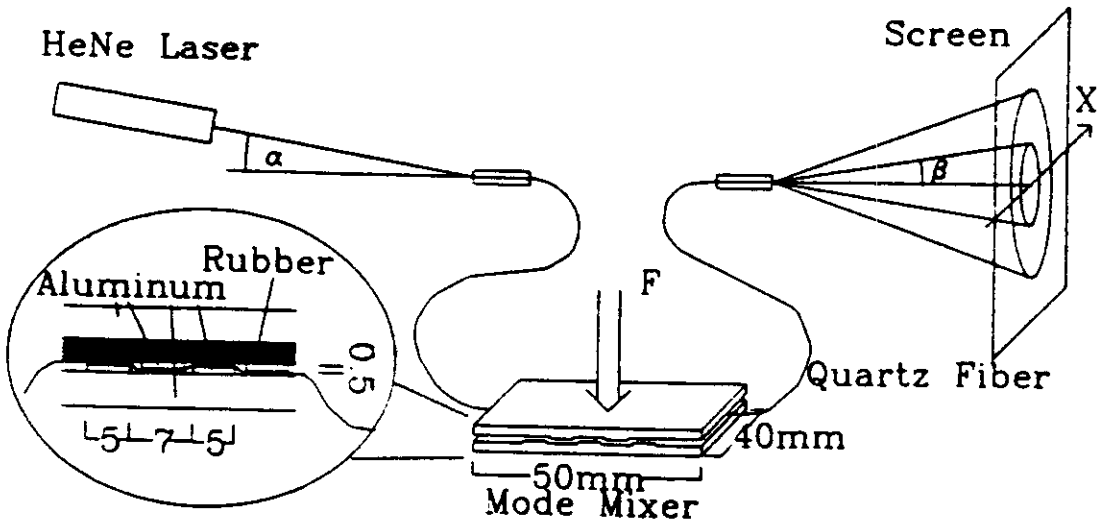

Fig. 5. Experimental setup to investigate mode coupling in a multimode quartz fiber. The light beam of a helium–neon laser is fed into the fiber at an angle α. The fiber is placed between two plates with a step profile. A sheet of rubber is placed between the top aluminum plate and the profile to protect the fiber. The plates can be pressed together with a force *F* to introduce microbending to the fiber. The light intensity leaving the fiber is measured with a photoresistor on a screen at a 15-cm distance from the fiber end along the X axis.

Stutz and Pitt (1997)
Appl. Optics, 36, 05

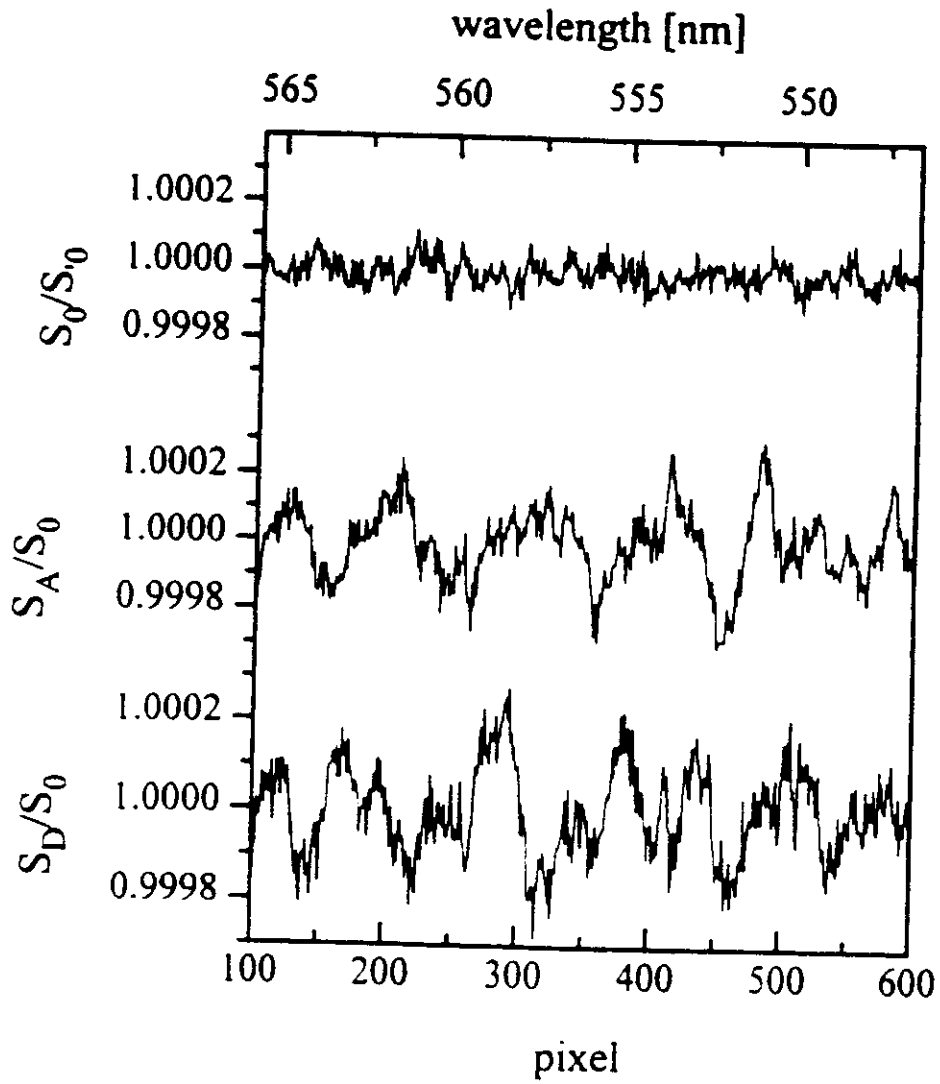

Fig. 8. Noise and residual spectral structure of a system, including a mode mixer (Figs. 5 and 7). The structures S_A/S_0 and S_D/S_0 are smaller by a factor of more than 10 compared with the results without a mode mixer (Fig. 2).

Stutz and Plath (1991)
App. Optics

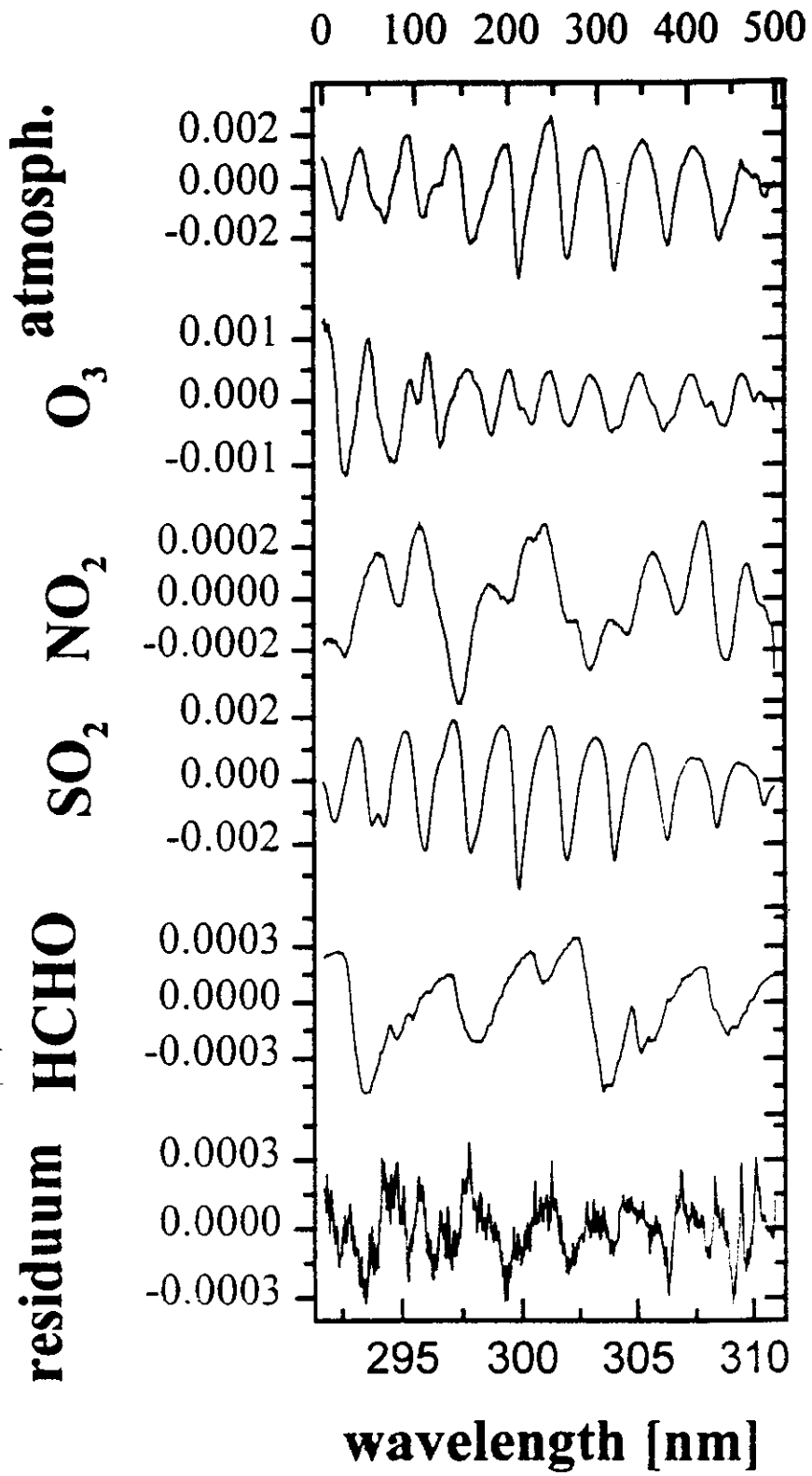
pixel
0 100 200 300 400 500
atmosph.
0.002
0.000
-0.002
O_3
0.001
0.000
-0.001
NO_2
0.0002
0.0000
-0.0002
SO_2
0.002
0.000
-0.002
HCHO
0.0003
0.0000
-0.0003
residuum
0.0003
0.0000
-0.0003
295 300 305 310
wavelength [nm]

Fig 9

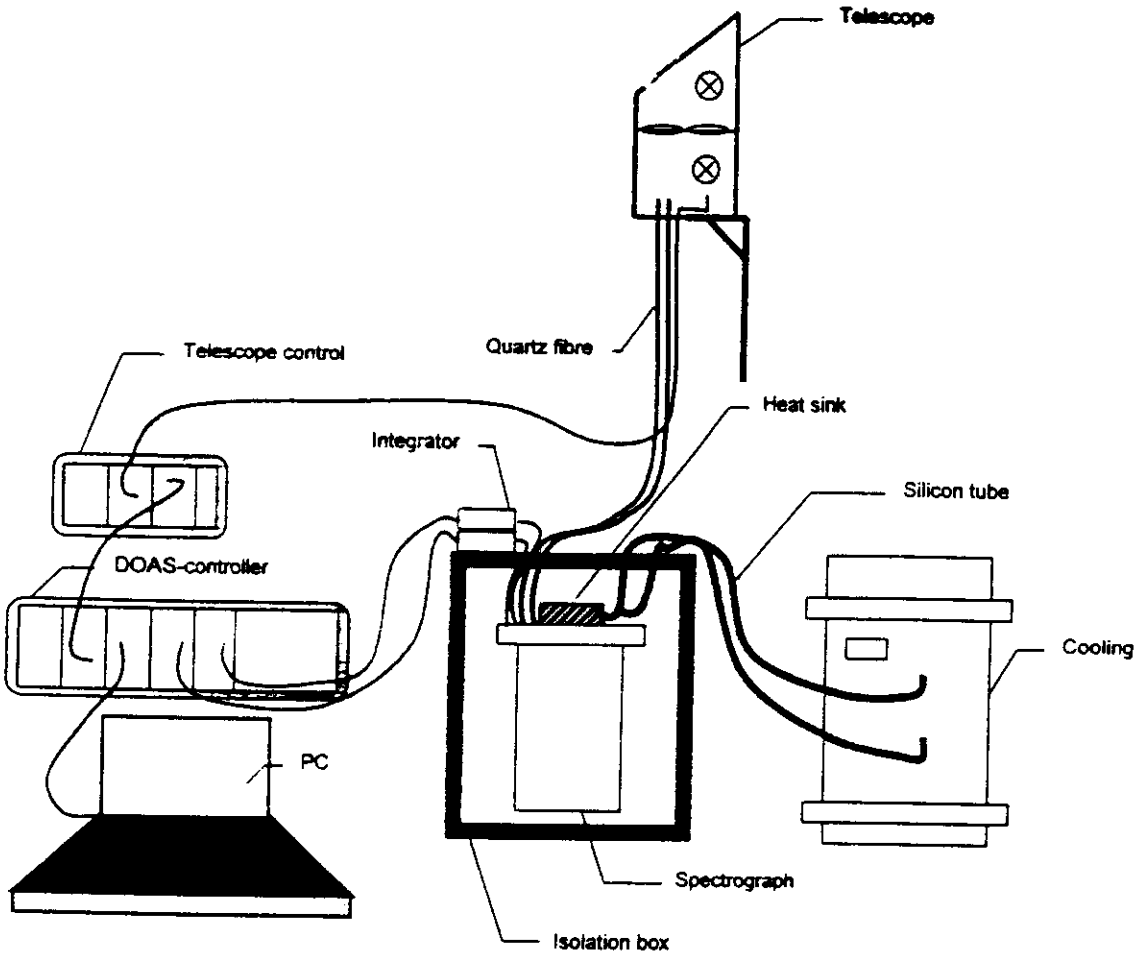
Telescope
Telescope control
Quartz fibre
Heat sink
Integrator
Silicon tube
DOAS-controller
Cooling
PC
Spectrograph
Isolation box

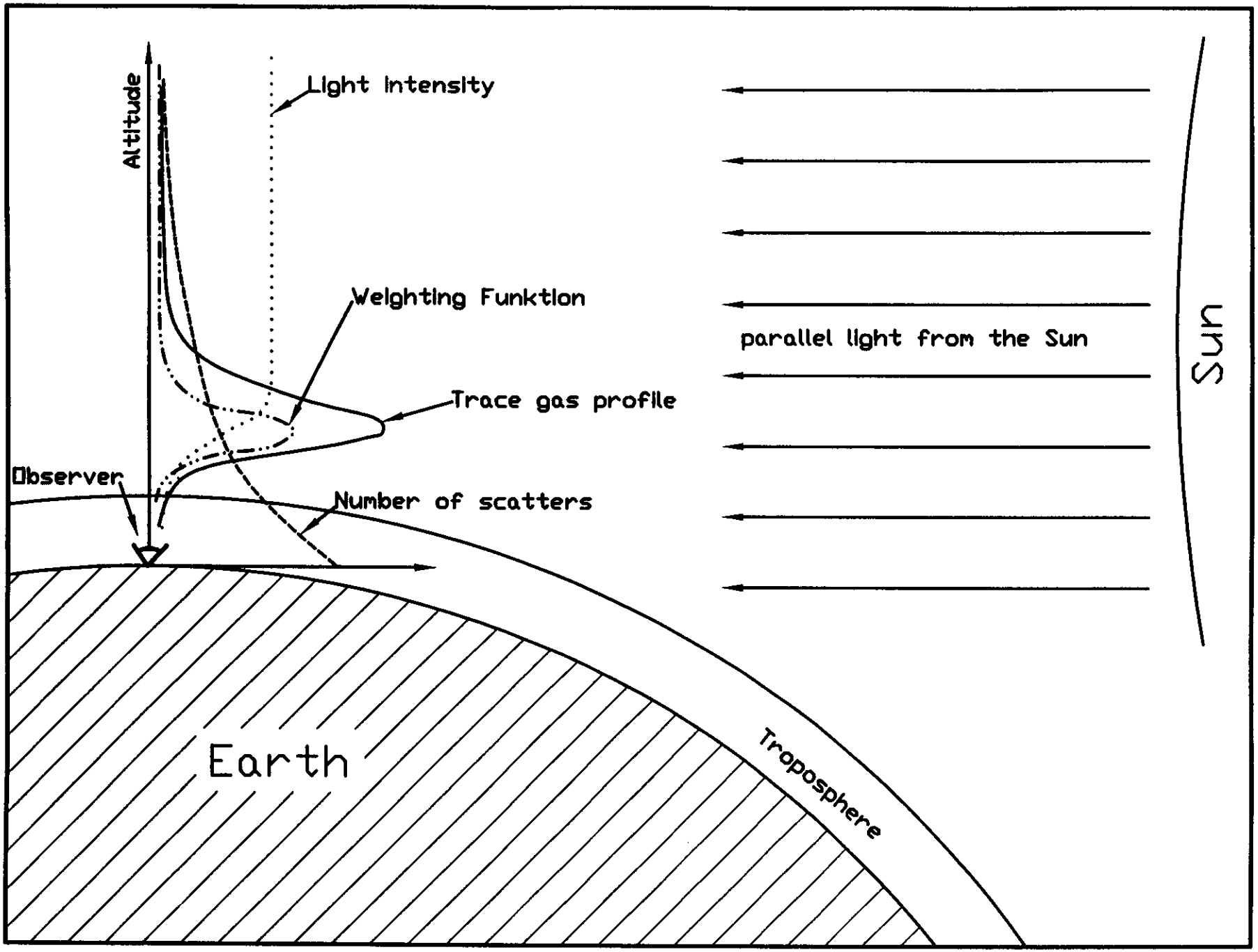
Altitude
Light intensity
Weighting Funktion
Trace gas profile
Observer
Number of scatters
parallel light from the Sun
Sun
Earth
Troposphere

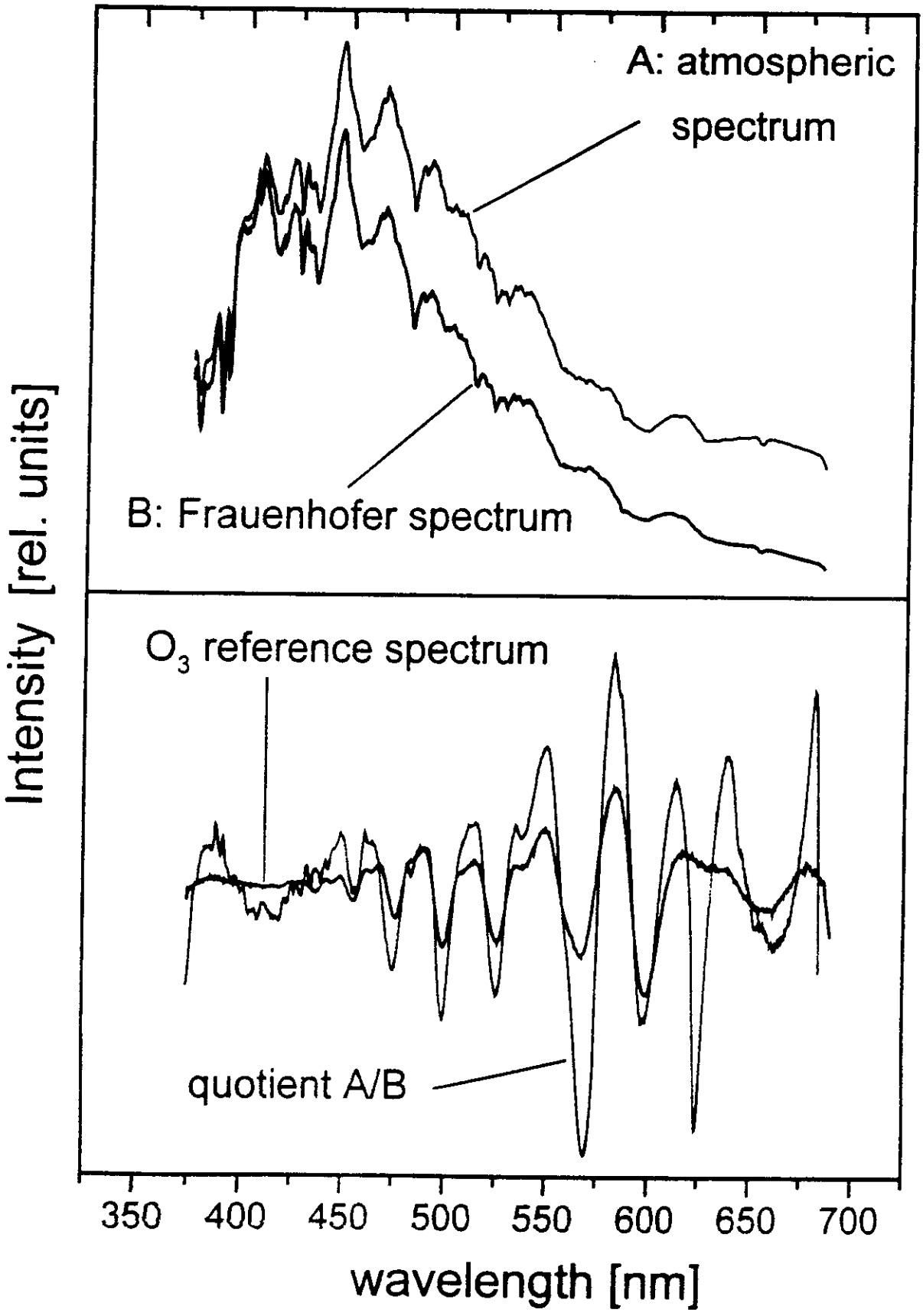
A: atmospheric spectrum
B: Frauenhofer spectrum
O_3 reference spectrum
quotient A/B
Intensity [rel. units]
350
400
450
500
550
600
650
700
wavelength [nm]

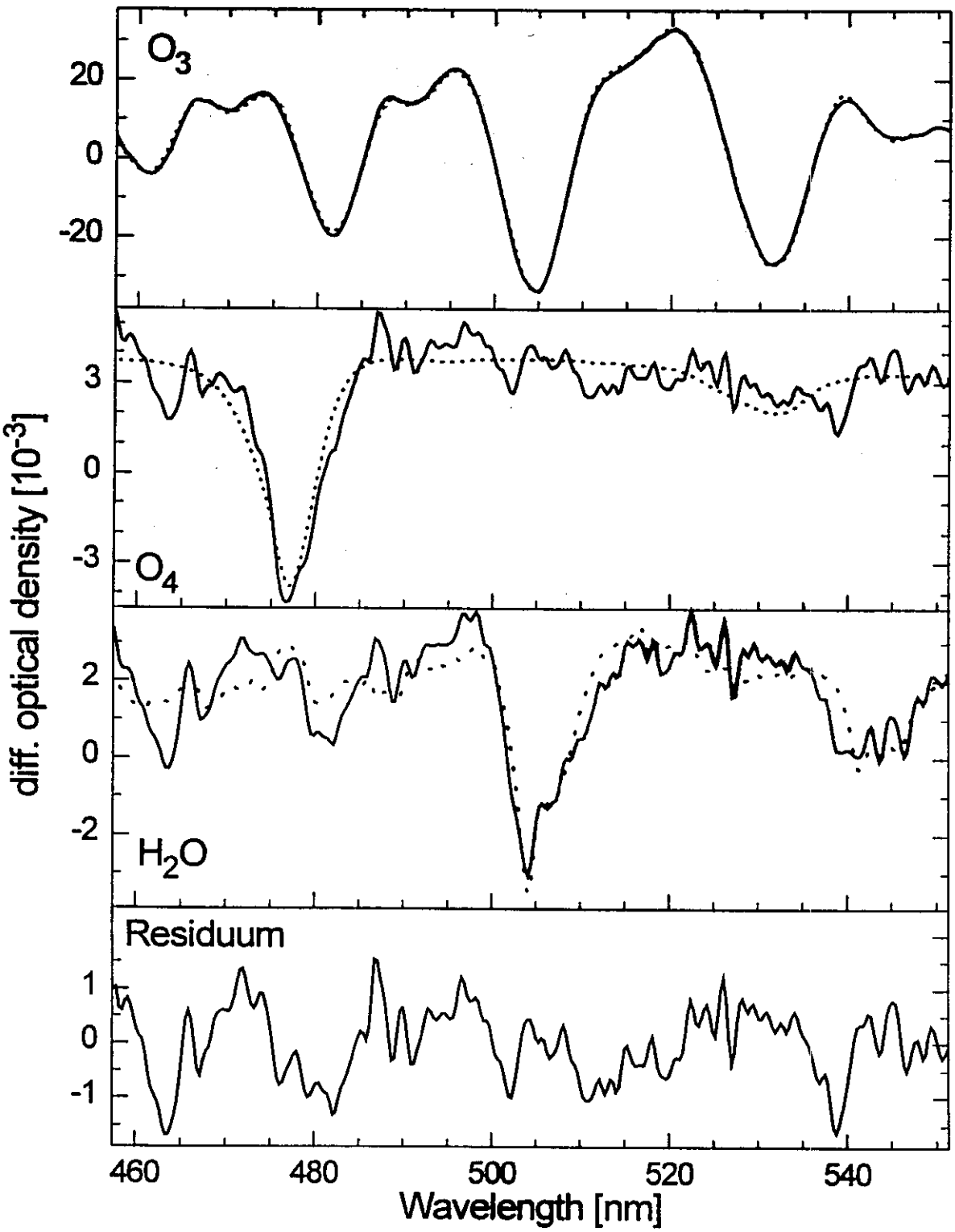
O3
20
0
-20
3
0
-3
O4
2
0
-2
H2O
Residuum
1
0
-1
460
480
500
520
540
Wavelength [nm]
diff. optical density [10-3]

Fig. 1

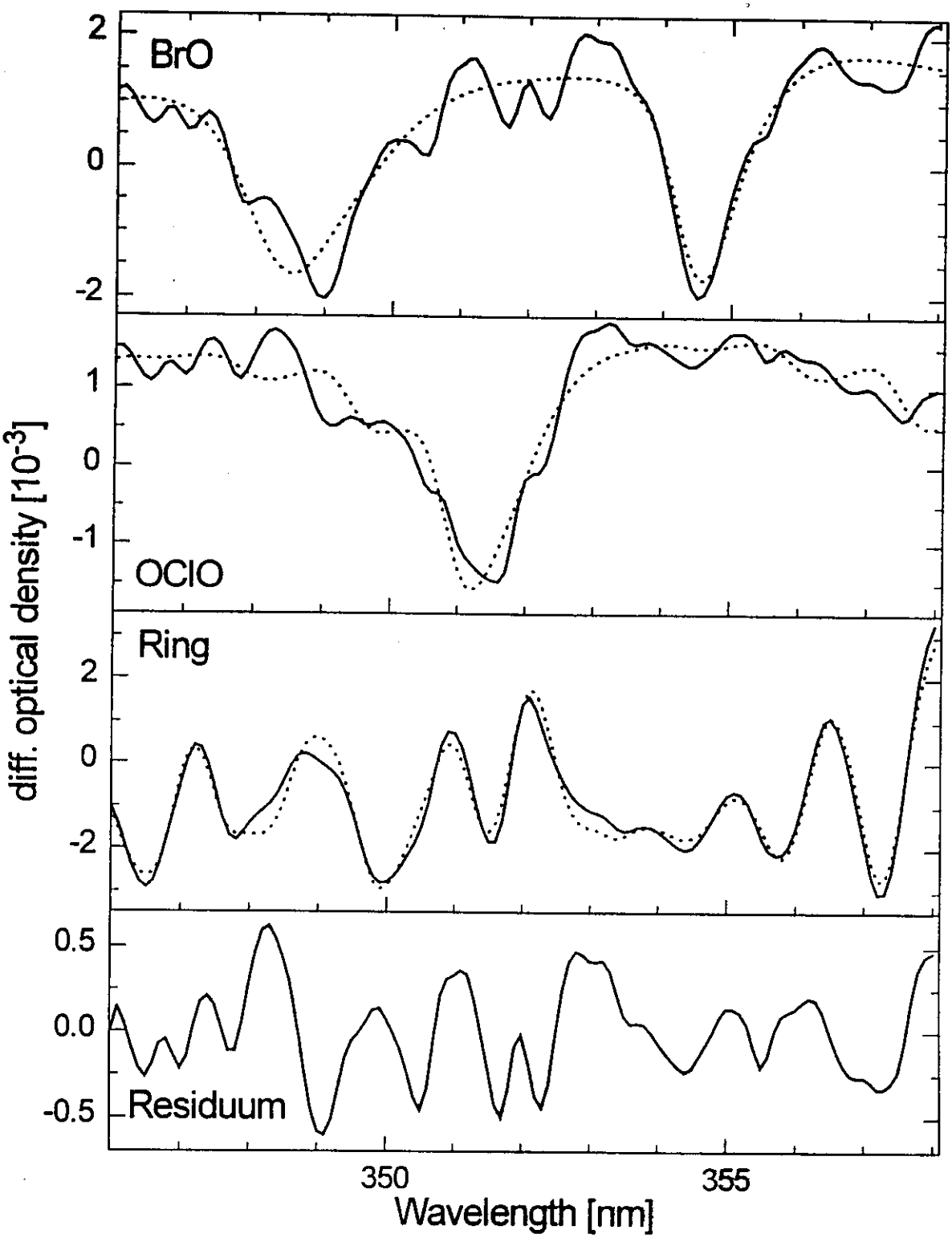
BrO
OClO
Ring
Residuum
diff. optical density [10-3]
Wavelength [nm]
2
0
-2
1
-1
0.5
0.0
-0.5
350
355

Fig. 3

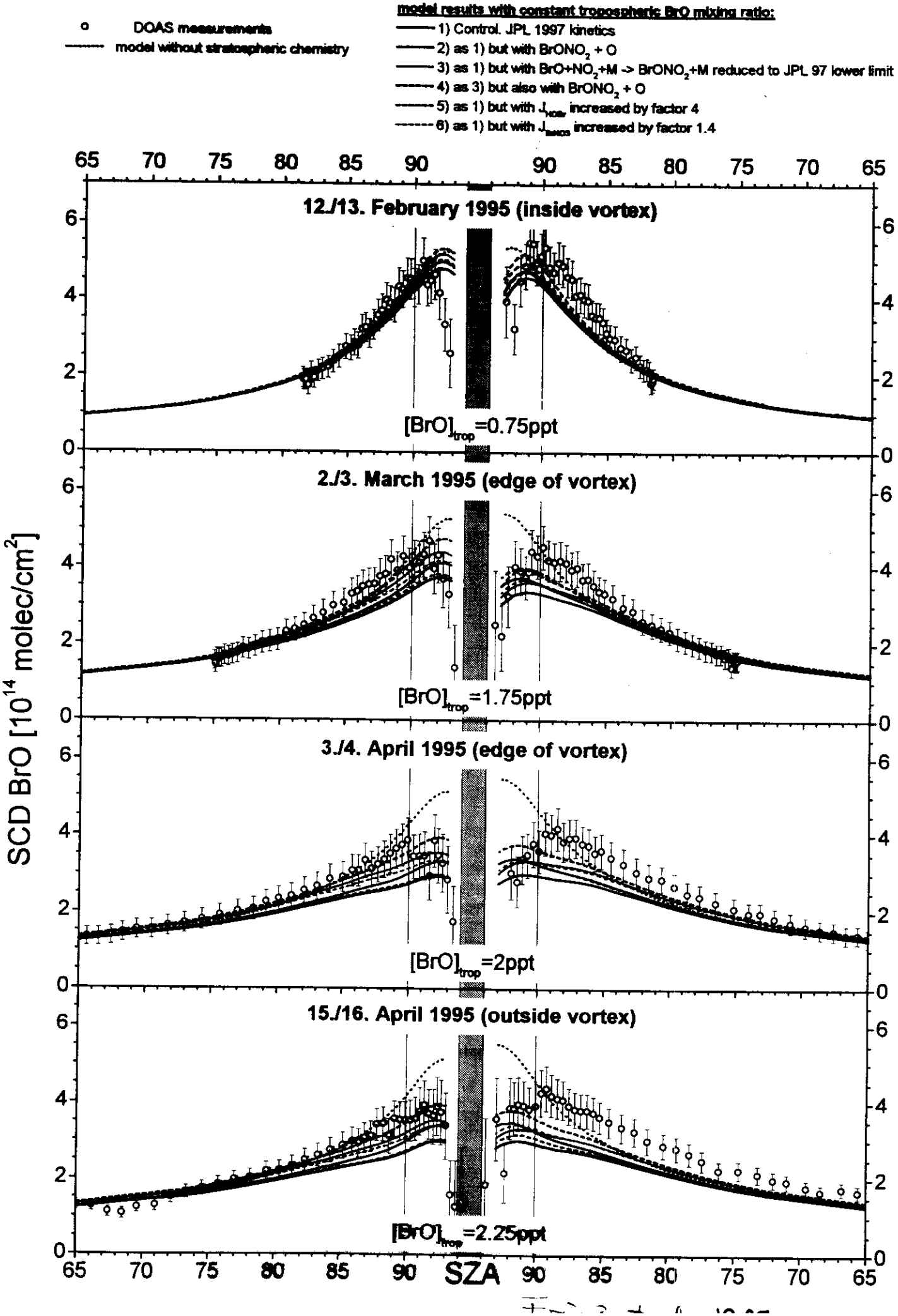
DOAS measurements
model without stratospheric chemistry
model results with constant tropospheric BrO mixing ratio:
1) Control. JPL 1997 kinetics
2) as 1) but with BrONO2 + O
3) as 1) but with BrO+NO2+M -> BrONO2+M reduced to JPL 97 lower limit
4) as 3) but also with BrONO2 + O
5) as 1) but with J(NO2) increased by factor 4
6) as 1) but with J(BrNO3) increased by factor 1.4
12./13. February 1995 (inside vortex)
[BrO]trop=0.75ppt
2./3. March 1995 (edge of vortex)
[BrO]trop=1.75ppt
3./4. April 1995 (edge of vortex)
[BrO]trop=2ppt
15./16. April 1995 (outside vortex)
[BrO]trop=2.25ppt
SCD BrO [10^14 molec/cm^2]
SZA
65 70 75 80 85 90 85 80 75 70 65
0 2 4 6

GOME total NO_2

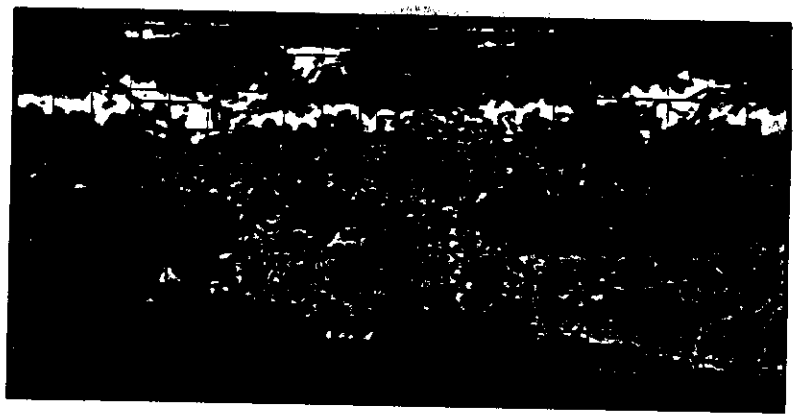

24.08.95 -27.08.95

28.08.95 - 30.08.95

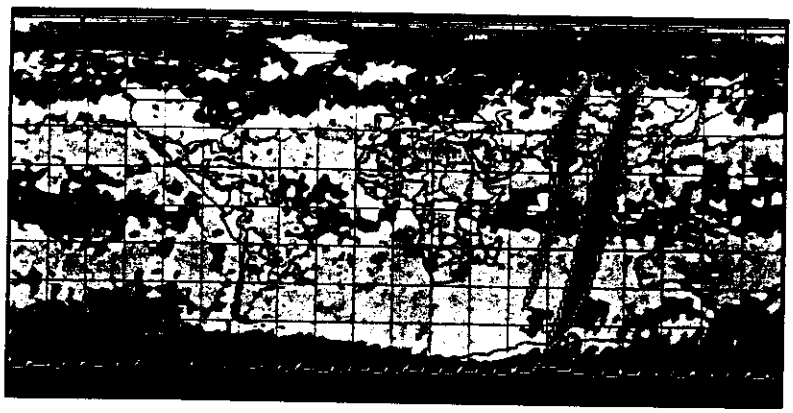

31.08.95 - 02.09.95

-Eisele et al. (1999)

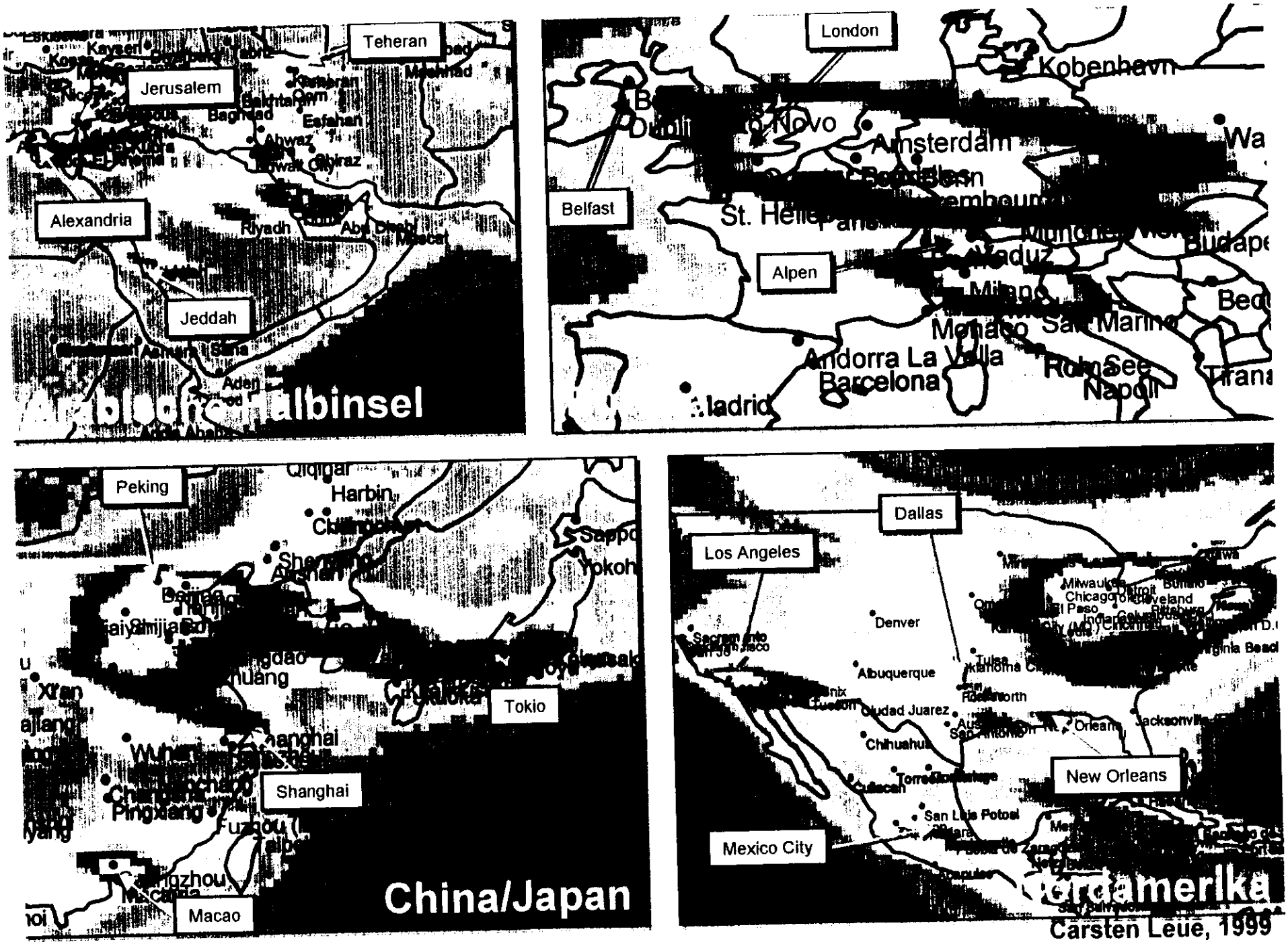
Teheran
Jerusalem
Alexandria
Jeddah
albinsel
London
Belfast
Alpen
Peking
Harbin
Tokio
Shanghai
Macao
China/Japan
Dallas
Los Angeles
Denver
Albuquerque
Ciudad Juarez
Chihuahua
New Orleans
Mexico City
Carsten Leue, 1999

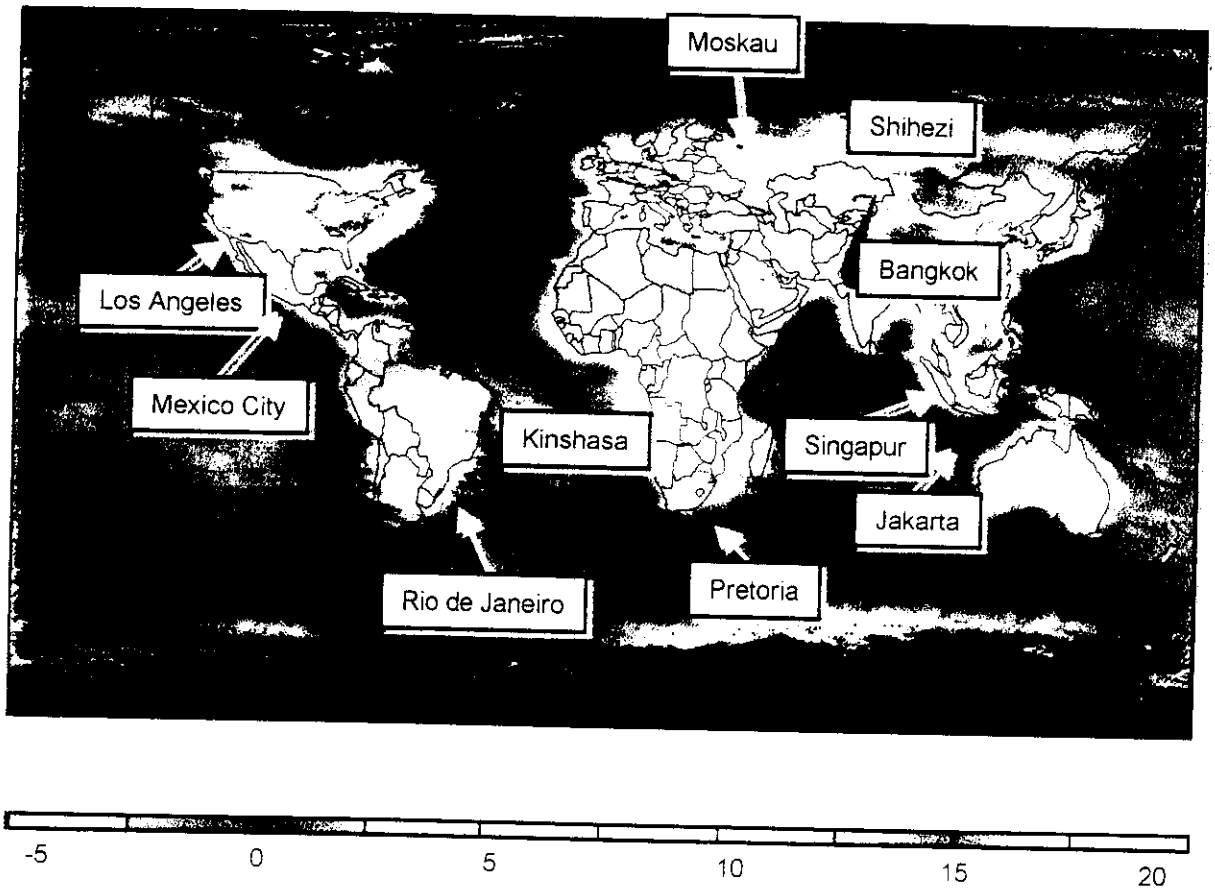

Vertical column of NO_2 [10^{14} molec/cm^2]

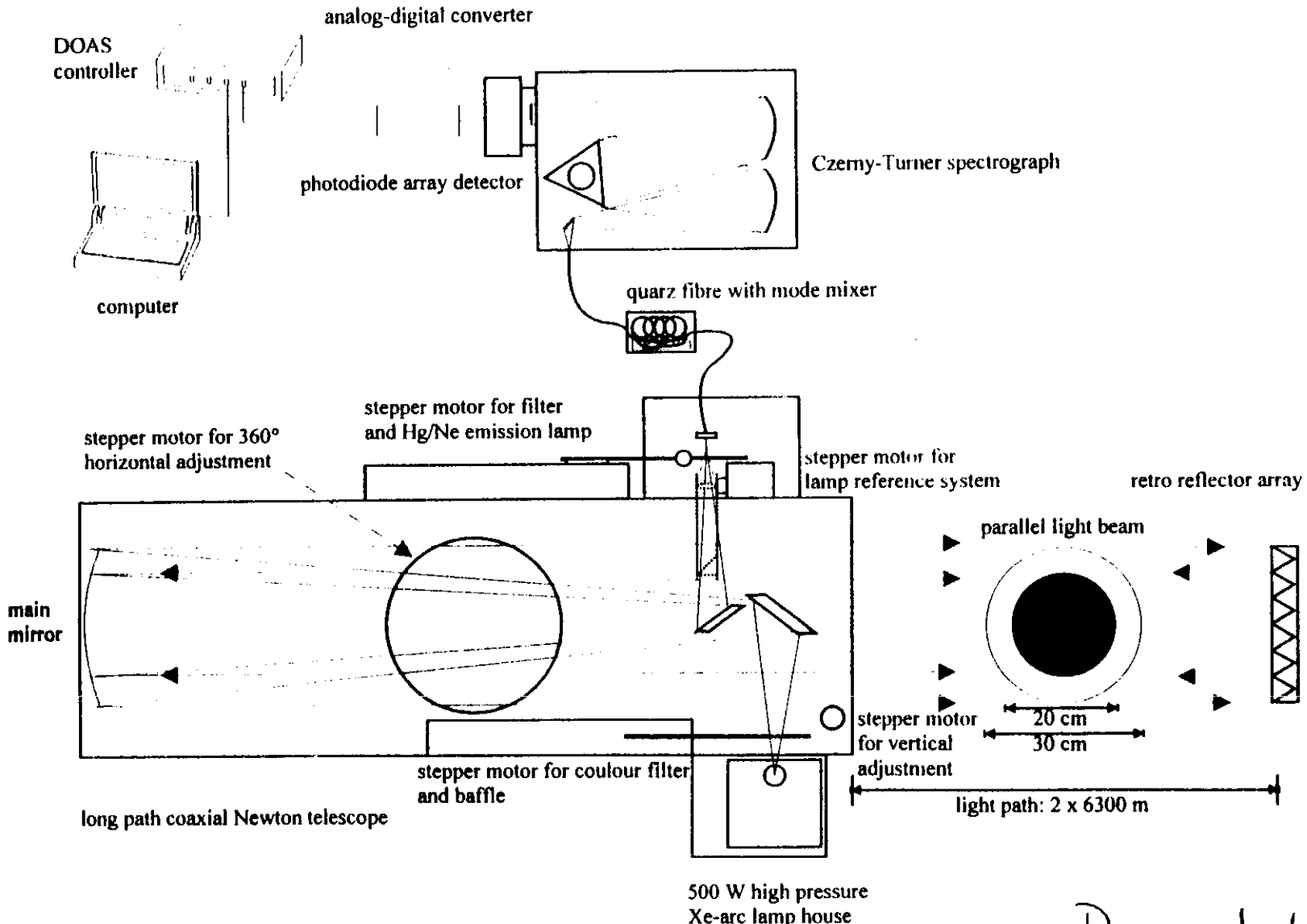

Darn et al. (1997)

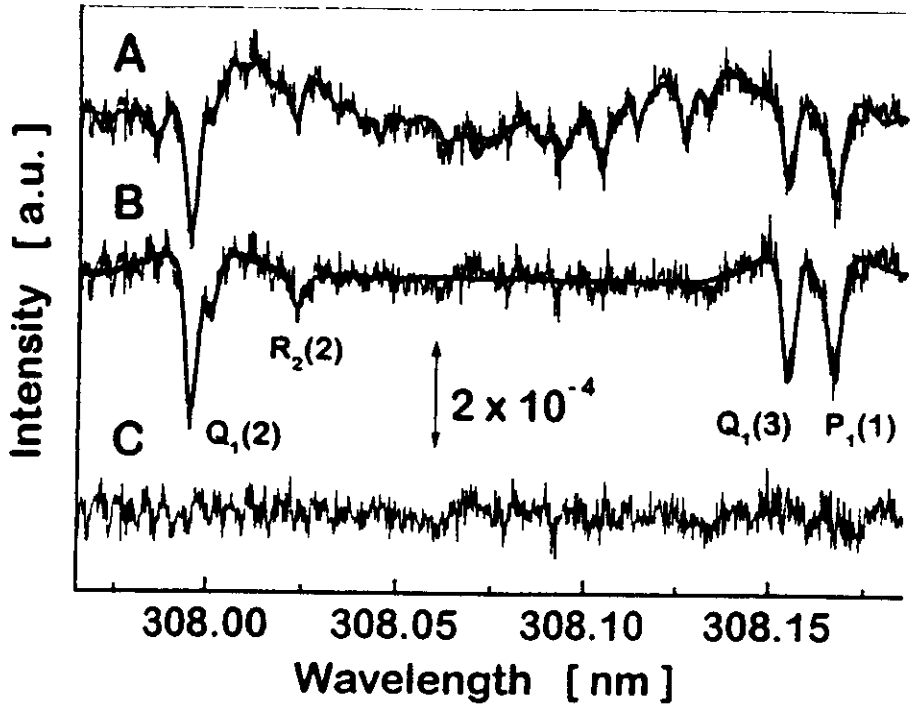
A
B
C
Intensity [a.u.]
R2(2)
2 x 10-4
Q1(2)
Q1(3)
P1(1)
308.00
308.05
308.10
308.15
Wavelength [nm]

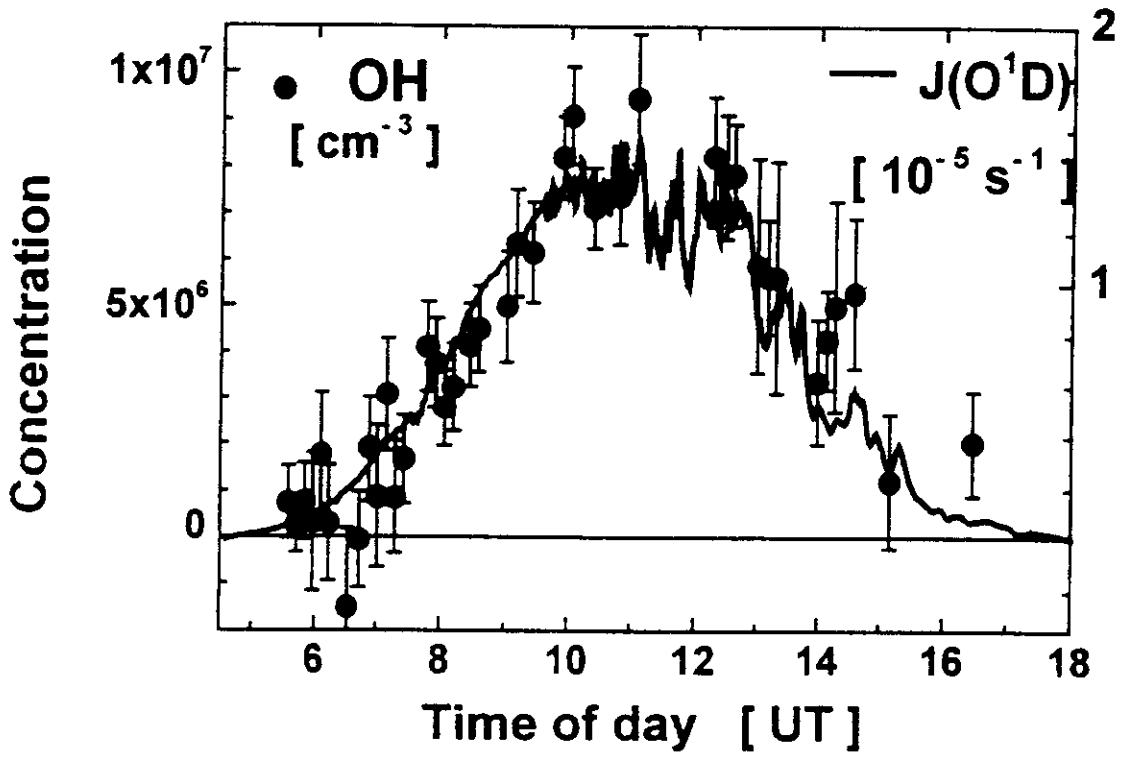
1x10^7
5x10^6
0
OH
[cm-3]
J(O1D)
[10-5 s-1]
2
1
Concentration
6
8
10
12
14
16
18
Time of day [UT]

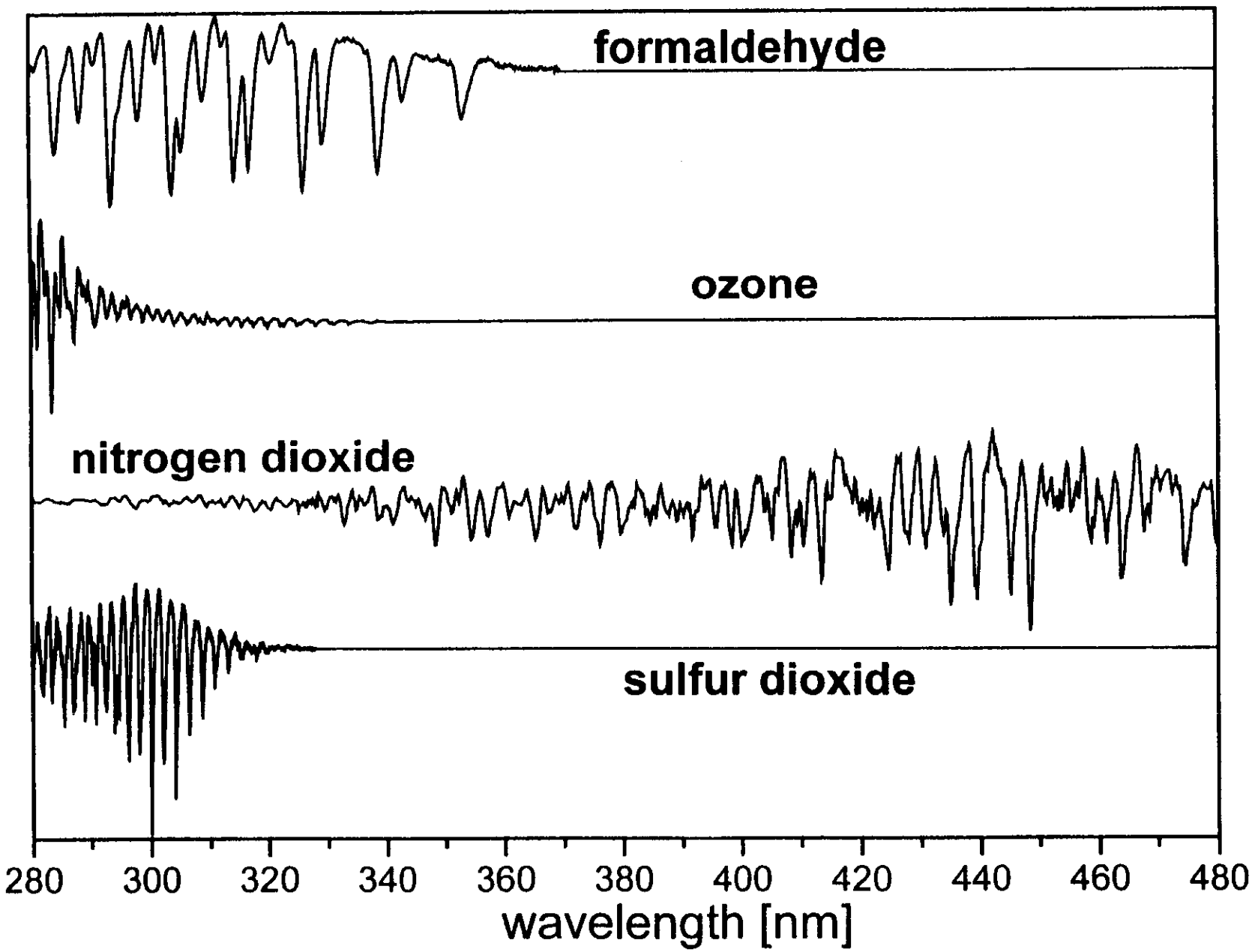
formaldehyde
ozone
nitrogen dioxide
sulfur dioxide
280
300
320
340
360
380
400
420
440
460
480
wavelength [nm]

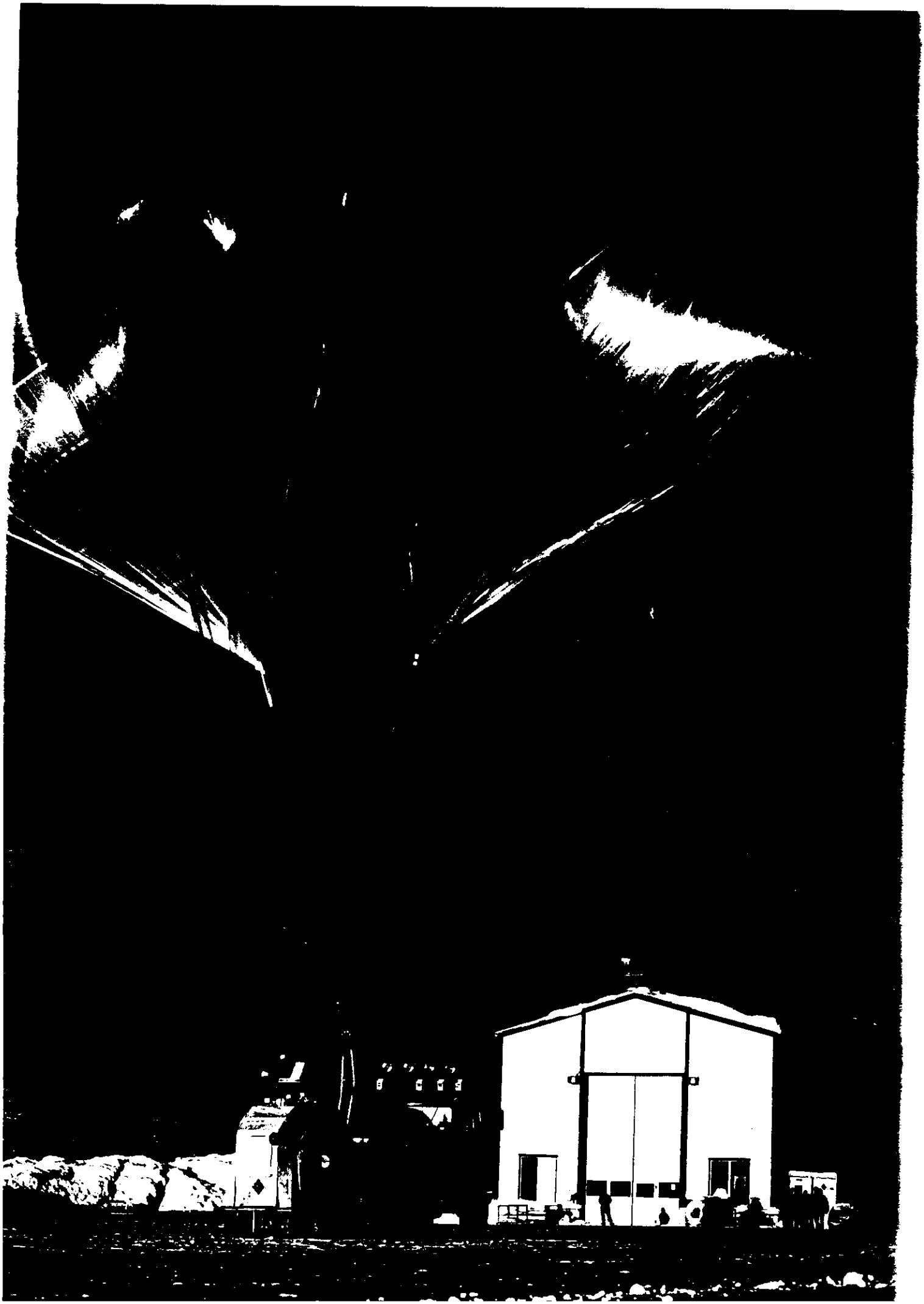

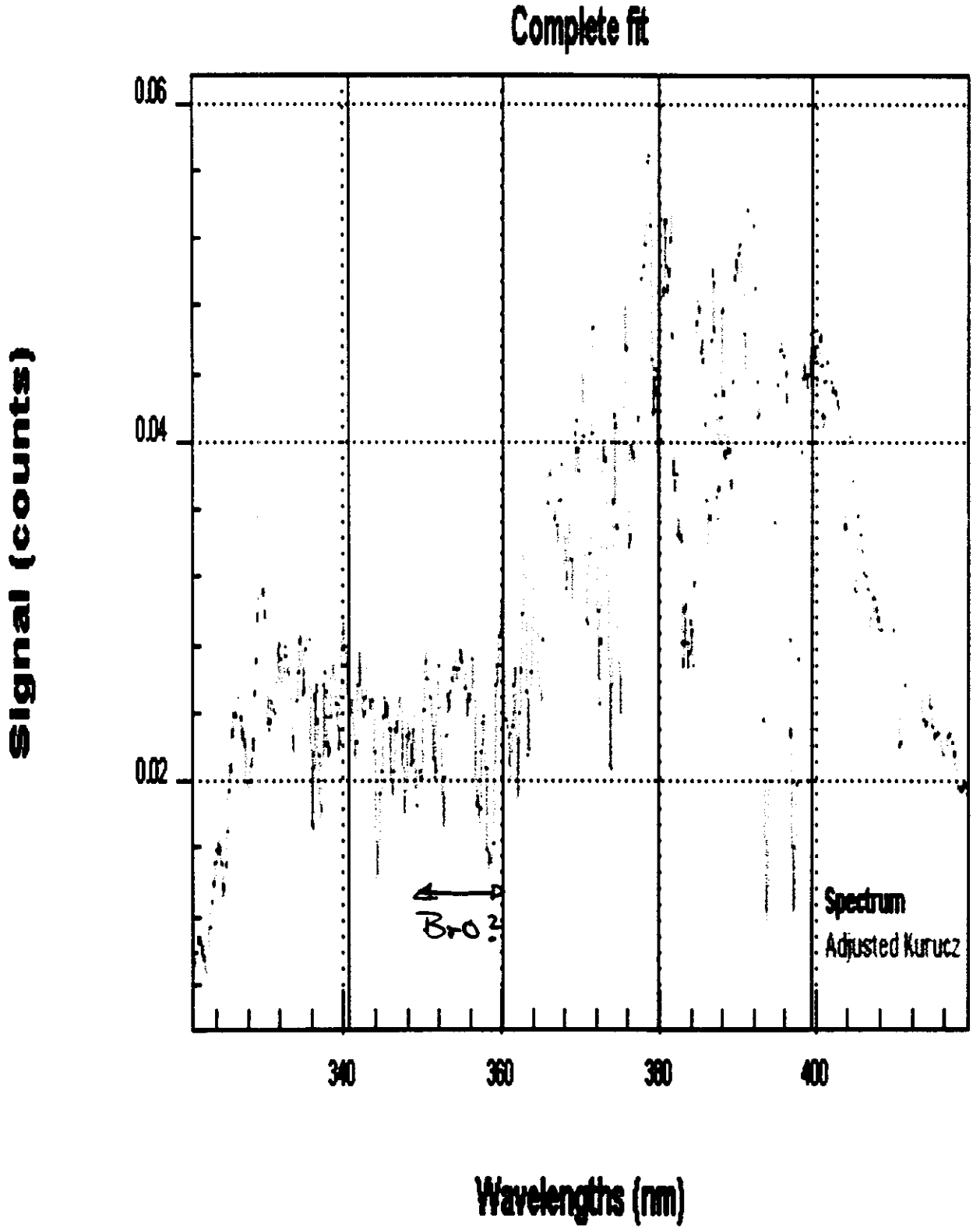
Complete fit
0.06
0.04
0.02
Signal (counts)
340
360
380
400
Wavelengths (nm)
BrO2
Spectrum
Adjusted Kurucz

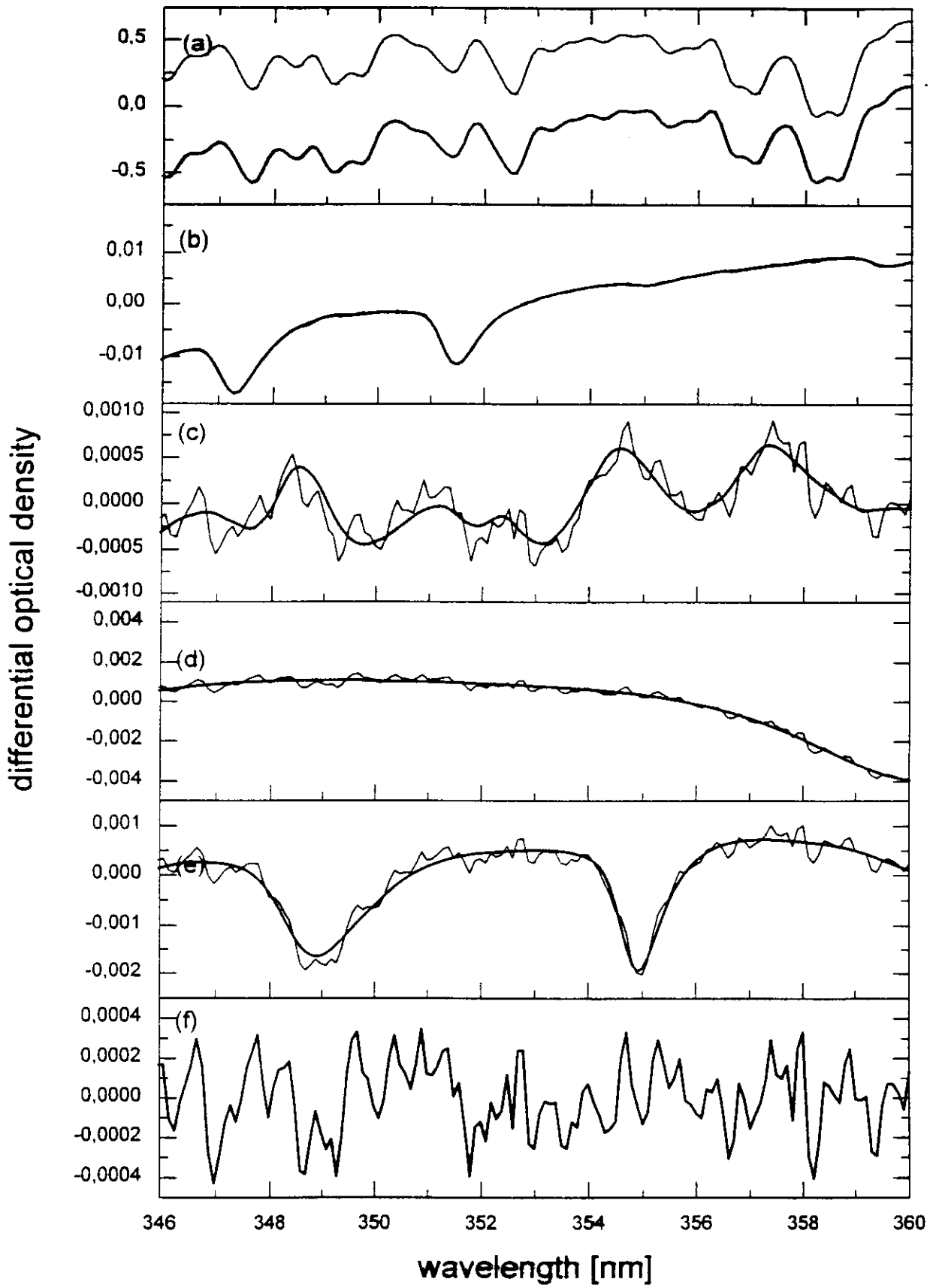

Fig: 2a

Fitzenberger et al. (1995)

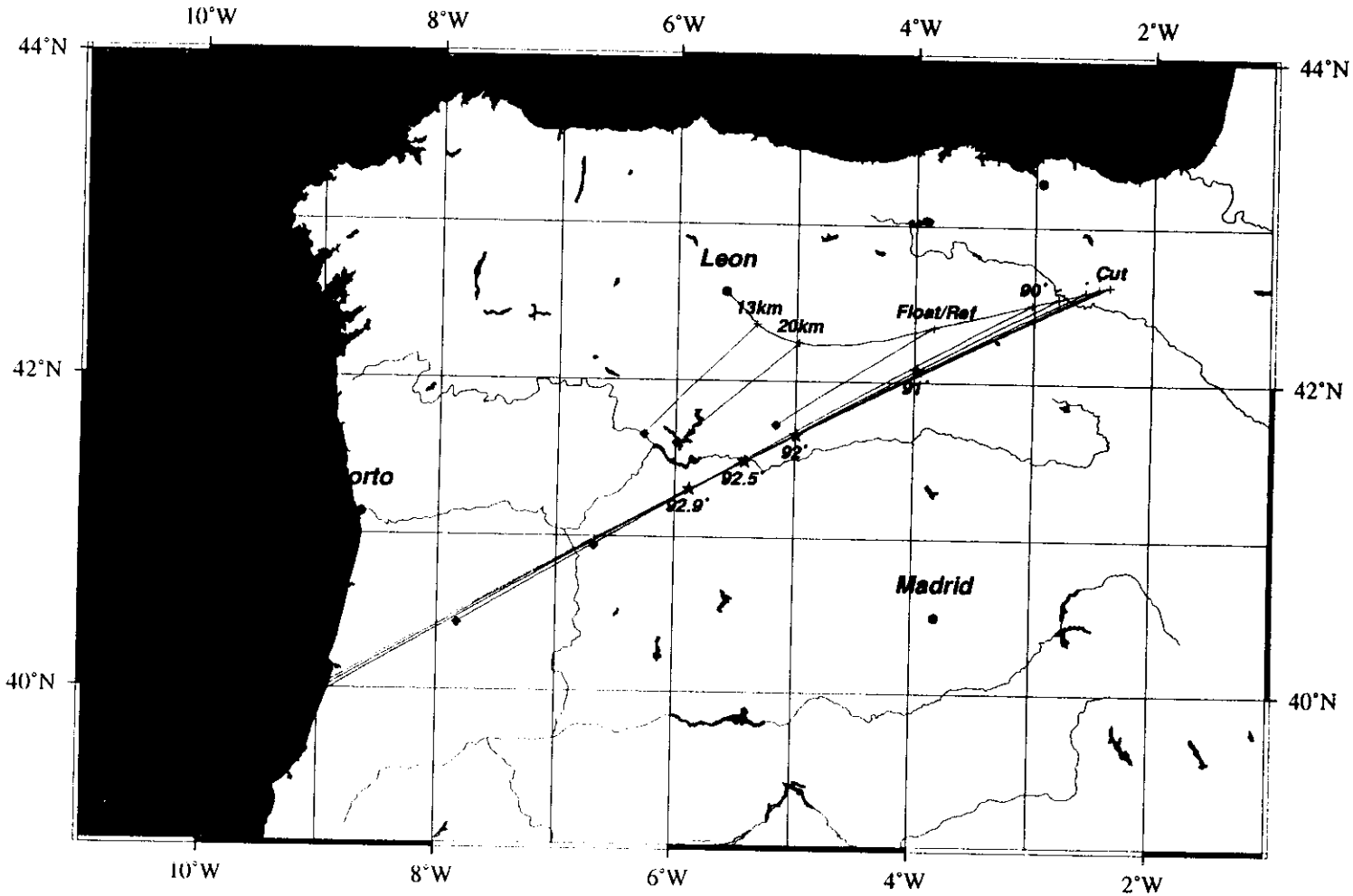
10°W
8°W
6°W
4°W
2°W
44°N
42°N
40°N
Leon
Cut
13km
20km
Float/Ref
90°
91°
92°
92.5
92.9°
Madrid

LPMA/DOAS PAYLOAD

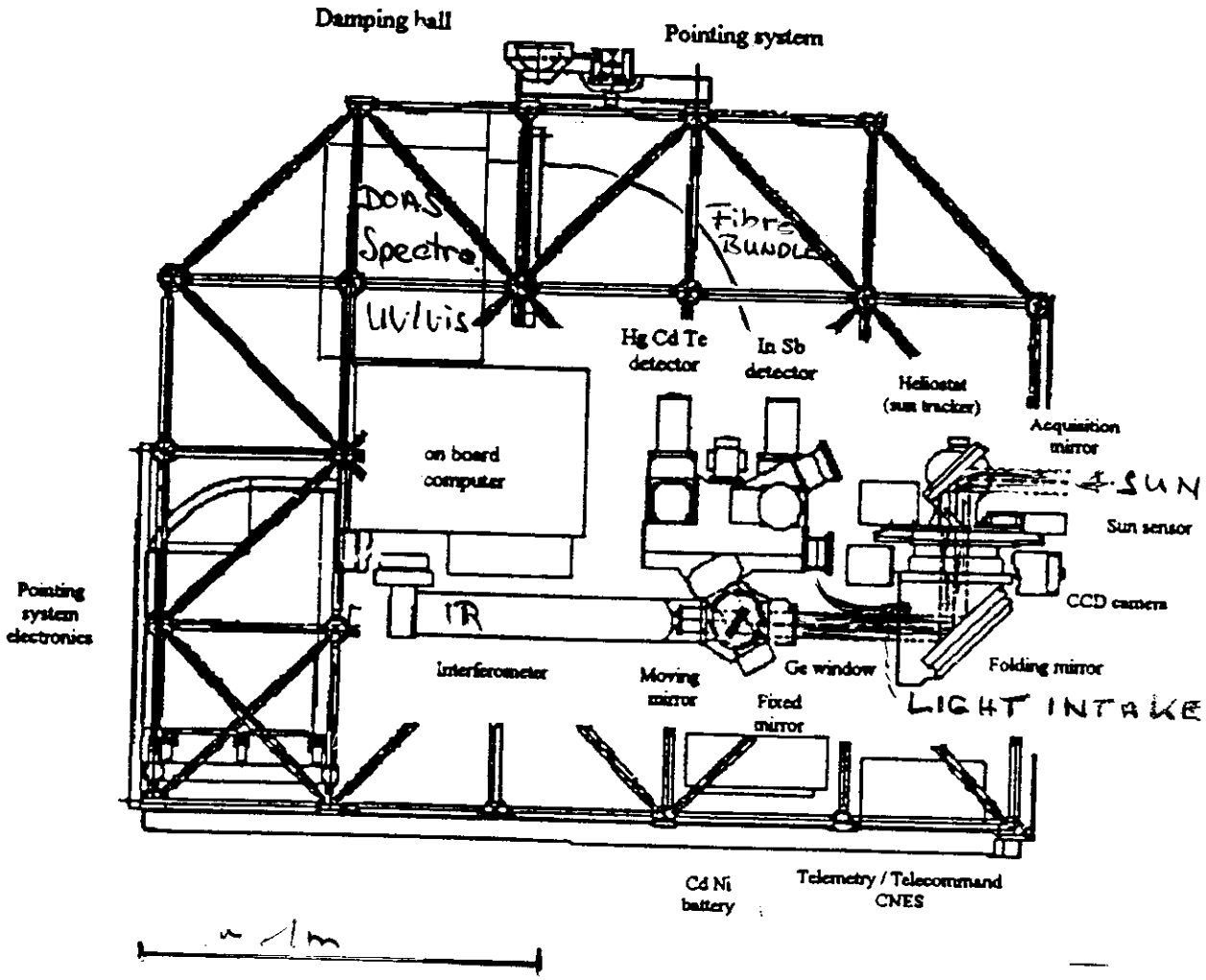

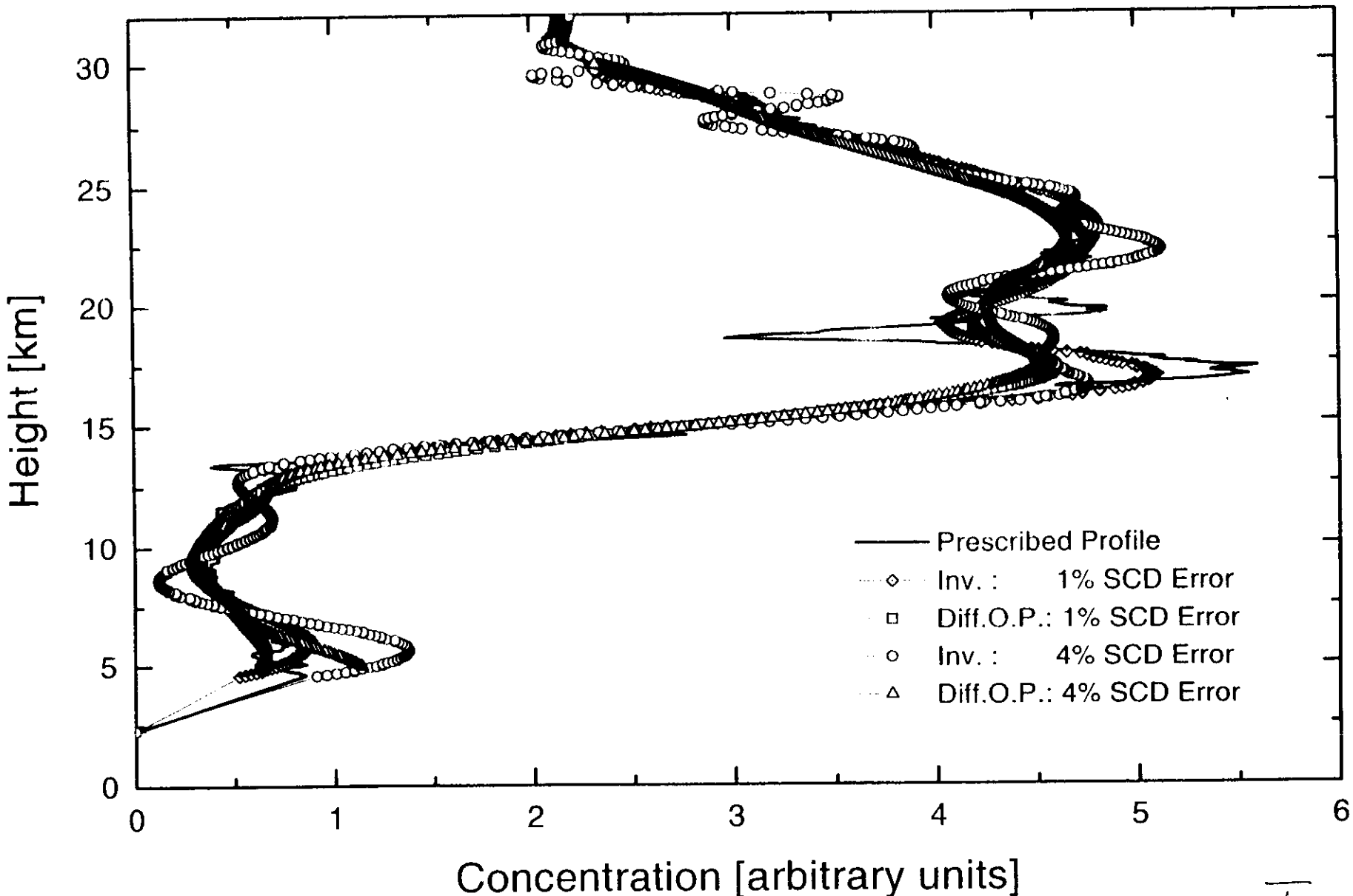
Height [km]
0
5
10
15
20
25
30
0
1
2
3
4
5
6
Concentration [arbitrary units]
Prescribed Profile
Inv. : 1% SCD Error
Diff.O.P.: 1% SCD Error
Inv. : 4% SCD Error
Diff.O.P.: 4% SCD Error

Fig. 6

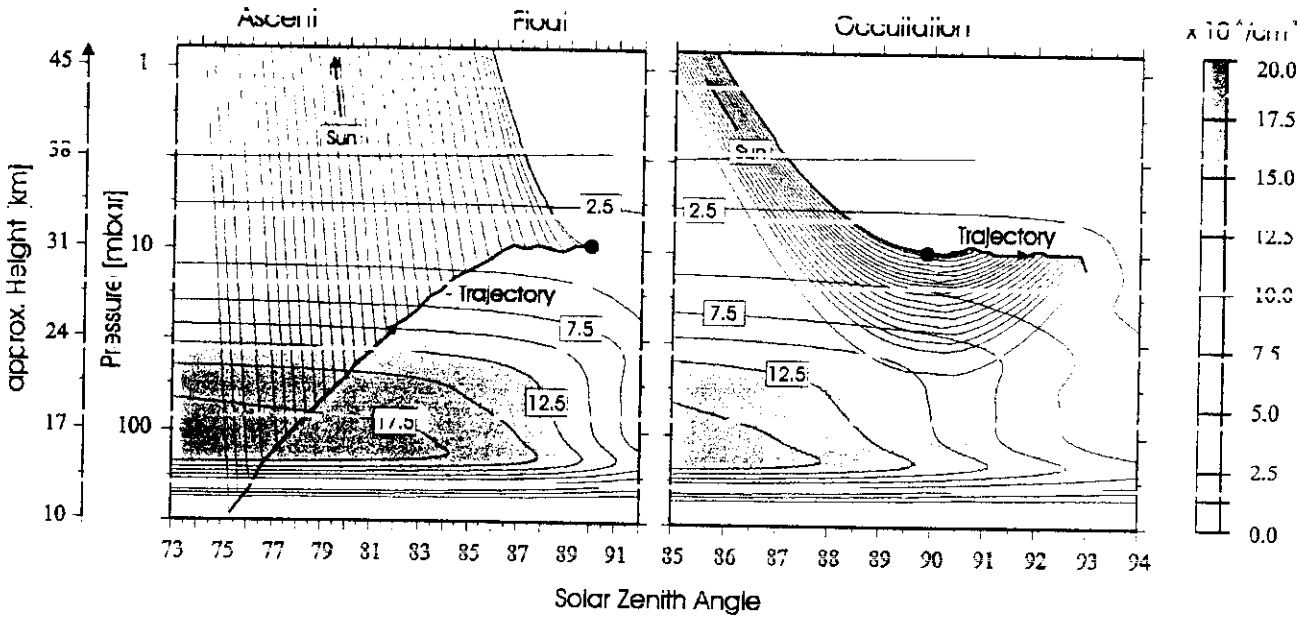

Figure 1: Harder et al.,

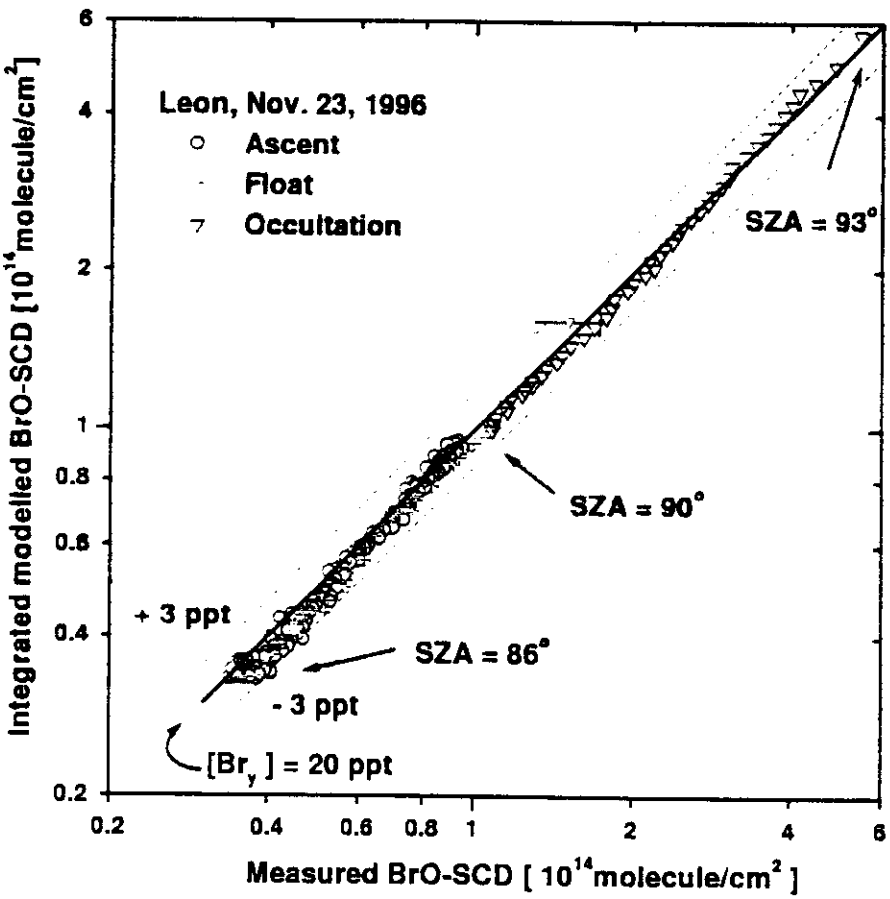

Fig. 2: Harder et al., 1999

Instrumental Set-Up

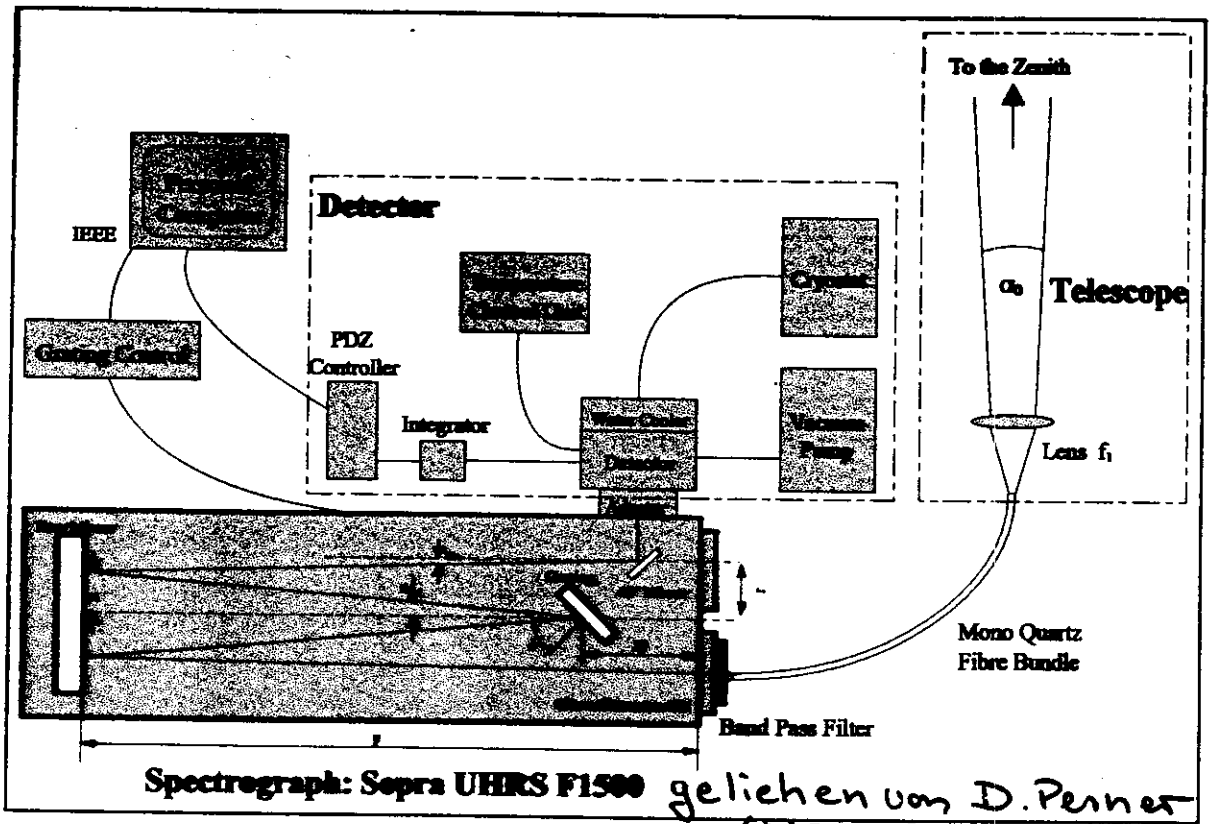

geliehen von D. Perner (MPI-Chemie, Mainz)

Spectrograph:

Spectral Range	763.0-778.0 nm
Field of View	0.86°
Focal Length	1500 mm
Aperture	f/13.5
Blazed Grating	316 rules/mm
Resolving Power(770 nm, 7th Order)	$\Delta\lambda$ = 19.5 pm
Transmission	5.3 %

Detector:

Photo Diode Array Dimension	1×1024, 2.5× 25.4 mm
Quantum Yield (770 nm)	40 %

Institut für Umweltphysik, University of Heidelberg

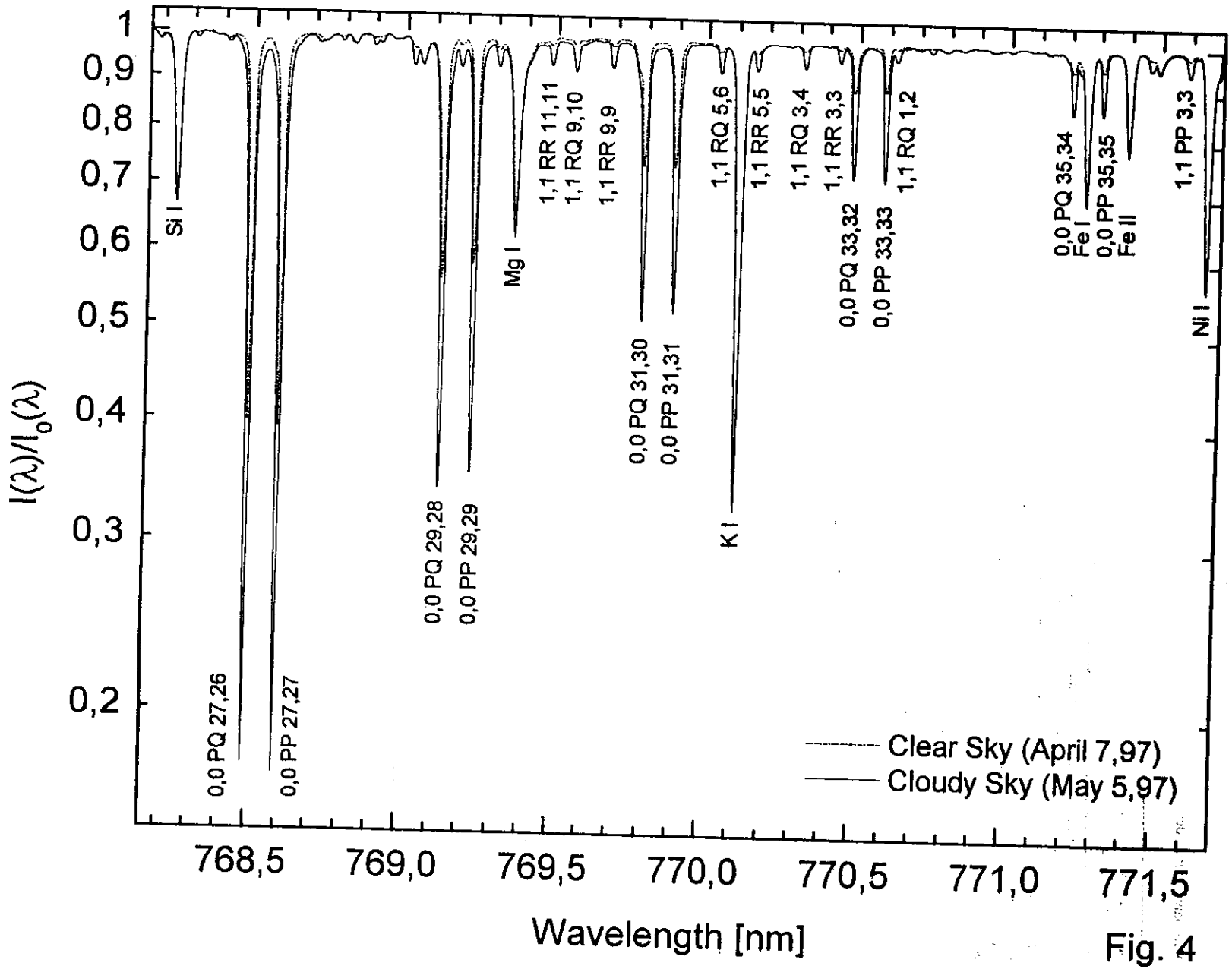

Fig. 4

Pfeilsticker et al. (1998)

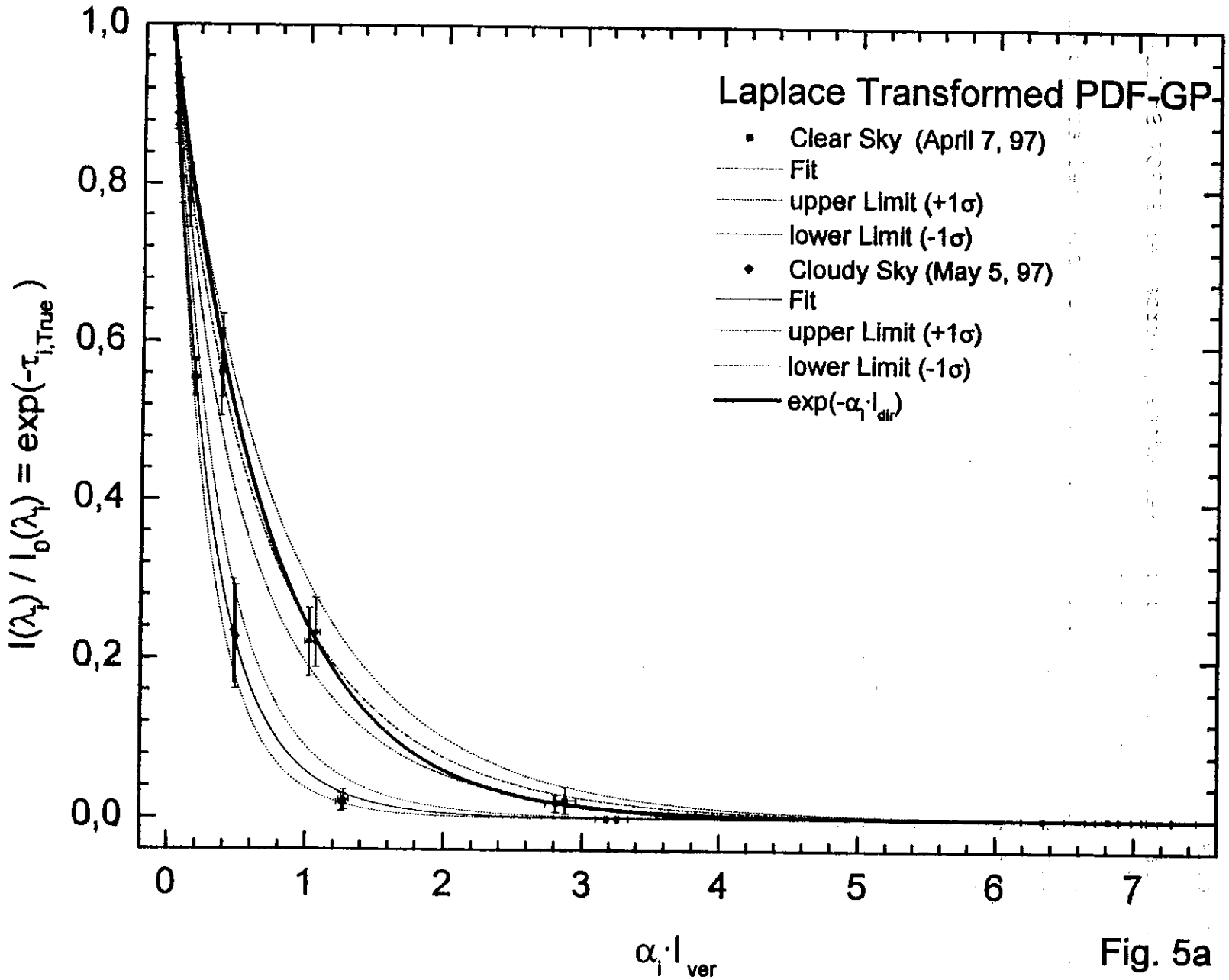

Fig. 5a

Pfeilsticker et al. (1998

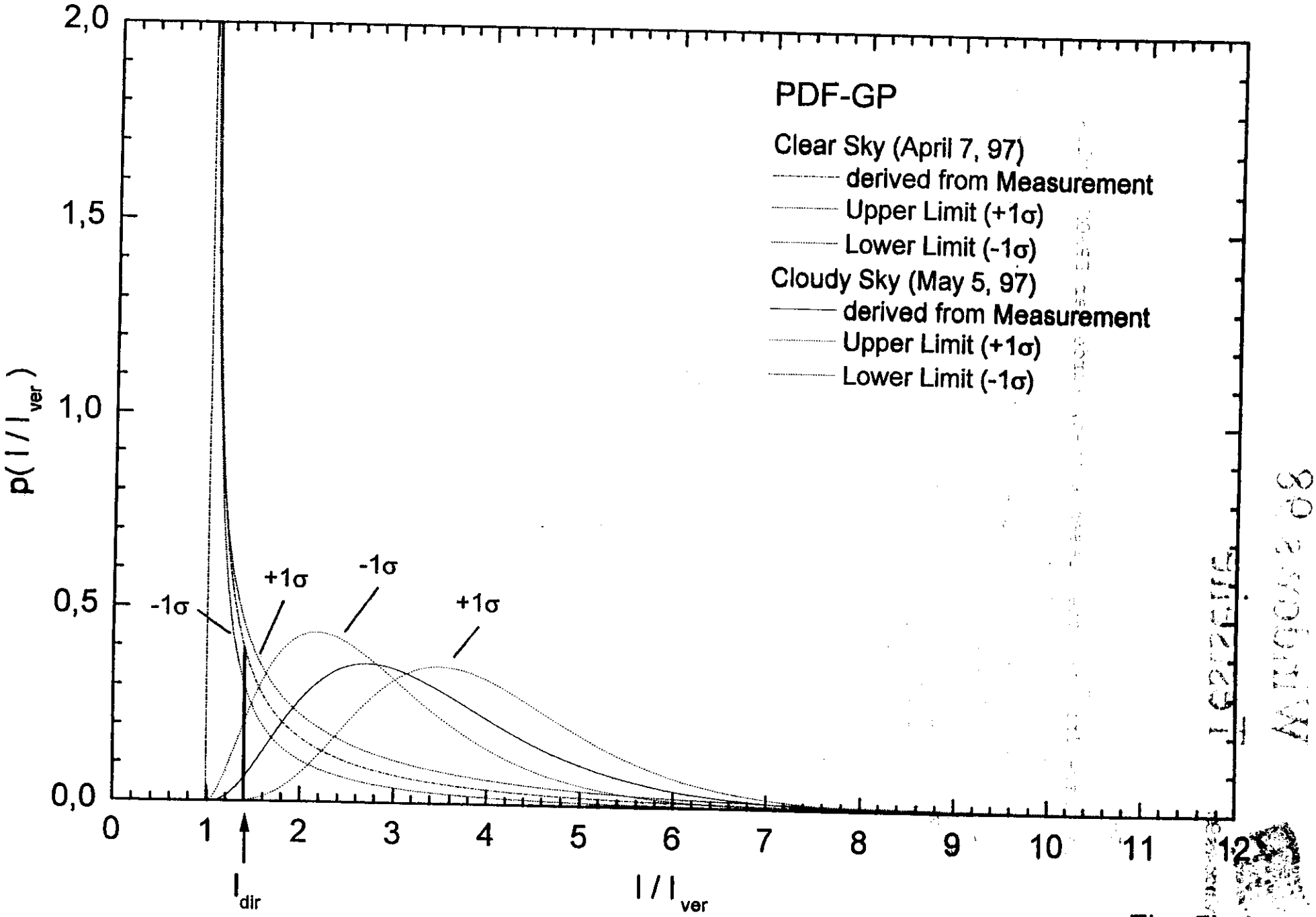

Fig. 5b

Pfeilsticker et al. (1998)

PDF-GPs for typical summer and winter cloudines